



# HOKKAIDO UNIVERSITY

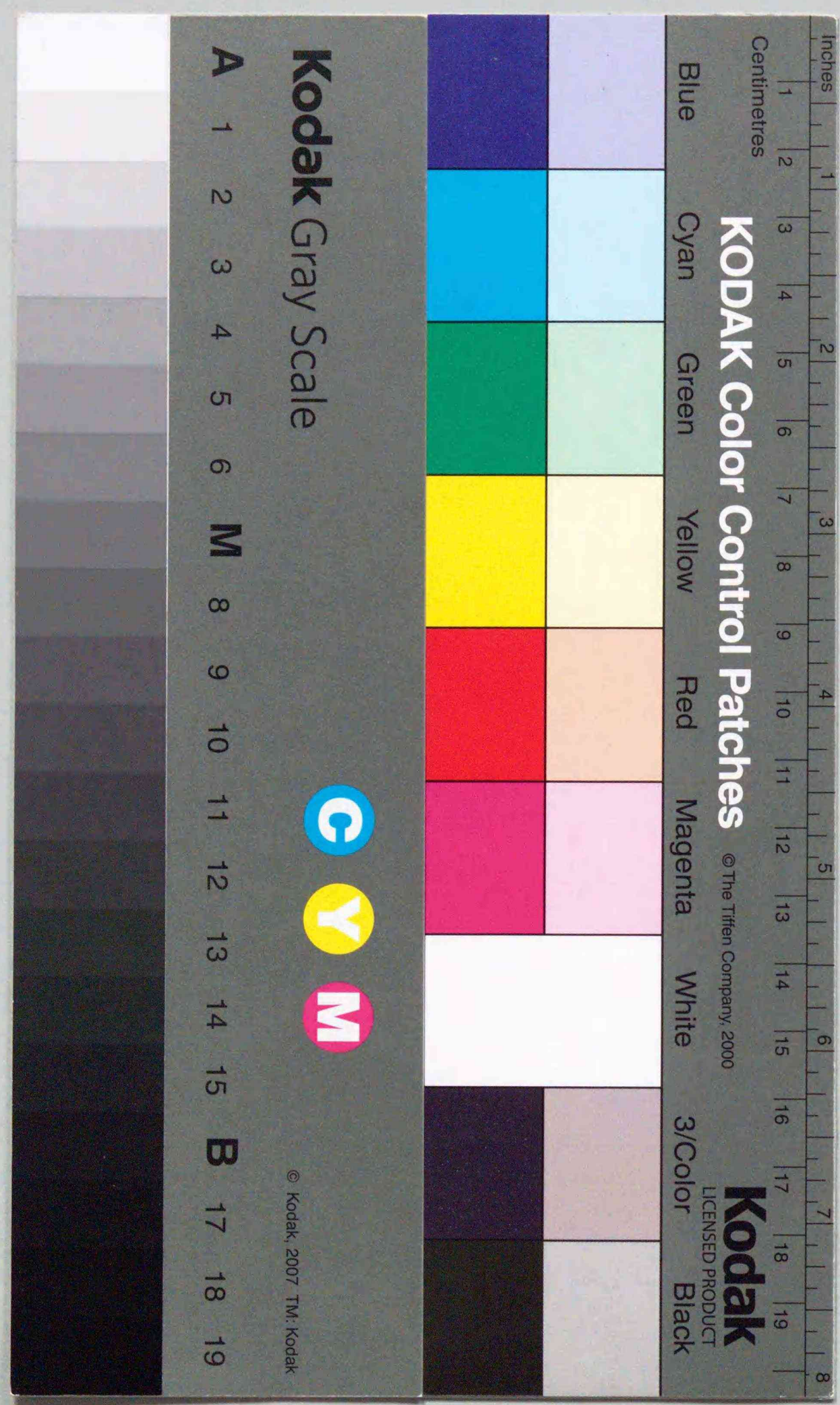
Title	Mechanical Effects of Pumping of Left Ventricular Assist Device on the Left Ventricular and Myocardial Function
Author(s)	Nakamura, Takao; 中村, 孝夫
Degree Grantor	北海道大学
Degree Name	博士(工学)
Dissertation Number	乙第4114号
Issue Date	1992-06-30
DOI	<a href="https://doi.org/10.11501/3089297">https://doi.org/10.11501/3089297</a>
Doc URL	<a href="https://hdl.handle.net/2115/49820">https://hdl.handle.net/2115/49820</a>
Type	doctoral thesis
File Information	000000251730.pdf



MECHANICAL EFFECTS OF PUMPING OF LEFT VENTRICULAR ASSIST DEVICE  
ON THE LEFT VENTRICULAR AND MYOCARDIAL FUNCTION

TAKAO NAKAMURA

June, 1992





C O N T E N T S

CHAPTER I	INTRODUCTION .....	1
1.1	INTRODUCTION .....	1
1.2	PURPOSE OF THIS STUDY .....	4
	REFERENCES .....	6
CHAPTER II	LEFT VENTRICULAR ASSIST DEVICE .....	7
2.1	CIRCULATORY ASSIST AND BLOOD PUMP .....	7
2.2	LEFT VENTRICULAR ASSIST DEVICE (LVAD) .....	10
	REFERENCES .....	12
CHAPTER III	ANALYSIS OF LEFT VENTRICULAR MECHANICS .....	15
3.1	INTRODUCTION .....	15
3.2	BULK AND REGIONAL MECHANICAL WORK .....	18
	REFERENCES .....	21
CHAPTER IV	EIGHT-CHANNEL ULTRASONIC DISPLACEMENT METER .....	23
4.1	INTRODUCTION .....	23
4.2	SYSTEM DESIGN .....	25
4.3	SENSOR DESIGN .....	28
4.4	RESOLUTION .....	30
4.5	IN VIVO PERFORMANCE TEST .....	33
4.6	DISCUSSION .....	36
4.7	SUMMARY .....	38
	REFERENCES .....	39

CHAPTER V	EFFECT OF DRIVE MODE	
	OF LEFT VENTRICULAR ASSIST DEVICE .....	43
5.1	INTRODUCTION .....	43
5.2	METHOD .....	44
5.2.1	Experimental protocol .....	44
5.2.2	Data analysis .....	49
5.3	RESULTS .....	51
5.3.1	Hemodynamic effect .....	51
5.3.2	Mechanical effect .....	55
5.3.3	Bulk mechanical work of the left ventricle .....	57
5.3.4	Regional mechanical work of the left ventricle .....	60
5.4	DISCUSSION .....	61
5.5	SUMMARY .....	66
	REFERENCES .....	67
CHAPTER VI	ACUTE EFFECT OF LEFT VENTRICULAR ASSIST DEVICE	
	ON THE ISCHEMIC HEART .....	69
6.1	INTRODUCTION .....	69
6.2	METHOD .....	70
6.2.1	Experimental protocol .....	70
6.2.2	Data analysis .....	75
6.3	RESULTS .....	77
6.3.1	Hemodynamic effect .....	79
6.3.2	Mechanical effect .....	84
6.3.2.1	Bulk mechanical work	
	of the left ventricle .....	85
6.3.2.2	Regional mechanical work	
	of the left ventricle .....	89

6.4	DISCUSSION .....	91
6.5	SUMMARY .....	95
	REFERENCES .....	96
CHAPTER VII	EFFECT OF LONG-TERM APPLICATION	
	OF LEFT VENTRICULAR ASSIST DEVICE	
	ON THE NORMAL HEART .....	98
7.1	INTRODUCTION .....	98
7.2	METHOD .....	100
7.2.1	Experimental procedure .....	100
7.2.2	Post-operative care and data acquisition .....	103
7.2.3	Data analysis .....	105
7.2.4	Histology .....	107
7.3	RESULTS .....	108
7.3.1	Feasibility	
	of the long-term ultrasonic measurements .....	110
7.3.2	Hemodynamics .....	111
7.3.3	Left ventricular dimension .....	115
7.3.4	Bulk and regional mechanical work .....	119
7.3.5	Histological study .....	123
7.4	DISCUSSION .....	127
7.5	SUMMARY .....	132
	REFERENCES .....	133
CHAPTER VIII	EFFECT OF LONG-TERM APPLICATION	
	OF LEFT VENTRICULAR ASSIST DEVICE	
	ON THE ISCHEMIC HEART .....	135
8.1	INTRODUCTION .....	135



CHAPTER I

INTRODUCTION

1.1 INTRODUCTION

The heart is one of the most important organs in the body, although it is a simple pump from the view point of engineering. Malfunction of the heart, particularly ischemic heart disease, is fatal and the mortality rate is extremely high.

To treat the ischemic heart disease, many internal medications have been developed and introduced first such as digitalis and nitroglycerin. Although this treatment is effective for the patients having minimal and moderate infarction, many patients still cannot be salvaged by these internal medicines. To these patients, several surgical methods called circulatory assist techniques have been applied (1,2), which include intra-aortic balloon pumping method (IABP) and veno-arterial bypass technique (VAB). However, it has been pointed out from clinical experiences that these mechanical support techniques are not still powerful enough to rescue the patients with more profound heart failure. To overcome the shortage of these methods, ventricular assist devices (VADs) have been developed as one of the most powerful means for the support of the damaged heart. The original concept of the VAD is to bypass the severely damaged ventricle, aiming to keep the systemic/pulmonary blood circulation under good condition as well as to rest the damaged heart and increase the coronary flow for recovery.

Cardiac transplantation is another currently available surgical way

to help patients with severely damaged, un-recoverable hearts. By virtue of the development of an immuno-control medicine (Cyclosporine-A), the transplantation is now the most successful method for those patients. However, there is a very important and serious problem with this method, which is that the number of donor hearts is always extremely short from the requirement and also donor hearts are not always available. For the past several years, VAD has been used as a bridging mean to cardiac transplantation to keep patients alive until their donor hearts become available.

Total artificial heart (TAH) is an alternative way to keep patients alive by substituting the damaged ventricles with two blood pumps. However, the application is limited to unrecoverably damaged hearts because the ventricles must be resected for the TAH application.

As mentioned above, VAD is applied in 2 ways:

- (i) to rescue damaged but recoverable hearts, and
- (ii) to bridge to heart transplantation for un-recoverable hearts.

It was reported that by the 31st of December, 1988, 451 and 142 clinical applications had been done in the categories of (i) and (ii), respectively (3,4).

Clinical application of VAD is expected to expand more with the increased knowledge of its high potential. To use this powerful and useful technique more effectively, basic studies of the effects of VAD on the natural heart have been conducted extensively. Most of them, however, were concerned with its hemodynamic effects in normal heart models.

Very few studies have been conducted on the effects of VAD from the stand point of cardiac mechanics, particularly on the mechanical effects of VAD on ischemic and infarcted hearts. To clarify the function of the

heart which is a mechanical pump, study on cardiac mechanics is essential in addition to hemodynamic study. Therefore, effects of VAD on the mechanical function of the natural heart, especially of the left ventricle, is one of the most important subjects to be studied for more effective use of this powerful means in clinical cases.

## 1.2 PURPOSE OF THIS STUDY

The main purpose of this study is to analyze bulk and regional mechanical behavior of the left ventricle during pumping of the left ventricular assist device (LVAD), which includes;

- (i) development of a method for the evaluation of the effects of cardiac assist on the left ventricular mechanics;
- (ii) design of a suitable measurement system which can be used for animal experiments;
- (iii) selection of the most effective drive mode of LVAD;
- (iv) study of the effects of LVAD on the bulk ventricular and local myocardial behavior;
- (v) study of the effects of LVAD pumping on the ischemic and normal myocardium in the ischemic heart model;
- (vi) evaluation of long-term effects of pumping;
- (vii) study of the recovery process of the failing heart supported by LVAD.

For the above-mentioned purposes, a sonomicrometer system was developed and applied for the study of the mechanical effects of LVAD in the normal and ischemic natural hearts both in acute and chronic animal experiments.

This dissertation is divided into 9 chapters.

CHAPTER I is the introduction including the purpose of this study.

CHAPTER II shows the concept, history, and state of the art of the techniques for circulatory assist, especially of ventricular assist devices.

In CHAPTER III, studies on the cardiac mechanics are briefly surveyed. After emphasizing the importance of cardiac mechanics for the

evaluation of effects of LVAD, methods used in this study for the analysis of the mechanical effects of LVAD pumping on the natural left ventricle are proposed.

To measure several important parameters including left ventricular diameter, myocardial segment length, and wall thickness which are required for the analysis described in CHAPTER III, an 8-channel ultrasonic displacement meter was developed. Design details and evaluation of the system are described in CHAPTER IV.

In the following chapters, protocols and results of animal experiments are described. First of all, effects of drive mode of LVAD on the left ventricular mechanics were studied by acute experiments on dogs having normal hearts, and the methods and results are described in CHAPTER V.

Based on these results, effects of LVAD on the cardiac mechanics were studied by acute experiments on canine hearts induced with myocardial ischemia. CHAPTER VI is devoted to describing this study.

After a series of the acute animal experiments, long-term effects of LVAD pumping on the normal heart and feasibility of long-term use of the sonomicrometers were studied using goats, and the experimental protocol and the results obtained are explained in CHAPTER VII.

As a final goal of this study, a series of chronic experiments were performed on goats with induced heart failure to observe the recovery process of the natural heart from the myocardial infarction by LVAD pumping, and are described in CHAPTER VIII.

CHAPTER IX is devoted to the conclusion and summary of this study.

## REFERENCES

1. Assisted Circulation. Ed: Unger F. Springer-Verlag 1979.
2. Assisted Circulation II. Ed: Unger F. Springer-Verlag 1984.
3. Miller CA, Pae WE, Pierce WS. Combined registry for the clinical use of mechanical ventricular assist device. -Postcardiotomy cardiogenic shock- ASAIO Trans 1990; 36: 43-46.
4. Pae WE, CA Miller, Pierce WS. Combined registry for the clinical use of mechanical ventricular assist pumps and the total artificial heart: third official report-1988. J Heart Transplant 1989; 8: 277-280.

## CHAPTER II

### LEFT VENTRICULAR ASSIST DEVICE

#### 2.1 CIRCULATORY ASSIST AND BLOOD PUMP

To maintain the blood circulation while resting the seriously damaged natural heart several mechanical support techniques have been developed such as intra-aortic balloon pumping (IABP) and veno-arterial bypass (VAB) methods, which are being used widely in clinical cases. They are called "circulatory assist" methods (1-3). It has been pointed out, however, that these means are not still powerful enough to rescue a number of profound heart diseases.

To salvage patients who have severely damaged hearts beyond the IABP capability or who cannot be weaned off from the cardiopulmonary bypass during open heart surgery, or to bridge patients to cardiac transplantation, a more powerful circulatory assist system called ventricular assist device (VAD) has been developed. As the natural ventricle is a simple pump from the engineering point of view, the VAD is also a kind of mechanical blood pump. To the VAD system, much interest has been directed because of its high ability (4): differently from the other cardiac assist systems, VAD has the capability of actively maintaining not only the blood pressure but also the circulatory blood volume.

For the patients whose ventricle(s) was (were) too severely damaged to recover by any methods, total artificial heart (TAH) has been developed. To apply TAH to those patients, both ventricles are resected

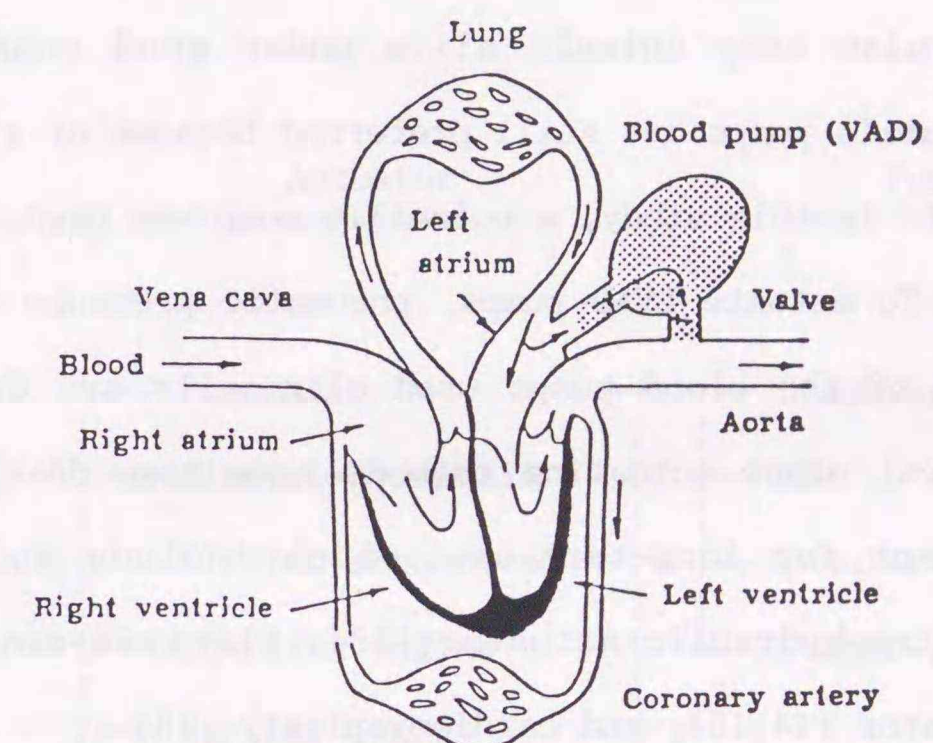
and replaced with two blood pumps (see Fig. 2.1). VAD is different from TAH (5): VAD is attached to a patient in order to bypass the left and/or right ventricles, keeping the heart intact as shown in Fig. 2.1. There are several variations for the use of VAD: VAD is applied to the left ventricle (LVAD), to the right ventricle (RVAD), or to both ventricles (BVAD). For the purpose of keeping blood circulation of patients having non-functioning hearts, for example, for the bridge use to cardiac transplantation, TAH or BVAD can be used (6). It has been reported recently that LVAD can maintain the blood circulation of whole body even if not only the left ventricle but also the right ventricle are fatally damaged (7). However, in the case that the natural heart is expected to recover, VAD should be selected with the ventricle(s) remained, and should be removed after recovery. Most cardiac assist devices are used temporarily for a short period to avoid the risk of severe infection and thromboemboli (8) anticipated in long-term use, for the recovery of natural heart or for the bridge to cardiac transplantation.

Historically, Kolff and Akutsu first kept alive a dog implanted with TAH pumps for 2 hours in 1957 (9). Since that experiment, many types of TAH and VAD systems have been developed; some of them have been used clinically since the middle of 1970's. Recent registries showed that 297 LVAD, 62 RVAD, 234 BVAD and 77 TAH had been used clinically and the hospital discharge rates were 24 % for cardiogenic shock cases and 45 % for bridge cases (73 % were transplanted) as of December 31, 1988 (8,10).

Since the left side of the heart is much more important than the right side for the systemic blood circulation, LVAD is usually considered as the first choice for the damaged heart. Because of excellent blood-volume unloading effect, ability of maintaining the

systemic blood circulation in the physiologically normal range, and improvement of coronary blood flow, LVAD is now considered to be the most powerful mechanical means to support the left ventricle.

VENTRICULAR ASSIST DEVICE (VAD)



TOTAL ARTIFICIAL HEART (TAH)

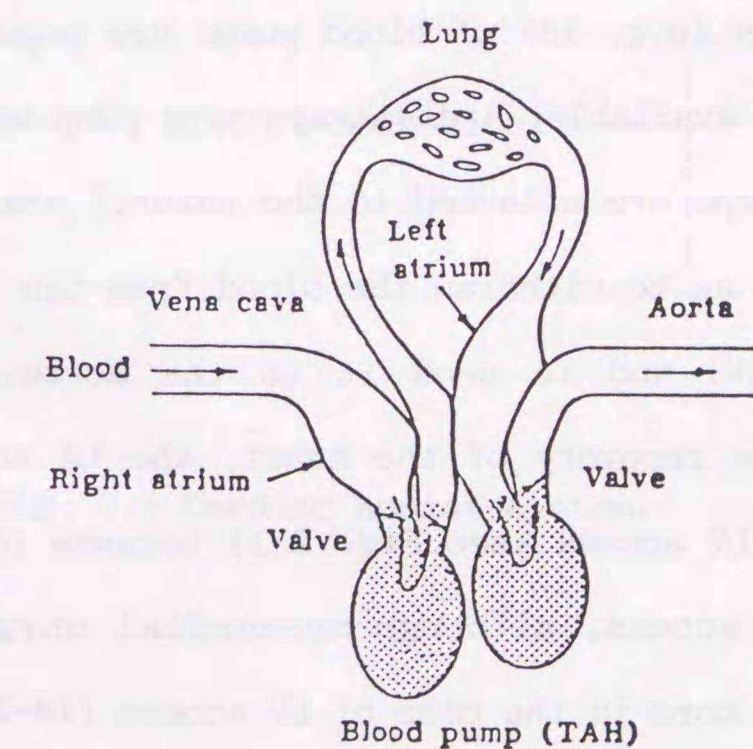


Fig. 2.1 Blood pump used as ventricular assist device (VAD) and total artificial heart (TAH).

## 2.2 LEFT VENTRICULAR ASSIST DEVICE (LVAD)

Figure 2.2 shows the classification of blood pumps developed so far. They are divided into pulsatile and non-pulsatile pumps. Since the natural heart is a pulsatile pump, most of the pumps developed as VAD are pulsatile pumps. It has been proven that non-pulsatile blood flow can also keep animals alive under good condition (11). However, pulsatile pumps are still preferred because of similarity to the natural heart. In this study, a pulsatile pump was used.

To actuate LVAD pumps, pneumatic pressure was used in this study. Most of the blood pumps used clinically are driven with this method. Several other actuating methods have been developed, mainly aiming to implant for long-term-use, which include solenoid actuator (12), electro-hydraulic actuator (13), electric-motor driven, mechanical actuator (14,15), and cardiomyoplasty (16).

There are several types of pumps, among which diaphragm (e.g. 17) and sac types (e.g. 18) of blood pumps are popular and some of them are commercially available. A diaphragm type pump was used in this study.

LVAD pumps are attached to the natural heart in two ways: they are implanted so as to withdraw the blood from the left atrium (LA) or left ventricle (LV) and to send it to the aorta. For the temporary use expecting the recovery of the heart, the LA access is much preferably used to the LV access (see Fig. 2.1) because of less myocardial damage with the LA access, although myocardial oxygen consumption can be reduced much more in the case of LV access (19-21). Since more blood can be withdrawn from LV than from LA, the LV access method is used for the case that the heart is un-recoverable. The LA access was employed in this study considering frequent clinical application of the method.

In summary, as one of the most popular VAD systems, a pneumatically driven, diaphragm-type blood pump with LA access was used in this study to evaluate effects of pumping on the left ventricular mechanics. This pump has been approved by Japanese government for clinical use (17).

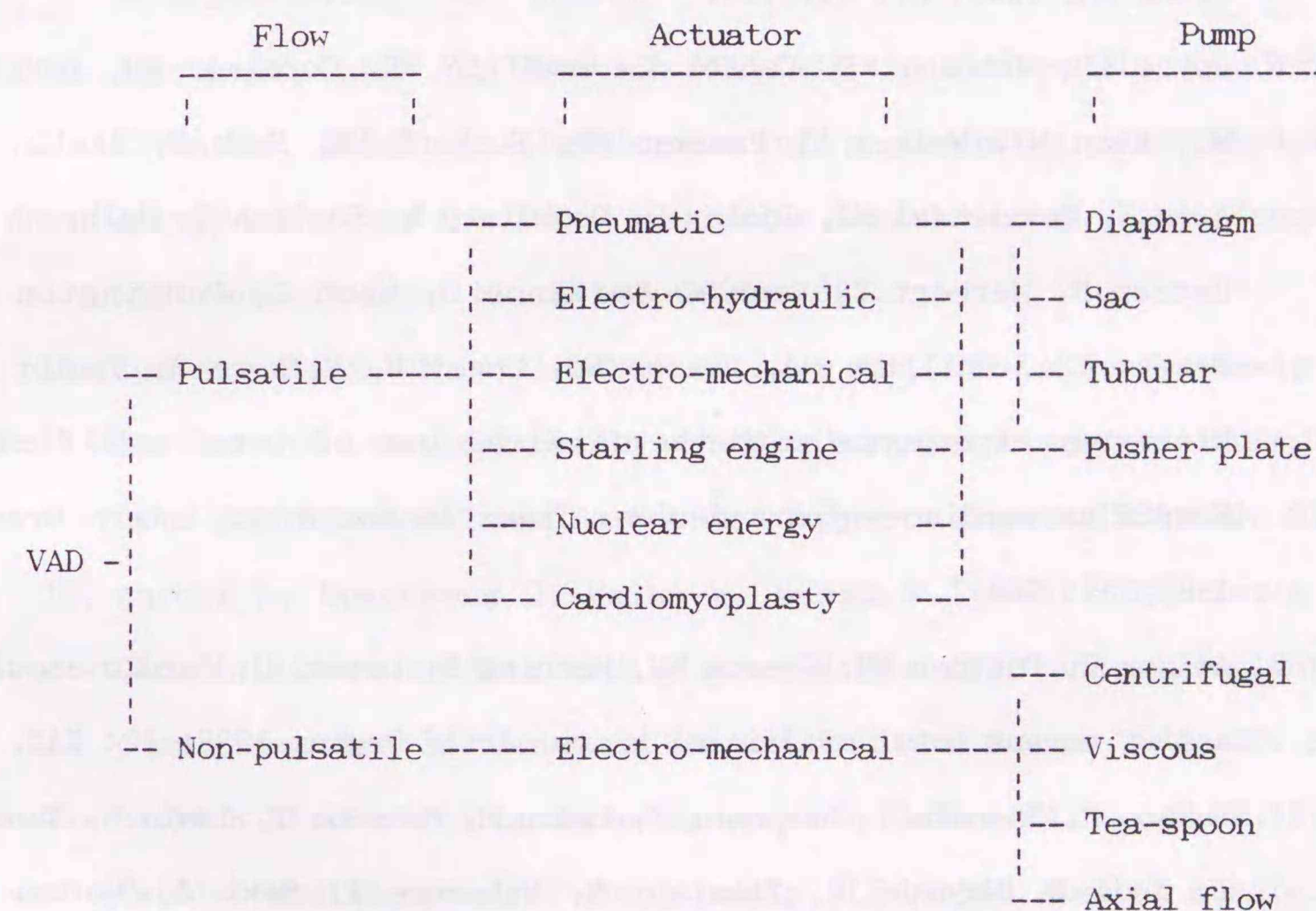


Fig. 2.2 Cardiac assist system.

REFERENCES

1. Assisted Circulation (Ed: Unger F). Springer-Verlag, 1979.
2. Assisted Circulation 2 (Ed: Unger F). Springer-Verlag, 1984.
3. New Developments in cardiac assist devices (Ed: S.Attar). Praeger, 1985.
4. Tsitlik JE. Circulatory support system entering the 1990's. IEEE Trans BME 1990; 37: 117-120.
5. Joyce LD, Johnson KE, Cabrol C, Griffith BP, Copeland JG, DeVries WC, Keon WJ, Wolner E, Frazier OH, Bucherl ES, Semb B, Akalin H, Aris A, Carmichael MJ, Cooley D, Dembitsky W, English T, Halbrook H, Hetzer R, Herbert Y, Keon WJ, Loisance D, Noon G, Pennington G, Peterson A, Phillips SJ, Pierce WS, Unger F, Pifarre R, Tector A. Nine year experience with the clinical use of total artificial hearts as cardiac support device. Trans Am Soc Artif Intern Organs 1988; 35: 703-7.
6. Aolner E, Portner PM, Pierce WS, Henning E, Losert U. Cardiovascular assist versus total artificial heart. Artif Organs 1988; 12: 242.
7. Takano H, Taenaka Y, Nakatani T, Umezu M, Matsuda T, Iwata H, Tanaka T, Noda H, Hayashi K, Takatani S, Nakamura T, Seki J, Akutsu T, Manabe H. Circulatory maintenance with a single artificial heart. Trans Am Soc Artif Intern Organs 1984; 30: 550-5.
8. Miller CA, Pae WE Jr, Pierce Ws. Combined registry for the clinical use of mechanical ventricular assist devices. ASAIO Trans 1990; 36: 43-6.
9. Kolff WJ. Artificial organs beyond the first 40 years. Life Support System 1984; 2: 1-14.
10. Pae WE Jr, Miller CA, Pierce WS. Combined registry for the clinical

- use of mechanical ventricular assist pumps and the total artificial heart: third official report-1988. J Heart Transplant 1989; 8: 277-80.
11. Nose Y. My life with the National Institutes of Health artificial heart program. Artif Organs 1990; 14: 174-190.
12. Portner PM. The Novacor heart assist system: development, testing and initial clinical evaluation. In: Artfi Heart 2 (Ed: Akutsu T), Sprenger-Verlag 1988: 89-97.
13. Jarvik RK, Lioi AP, Isaacson MS, Orth J, Nielsen SD, Kessler TR, Olsen DB, Kolff WJ. Development of a reversing electrohydraulic energy converter for left ventricular assist device. Final Report of NIH contract/grant No. NO1-HV-72975 1982.
14. Igo SR, Fuqua JM, McGee MG, Creager GJ, Pool GE, Krudewig TW, Fraizier OH. An implantable ventriular assist system: chronic in vivo performance. Trans Am Soc Artif Intern Organs 1984; 30: 81-5.
15. Anyder A, Rosenberg G, Weiss W, Huang W, Landis D, Pierce WS. Chronic animal studies with a motor-driven LVAD and an implantable compliance chamber. Trans Am Soc Artif Intern Organs 1984; 30: 92-7.
16. Badylak SF, Stevens L, Janas W, Gray MH, Gedded LA, Voorhees III WD. Cardiac assistance with electrically stimulated skeltal muscle. Med & Biol Eng & Comput 1989; 27: 159-62.
17. Takano H, Taenaka Y, Noda H, Kinoshita M, Yagura A, Tatsumi E, Sekii H, Sasaki E, Umezu M, Nakatani T, Kyo S, Omoto R, Akutsu T, Manabe H. Multi-instisutional studies of the National Cardiovascular Center ventricular assist system: use in 92 patients. Trans Am Soc Artif Intern Organs 1989; 35: 541-4.
18. Atsumi K. Ventricular assistance: development and clinical application of a new device. In: Assisted circulation 2 (Ed: Unger

F) Springer-Verlag 1984: 100-114.

19. Pierce WS, Aaronson AE, Prohet GA, Williams DR, Waldhausen JA. Hemodynamic and metabolic studies during two types of left ventricular bypass. Surg Forum 1972; 23: 176-8.
20. Eugene J, Moore-Jeffries EW, Ott RA, Haiduc NJ. Left atrial-to-aortic assistance: effect of in-line venting on myocardial oxygen consumption. Heart Transplant 1984; 3: 329-35.
21. La Farge CG, Schoen FJ, Monroe RG, Bernhard WF. Left atrium-to-aorta versus left ventricle-to aorta bypass: the Lewis and Anrep effects. ASAIO J 1985; 8: 191-204.

### CHAPTER III

#### ANALYSIS OF LEFT VENTRICULAR MECHANICS

##### 3.1. INTRODUCTION

Because the heart is a sort of mechanical pumps, to know the mechanical characteristics of the bulk heart as well as the local myocardium is one of the most important subjects to understand the heart function. From the hemodynamical view point, many parameters have been proposed and used to analyze and evaluate the cardiac function (contractility), including time-domain derivative of the positive slope of left ventricular pressure ( $dP/dt$ ) (1), tension time index (TTI) (2), their modifications (3), max. negative  $dP/dt$  (4), and time constant of the negative slope of left ventricular pressure (5,6). In addition, mean fiber shortening velocity (Mean Vcf) (7), end-systolic pressure-volume relation ( $E_{max}$ ) (8), and left ventricular pressure-volume area (PVA) (9) have been proposed for more direct and accurate evaluation of cardiac mechanics.

Bulk stroke work of the left ventricle and mechanical external work done by the local myocardium are the most basic parameters. Because the myocardial infarction is often caused by blockage of coronary artery and has a local nature, regional myocardial work is particularly important for the evaluation of local myocardial infarction. A method to obtain the local myocardial stroke work has been proposed (10,11) in which anisotropic nature of the heart is taken into account.

These parameters proposed for the evaluation of ventricular

function are summarized in Table III.I (1).

In this study, "mechanical external work" done by the local myocardium and by the whole left ventricle were used for the evaluation of local and bulk ventricular function, respectively. The details of the method for obtaining these parameters are described in this chapter.

Table III.I Ventricular performance indexes.

Index	Definition
<u>Isovolumetric indexes</u>	
Vmax	Maximum velocity of shortening from velocity curve extrapolated to zero force.
max dP/dt	Maximum rate of rise of ventricular pressure (DP).
DP time	Time from beginning of systole to DP.
P <sub>0</sub>	Ventricular pressure at DP.
R time	Time for ventricular pressure to rise from 25 to 45 mmHg.
DP/P	Maximum dP/dt divided by ventricular pressure.
DP/DEV P	Maximum dP/dt divided by ventricular pressure minus end-diastolic ventricular pressure.
DP/KP	Same as DP/P, but using an elastic modulus constant of 28-32.
DP/P <sub>0</sub>	DP divided by ventricular pressure at DP.
IIT	Integrated isometric tension: area under ventricular pressure curve from beginning of systole to 1.5xDP time.
DP/IIT	DP divided by IIT.
DP <sub>40</sub>	dP/dt at ventricular pressure of 40 mmHg.
FRCP <sub>50,75</sub>	DP/P + d <sup>2</sup> P/dt <sup>2</sup> /DP at ventricular pressures of 50 and 75 mmHg.
PEP	Pre-ejection period.
Vce	Contractile element velocity (same as Vmax).
<u>Ejection indexes</u>	
Vcf	Velocity of circumferential fiber shortening at peak left ventricular wall tension.
Peak Vcf	Maximum velocity of shortening.
Mean Vcf	Mean velocity during ejection.
EF	Ejection fraction = (stroke volume)/(end-diastolic volume).
PVP	Peak ventricular pressure.
Max E(t)	Maximum pressure-volume ration.
BMW	bulk mechanical external work = (bulk stroke work of ventricle)/(heart rate).
RMW	Regional mechanical external work = (regional stroke work of myocardium)/(heart rate)
E <sub>max</sub>	End-systolic pressure-volume relation.
PVA	Left ventricular pressure-volume area.
<u>Combined indexes</u>	
PVP time	Time from beginning of systole to PVP.
Systolic time	Length of systole.
FOM	Figure of merit = (PVP time)x(heart rate).

### 3.2 BULK AND REGIONAL MECHANICAL WORK

Bulk and regional mechanical behavior of the left ventricle have been extensively studied in the field of cardiac mechanics (10-14). Little et al. (12) studied anisotropic change of left ventricular diameter, and anisotropic behavior of regional muscular length was observed by Lew and LeWinter (13). These results suggest that we should analyze both whole and regional behavior of the left ventricle multi-dimensionally for precise evaluation of ventricular function: at least three different diameters should be measured to analyze bulk behavior of the left ventricle, and two segmental lengths in different directions for regional mechanics of the myocardium.

As reported by Suga et al., mechanical work of the ventricle is closely related to myocardial oxygen consumption (15): reduction of the left ventricular work corresponds to decrease in the myocardial oxygen consumption. Thus, the left ventricular mechanical work could be one of the most useful indices for the evaluation of mechanical effects of LVAD pumping.

In this study, left ventricular bulk stroke work was calculated from the left ventricular pressure-volume relationship in a cardiac cycle. The ventricular pressure-volume relation forms a counterclockwise loop, and the area inside the loop gives external mechanical stroke work done by the left ventricle. To obtain this loop, left ventricular pressure (LVP) and volume (LVV) must be measured simultaneously and accurately.

In the field of cardiac mechanics, for the measurement of LVP, implantable wire strain gauge-type pressure transducers have been employed to avoid the distortion and phase delay of the LVP signals.

This type of transducer was used in this study.

Ultrasonic transit-time technique using a pair of implantable miniature sensors has been widely used to measure the left ventricular dimensions. Rushmer et al. (16) first measured left ventricular diameter by this method. Because of anisotropic behavior of the left ventricle as stated above, at least three different diameters and two segmental length in the different directions should be measured to analyze bulk behavior of the left ventricle (12) and regional mechanics of the myocardium (13), respectively. Since ultrasonic displacement meters (i.e. sonomicrometers) commercially available are equipped with only 4 channels, they cannot be used for the purpose of this study. To overcome this drawback, an 8-channel sonomicrometer system was newly designed, the detail of which is described in the next chapter.

To obtain the LVV, a long axis inner diameter and two short axis diameters parallel and perpendicular to the septum were measured simultaneously by means of the newly designed ultrasonic sonomicrometer. By using the measured diameters, LVV can be calculated by:

$$LVV = \frac{\pi}{6} LD \cdot SDp \cdot SDn, \quad (3.1)$$

where the shape of the left ventricular cavity was assumed ellipsoidal (11,12).

Calculation of the LVV from only three diameters still might be criticized because the shape of the left ventricular cavity is not a simple ellipsoid. The ventricular shape is distorted by open chest surgery and by induction of local ischemia. Besides, sensors might not be always embedded at prescribed positions. It has been reported, however, that the linear correlations between the LVV calculated from three ventricular diameters measured by the ultrasonic technique and

that by the other conventional methods, are excellent (11,12). Based on these results, three ventricular diameters were measured in this study.

To calculate local myocardial work, myocardial wall tension-area relation was utilized (10,11). This relation is similar to the left ventricular pressure-volume relation; the area inside the loop gives regional myocardial work.

Regional wall tension (Tw) was calculated from measured left ventricular diameters and pressure using the law of Laplace for thin-layered spherical model (17,18), which is given by:

$$Tw = \frac{r \cdot P}{2}, \quad (3.2)$$

where r is the radius of the sphere and P the internal pressure. The radius r was calculated from measured diameters by a method described in each chapter, and left ventricular pressure was used for P in this study.

Local subendocardial area (Am) is given by a rhombus area surrounded by 2 pairs of ultrasonic sensors embedded in the subendocardium to measure segment lengths in orthogonal directions (LS and SS), and is calculated by:

$$Am = \frac{LS \cdot SS}{2}, \quad (3.3)$$

These measured parameters were fed into a mini-computer system and bulk and regional stroke work done were calculated using an algorithm shown in APPENDIX A.1. Then, the bulk and regional stroke work were normalized by left ventricular weight and regional myocardial volume, respectively, and, then, they were normalized by the heart rate to obtain each average work per second.

#### REFERENCES

1. Abel FL, McCutcheon EP. *Cardiocascular function: principles and applications*. Little, Brown & Co. 1979.
2. Guyton AC. *Textbook of medical physiology* (5th ed). W.B. Saunders Co./ Igaku Shoin 1976.
3. Siegel JH, Sonnenblick EH. Quantification and prediction of myocardial failure. *Arch Surg* 1964; 89: 1026-36.
4. Weisfeldt ML, Scully HE, Frederiksen J, Rubenstein JJ, Pohost GM, Beierholm E, Bello AG, Daggett WM. Hemodynamic determinants of maximum negative dP/dt and periods of diastole. *Am J Physiol* 1974; 227: 613-21.
5. Weiss JL, Frederiksen JW, Weisfeldt ML. Hemodynamic determinants of the time-course of fall in canine left ventricular pressure. *J Clin Invest* 1976; 58: 751-60.
6. Frederiksen JW, Weiss JL, Weisfeldt ML. Time constant of isovolumic pressure fall: determinants in the working left ventricle. *Am J Physiol* 1978; 235: H701-6.
7. Karliner JS, Gault JH, Eckberg D, Mullins CB, Ross J Jr. Mean velocity of fiber shortening: a simplified measure of left ventricular myocardial contractility. *Circulation* 1971; 44: 323-33.
8. Suga H, Sagawa K, Shoukas AA. Load independence of the instantaneous pressure-volume ratio of the canine left ventricle and effects of epinephrine and heart rate on the ratio. *Circ Res* 1973; 32: 314-22.
9. Suga H. Cardiac mechanics and energetics. *J Physiol Soc Jpn* 1982; 44: 89-98.
10. Sugawara M, Tamiya K, Nakano K. Regional work of the ventricle: wall tension-area relation. *Heart and Vessels* 1985; 1: 133-44.

11. Goto Y, Suga H, Yamada O, Igarashi Y, saito M, Hiramori K. Left ventricular regional work from wall tension-area loop in canine heart. Am J Physiol 1986; 250: H151-8.
12. Little WC, Freeman GL, O'Rourke RA. Simultaneous determination of left ventricular end-systolic pressure-volume and pressure-dimension relationships in closed-chest dogs. Circulation 1985; 71: 1301-8.
13. Lew WYW, LeWinter MM. Regional comparison of midwall segment and area shortening in the canine left ventricle. Circ Res 1986; 58: 678-91.
14. Matre K, Hexeberg E, Lekven J. Interpretation of myocardial contraction recorded from local segments. Cardiovasc Res 1985; 19: 193-200.
15. Suga H. Total mechanical energy of a ventricle model and cardiac oxygen consumption. Am J Physiol 1979; 236: H498-505.
16. Rushmer RF, Franklin DL, Ellis RM. Left ventricular dimensions recorded by sonocardiometry. Circ Res 1956; 4: 684-8.
17. Fung YC. Biomechanics: mechanical properties of living tissues. Springer-Verlag 1981.
18. Caro CG, Pedley TJ, Schroter RC, Seed WA. The mechanics of the circulation. Oxford University Press 1978.

## CHAPTER IV

### EIGHT-CHANNEL ULTRASONIC DISPLACEMENT METER

#### 4.1 INTRODUCTION

Since the pioneer work of Rushmer et al. (1), a variety of ultrasonic dimension gauges have been developed to measure ventricular diameter (e.g., 1-4), myocardial segment length (e.g., 5), and vascular diameter (e.g., 6-10). In these systems, dimensions are determined from the transit time of an ultrasonic pulse wave between a pair of sensors embedded in biological tissues. Four-channel systems are commercially available for the study of cardiovascular physiology and mechanics, and have been applied to measure the diameter, segment length, and wall thickness of the ventricles. For the detailed study of cardiac mechanics, it is necessary to determine not only the regional myocardial characteristics but also the bulk ventricular behavior. However, very few studies have been reported on the simultaneous measurement of the regional dimensions of cardiac muscle and the ventricular diameter, because of the shortage of channel numbers incorporated in these systems.

In the commercially available four-channel systems, cut-off frequencies of the output low-pass filters (LPFs) are around 100 Hz, pulse repetition frequencies (PRFs) are between 1 and 2 kHz, and maximum measurable distances are designed to be longer than 250 mm for a very wide variety of applications. For the design of a system with more than four channels, the PRF must be lowered, which results in worse

resolution. Although the resolution would be improved if the cut-off frequency of the output signal is decreased, the frequency response might be slower. However, if we design a system with a shorter measurable distance than 250 mm, we can increase the channel number without reduction in the resolution. For the measurement of ventricular dimensions, it is sufficient to be able to determine the distance up to 100 mm because the longest dimension (long axis diameter) in the ventricle is estimated to be less than 100 mm in animals weighing up to several tens of kilograms.

Considering these factors, an ultrasonic displacement meter for eight pairs of implantable miniature sensors was designed. This chapter deals with the design specifications, resolution, and performance of the system.

## 4.2 SYSTEM DESIGN

As the ultrasonic pulse propagates at a speed of around 1.5 mm/ $\mu$ s in biological soft tissues (11), the distance between a pair of miniature sensors can be calculated from the pulse transit time. Fig. 4.1 shows the block diagram of the newly designed displacement meter. One of the paired sensors is driven by the pulse train generated by each driver. The RPF and pulse-halfwidth are 1.95 kHz and 0.5  $\mu$ s, respectively. The amplitude of the driving pulse is manually adjustable between 60 and 110 V according to the measuring distance and the ringing characteristics of each sensor. The RPF was determined to be low enough for the measurement of ventricular diameter (12). To generate the pulse train, a source frequency of 1 MHz is divided by the frequency divider consisting of a nine-stage binary counter. The cyclic period of the ultrasonic pulses (512  $\mu$ s) is divided into successive 64  $\mu$ s periods by a decoder for the eight-channel operation. Each divided period corresponds to the maximum measurable distance (96 mm) in the system.

The pulse wave emitted by one of a pair of sensors is received by the other after the transit time which is proportional to the distance between two sensors has elapsed. A miniature pre-amplifier, which is a source follower circuit consisting of a field-effect transistor, was inserted in the cable near the receiving sensor to decrease the line impedance, to suppress the signal attenuation and to improve the signal-to-noise ratio. By virtue of the pre-amplifier, the RF signals were attenuated by only 3 dB in a 5 m cable, whereas the length of the cable was limited to only 2 m without the pre-amplifier.

After being amplified by an RF amplifier (45 dB), the pulse train of the received signal is detected by a voltage comparator. The

threshold level for the detection is manually adjustable according to the amplitude of the received RF signal.

The function of the comparator is inhibited by two gating signals. One of these signals is generated from a monostable multivibrator which is triggered at the time of emission of ultrasonic pulses. This signal gates a large noise component which is mixed with the received signals by the capacitive coupling between a pair of sensors when the ultrasonic pulse is emitted. The duration of the noise is dependent on the amplitude and waveform of the driving pulse and the ringing and coupling characteristics of the sensors. In addition to this noise component, various other noises are mixed with the signal component in the case of long distance measurement. The gating duration should be set longer than the duration of these noise components. In this system, the pulse width generated by the multivibrator, i.e. the gating duration, is manually adjustable in the range 1-47  $\mu$ s which corresponds to the distance range 1.5-70.5 mm. The minimum measurable distance in this system is determined by the minimum gating duration.

The other gating signal is generated from a flip-flop circuit. Once the pulse train in the received signal is detected by the voltage comparator, the flip-flop is set to inhibit the function of the comparator to improve the signal-to-noise ratio. It is reset when the next ultrasonic pulse is emitted.

Transit time of the pulse wave is modulated into a pulse width by another flip-flop circuit. The pulse-width modulator (PWM) is set when the ultrasonic pulse is emitted and is reset when the received pulse train is detected. This pulse-width-modulated signal is then converted into a voltage signal by an LPF which has a cut-off frequency of 80 Hz and an attenuation coefficient of -18 dB per octave. The filtered signal

is amplified to an appropriate magnitude by a buffer amplifier.

Two reference signals are generated for the calibration of distance from the same frequency divider (counter) as used for the emission of the PRF signal. The outputs of the fourth (62.5 kHz) and fifth (31.25 kHz) stages of the counter are used as the calibration signals for 24 and 48 mm, respectively. These signals are also fed into the PWM.

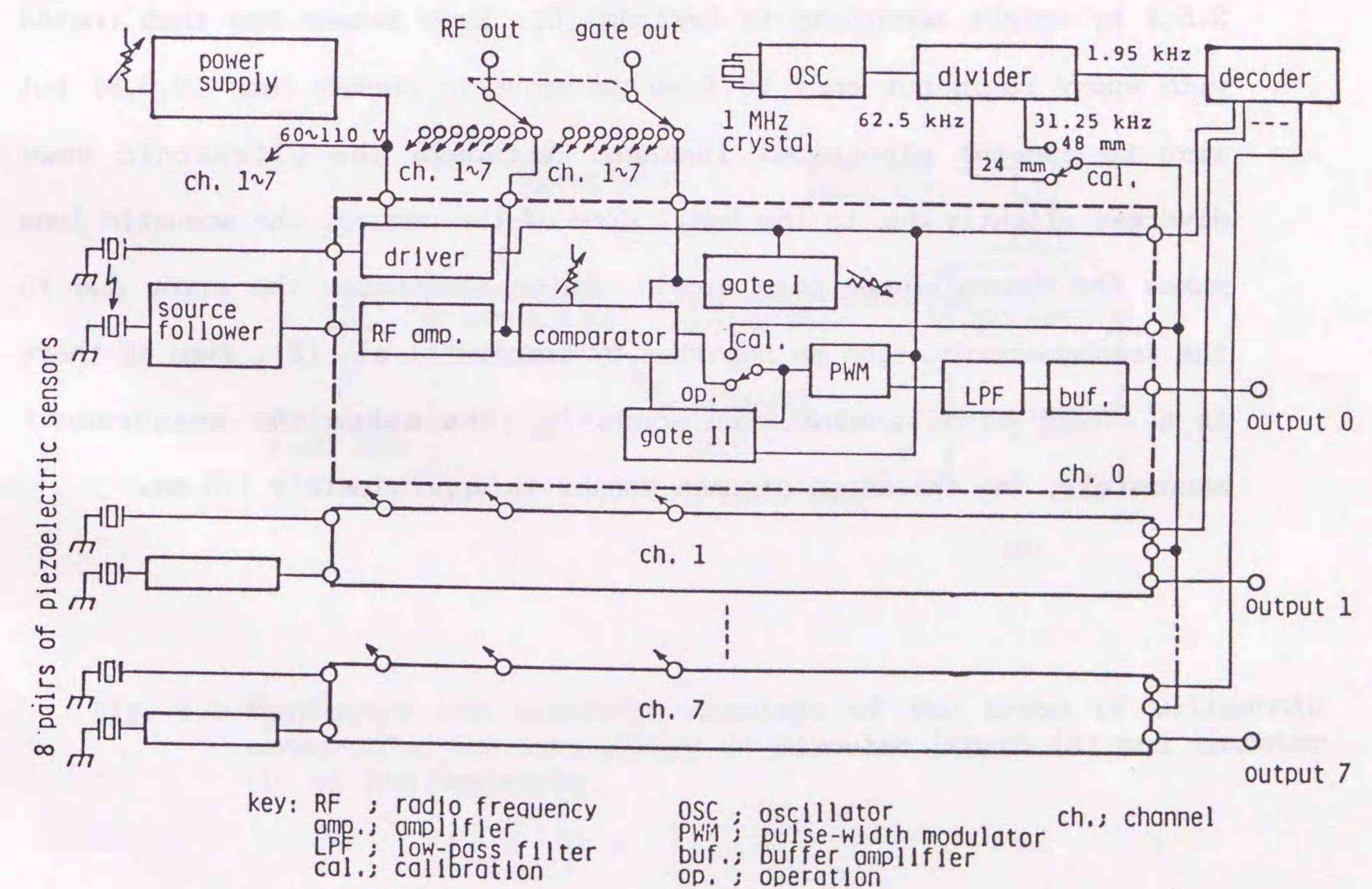


Fig. 4.1 Eight-channel ultrasonic displacement meter.

#### 4.3 SENSOR DESIGN

Figure 4.2 shows two types of sensors used for the measurements of (a) myocardial segment length and (b) ventricular diameter. A pair of sensors of each type is used for the measurement of these dimensions.

Each sensor was made of a disk of 2 mm diameter cut from a 5 MHz lead zirconate titanate ceramic plate (Piezotite, Murata, Kyoto, Japan). The electrical wires were attached perpendicularly to the disk surface for the measurement of ventricular diameter and parallel to it for the muscular length. After a pair of fine electrical wires made of stainless steel were bonded to the disk, tungsten-loaded epoxy foils were attached to both surfaces of the disk to reduce the reflection of ultrasonic pulses. The ratio of tungsten powder to epoxy resin of the foil was 3.5:1 by weight according to Bertram (6). Each sensor was then coated with epoxy resin not only to form an acoustic convex lens (2,5,8) but also to prevent electrical leakage. Although the ultrasonic beam diverges slightly due to the small size of the sensor, the acoustic lens makes the beam diverge more widely, which eliminates the error due to the transducer rotation as reported by Tomoike et al. (8). Even if there is a sensor misalignment, the acoustic lens makes the measurement accurately. The thickness of each sensor is approximately 1.5 mm.

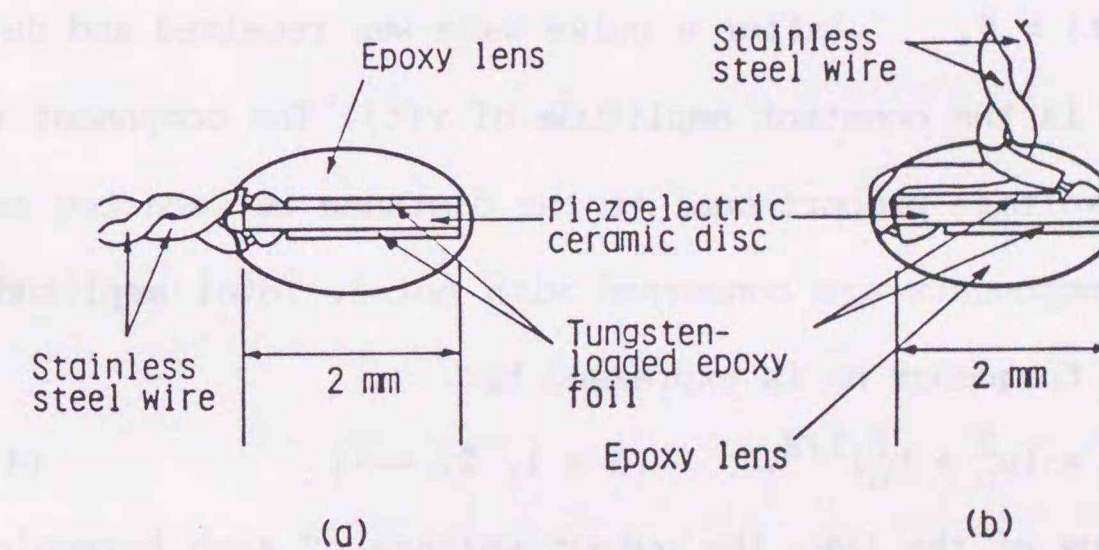
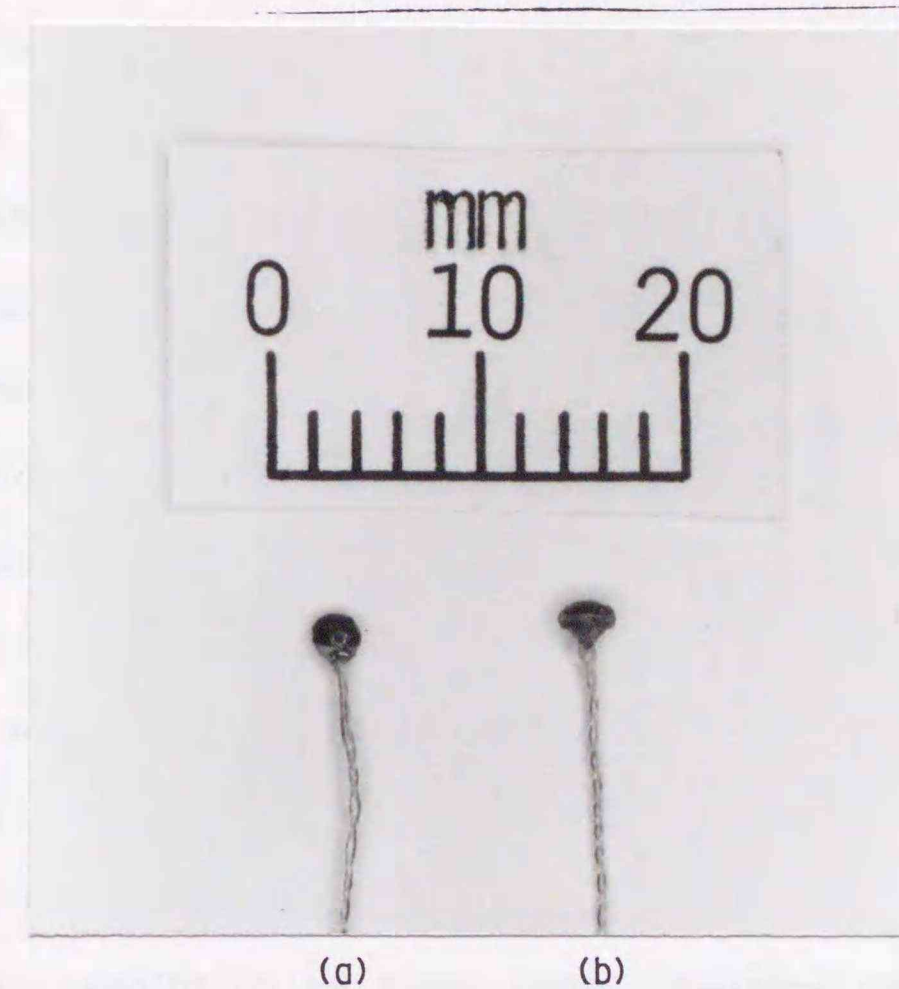


Fig. 4.2 Photograph and schematic drawings of two types of ultrasonic sensors for the measurement of muscular length (a) and diameter (b) of the ventricle.

#### 4.4 RESOLUTION

Pulse width-modulated signal,  $v(t)$ , in a cyclic period ( $T$ ) is expressed by Fourier spectra as follows:

$$v(t) = a_0 + \sum_n (a_n \sin(n\omega t) + b_n \cos(n\omega t)), \quad (4.1)$$

where

$$\omega = 2\pi/T,$$

$$a_0 = (1/T) \int_0^T v(t) dt,$$

$$a_n = (2/T) \int_0^T v(t) \cdot \sin(n\omega t) dt,$$

and

$$b_n = (2/T) \int_0^T v(t) \cdot \cos(n\omega t) dt.$$

In the present system,

$$T = 1/1.95 \text{ (ms)},$$

$$v(t) = E, \quad (\text{until a pulse wave is received and detected})$$

and

$$v(t) = 0, \quad (\text{after a pulse wave was received and detected})$$

where  $E$  is the constant amplitude of  $v(t)$ . The component  $a_0$  corresponds to the voltage proportional to the distance between two sensors and the other components are concerned with noise. Total amplitude ( $A_n$ ) of the angular frequency  $n\omega$  is expressed by:

$$A_n = (a_n^2 + b_n^2)^{1/2}. \quad (n = 1, 2, \dots) \quad (4.2)$$

By virtue of the LPF, the output voltage of each harmonic component is negligibly small compared with that of the  $A_1$  component in this system.

Thus the static resolution depends mainly upon the  $A_1$  component and the minimal resolution is obtained when  $A_1$  is maximum.  $A_1$  is maximum when the pulse wave is detected at  $64 \mu\text{s}$  ( $T/8$ ) after the pulse emission, that is, when the maximum measurable distance is measured, and the maximum value is  $0.244E$ . Being attenuated 80 dB by the LPF, the peak-to-peak

voltage of the maximum  $A_1$  ( $0.488E$ ) is reduced to  $2.45 \times 10^{-5}E$ . Since the voltage of  $E/8$  corresponds to the distance of 96 mm, this attenuated voltage is equivalent to the distance of  $18.8 \mu\text{m}$ , which is the static resolution of the system.

Dynamic resolution of the system is calculated by dividing the deformation velocity of the left ventricle by the PRF. If we assume that the left ventricular diameter changes 10 mm for the period of 0.15 s at the heart rate of 120 bpm and that the maximum deformation velocity is five times as much as the average velocity in this period (333 mm/s), the resolution is about  $170 \mu\text{m}$ . If the muscular length of ventricular wall changes 2 mm under the same condition, the resolution is about 34  $\mu\text{m}$ . The dynamic resolution in these cases is 1.7 % of the reference dimension.

Specifications of the system are summarized in Table IV.I.

TABLE IV.I Specification of the system.

Channel number	= 8
Pulse repetition frequency	= 1.95 kHz
Driving pulse amplitude	= 60 to 110 V
Driving pulse duration	= 0.5 $\mu$ s
Output low-pass filter	
Cut-off frequency	= 80 Hz
Attenuation coefficient	= -18 dB per octave
Measurable distance	= 1.5 to 96 mm
Calibration distance	= 24 and 48 mm
Static resolution	= 18.8 $\mu$ m
Dynamic resolution	= 1.7 %
	of the reference dimension
Dimensions of sensor	
Diameter	= 2 mm
Thickness	= 1.5 mm

#### 4.5 IN VIVO PERFORMANCE TEST

After the linearity between the distance between a pair of sensors and the output voltage of the system had been confirmed ( $r = 1.000$ ) by an in vitro calibration test, this system was applied to measure eight dimensions in the left ventricle (LV) of a mongrel dog. As shown in Fig. 4.3 three pairs of sensors were inserted into LV cavity and attached to the endocardium to measure a long axis diameter and two short axis diameters parallel and perpendicular to the septum. Four pairs of sensors were embedded in the subendocardium of the LV free wall. Two pairs were implanted in the central region of the free wall and the other two were positioned in the distributing area of the left anterior descending coronary artery (LAD). Two pairs in each location were oriented so as to measure the muscular length in the orthogonal (equatorial and meridian) direction. The remaining pair of sensors was used to measure the wall thickness in the central region of the free wall. The aortic pressure was changed from 110 mmHg to 108 mmHg by the implantation of these sensors. At the same time, the left atrial pressure and aortic blood flow became 13 mmHg and 2.5 l/min, respectively, from 10 mmHg and 2.3 l/min. Ischaemia was induced by the LAD ligation at the proximal position to the first diagonal branch.

All data were acquired by a data recorder (XR-510, Teac, Tokyo, Japan) and then analyzed off-line by a mini-computer system (PDP-11/44, DEC, Maynard, Massachusetts, U.S.A.). Fig. 4.4 shows an example of the computer output of phasic tracing of the hemodynamic and dimensional data obtained after the LAD ligation. Waveforms of the dimensional data were magnified by the computer. The ventricular diameters (LD, SDn and SDp) and segment lengths (LSn and SSn) in normal area changed out of

phase by around  $90^\circ$  compared with the change in the left ventricular pressure. The meridian segment length (LSi) in the ischemic area did not change so much. The change of the equatorial segment length in the ischemic area (SSi) was shifted by around  $180^\circ$  phase compared with that in the normal area (SSn). The change in the wall thickness (WT) was out of phase by around  $180^\circ$  from the change of segment length in the normal area.

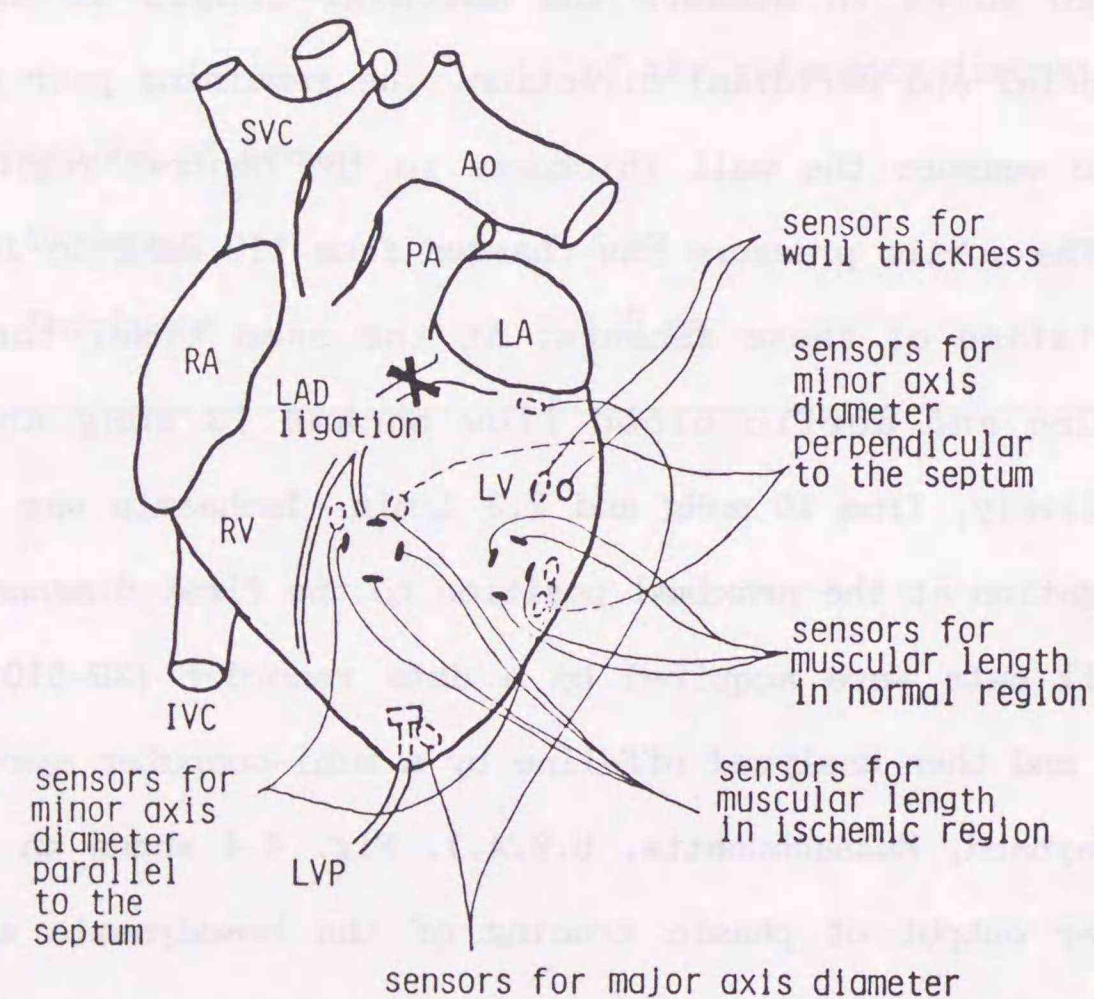


Fig. 4.3 Experimental arrangement. Ao, aorta; IVC, inferior vena cava; LA, left atrium; LAD, left anterior descending coronary artery; LV, left ventricle; LVP, LV pressure; PA, pulmonary artery; RA, right atrium; RV, right ventricle; SVC, superior vena cava.

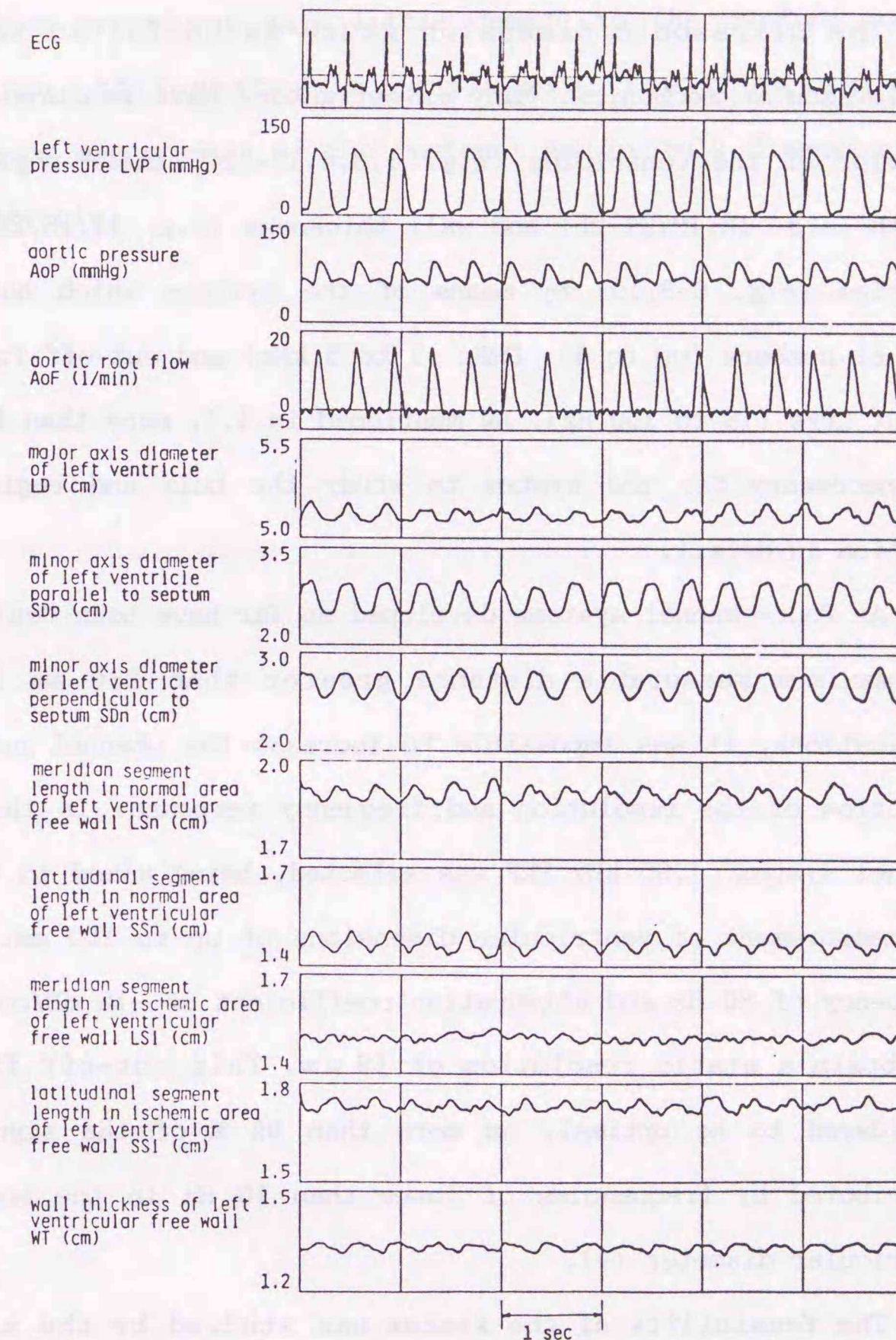


Fig. 4.4 Phasic tracings of hemodynamic and dimensional data after ligation of the left anterior descending coronary artery.

#### 4.6 DISCUSSION

The ultrasonic dimension gauge is useful in the study of cardiovascular mechanics. Many investigators have measured the dynamic behavior of the ventricles (e.g. 1,3,4,13-21), their regional segment length (e.g. 18,19,21-25) and wall thickness (e.g. 14,18,20,23-28), and arteries (e.g. 6-8,10) by means of the systems which have different channel numbers (up to 4), PRFs (1 to 5 kHz) and cut-off frequencies of output LPFs (16 to 150 Hz). As mentioned in 4.1, more than four channels are necessary for the system to study the bulk and regional cardiac function in detail.

As four-channel systems developed so far have been designed to have the maximum measurable distance greater than 250 mm for various applications, it was impossible to increase the channel number without reduction of the resolution and frequency response. In the present 8-channel system, 1.95 kHz PRF was selected, being aimed to apply it for the measurement of ventricular dimensions of up to 100 mm. The cut-off frequency of 80 Hz and attenuation coefficient of -18 dB/oct was chosen to obtain a static resolution of 19  $\mu$ m. This cut-off frequency is considered to be optimal, as more than 99 % of the signal power is contributed by frequencies of lower than 10 Hz in the measurement of ventricular diameter (4).

The feasibility of the system was studied by the simultaneous eight-channel measurement of ventricular dimensions in a canine heart. By the pre-amplifiers inserted in the cables, the received signals could be transferred more than 5 m without large attenuation even in the measurement of the long axis diameter of the ventricle. Changes in the ventricular diameter, myocardial length and wall thickness were

reasonable, as shown in Fig. 4.4. The hemodynamic data were not changed much by the implantation of sensors, which indicates that the implantation procedures gave little damage to the cardiac muscle. In conclusion, this system is very useful for the eight-channel simultaneous measurement of the regional and/or bulk dimensions of the left ventricle.

#### 4.7 SUMMARY

For the study of bulk and regional mechanical behavior of the ventricle, an eight-channel ultrasonic displacement meter for implantable miniature sensors was developed to measure ventricular dimensions and myocardial segment lengths.

The distance between a pair of sensors is measured by the transit-time technique of ultrasonic pulse wave. The pulse repetition frequency (PRF) is 1.95 kHz and pulse interval (512  $\mu$ s) is divided for eight-channel operation. Measurable distance is between 1.5 and 96 mm. The theoretical static resolution calculated from the PRF and the cut-off characteristics of the output low-pass filter (80Hz and -18 dB/oct) was 19  $\mu$ m. The dynamic resolution calculated from the PRF and the deformation velocity was 1.7 % of the reference dimension.

Preliminary in vivo tests showed that the system is useful to measure the segment length, wall thickness, and diameter of the left ventricle.

#### REFERENCES

1. Rushmer RF, Franklin DL, Ellis RM. Left ventricular dimensions recorded by sonocardiometry. *Circ Res* 1956; 4: 684-8.
2. Stegall HF, Kardon MB, Stone HL, Bishop VS. A portable, simple sonomicrometer. *J Appl Physiol* 1967; 23: 289-93.
3. Patrick TA, Vatner SF, Kemper WS, Franklin D. Telemetry of left ventricular diameter and pressure measurements from unrestrained animals. *J Appl Physiol* 1974; 37: 276-81.
4. Stinson EB, Rahmoeller G, Tecklenberg PL. Measurement of internal left ventricular diameter by a tracking sonomicrometer. *Cardiovasc Res* 1974; 8: 283-9.
5. Goodman CA, Castellana FS. A digital sonomicrometer for two-point length and velocity measurements. *Am J Physiol* 1982; 243: H634-9.
6. Bertram CD. Ultrasonic transit-time system for arterial diameter measurement. *Med & Biol Eng & Comput* 1977; 15: 489-99.
7. Sia JB, Pace DG, Osborne MW, Zanko MT, Kovzelove F. An improved signal processor for the ultrasonic dimension gauge. *Cardiovasc Res* 1980; 14: 490-4.
8. Tomoike H, Ootsubo H, Sakai K, Kikuchi Y, Nakamura M. Continuous measurement of coronary artery diameter in situ. *Am J Physiol* 1981; 240: H73-9.
9. Nakamura T, Hayashi K, Taenaka Y, Umezu M, Nakatani T, Takano H. Ultrasonic flowmeter for implantable miniature sensors. *Med & Biol Eng & Comput* 1986; 24: 235-42.
10. Drews TA, Lamping KG, Laighlin DE, Dole WP. Digital sonomicrometer system for measuring small vascular diameter in situ. *Med & Biol Eng & Comput* 1987; 25: 420-7.

11. Wells PNT. Biomedical Ultrasonics. Academic Press, 1977.
12. Nakamura T, Hayashi K, Seki J, Nakatani T, Noda H, Fukuda S, Takano H, Akutsu T. Eight-channel ultrasonic displacement meter for the measurement of myocardial dimensions during cardiac assist. Proc IEEE 1985 Ultrasonics Symp, San Francisco, 1986: 860-3.
13. Horwitz LD, Bishop VS, Stone HL, Stegall HF. Continuous measurement of internal left ventricular diameter. J Appl Physiol 1968; 24: 738-40.
14. Rankin JS, McHale PA, Arentzen CE, Ling D, Greenfield JC Jr, Anderson RW. The three-dimensional dynamic geometry of the left ventricle in the conscious dog. Circ Res 1976; 39: 304-13.
15. Sodums MT, Badke FR, Starling MR, Little WC, O'Rourke RA. Evaluation of left ventricular contractile performance utilizing end-systolic pressure-volume relationship in conscious dogs. Circ Res 1984; 54: 731-9.
16. McRitchie RJ, Blood R, Chalmers JP. Measurement of myocardial contractility in conscious rabbits. Am J Physiol 1984; 246: H293-5.
17. Little WC, Badke FR, O'Rourke RA. Effect of right ventricular pressure on the end-diastolic left ventricular pressure-volume relationship before and after chronic right ventricular pressure overload in dogs without pericardia. Circ Res 1984; 54: 719-30.
18. Lee JD, Sasayama S, Kihara Y, Ohyagi A, Fujisawa A, Yui Y, Kawai C. Adaptations of the left ventricle to chronic volume overload induced by mitral regurgitation in conscious dogs. Heart & Vessels 1985; 1: 9-15.
19. Kaseda S, Tomoike H, Ogata I, Nakamura M. End-systolic pressure-volume, pressure-length, and stress-strain relations in canine

- hearts. Am J Physiol 1985; 249: H648-54.
20. Crozatier B, Bacal O, Belot J-P, Caillet D. End-systolic left ventricular pressure-dimension shift during acute relief of volume overload in the conscious dog. Am J Cardiol 1985; 55: 1102-6.
21. Nakamura T, Hayashi K, Seki J, Nakatani T, Noda H, Fukuda S, Takano H, Akutsu T. Bulk and regional mechanical work of ischemic heart during left ventricular assistance. In: Progress in Artif Organs-1985, ISAO Press, 1986: 447-51.
22. Heyndrickx GR, Millard RW, McRitchie RJ, Maroko PR, Vatner SF. Regional myocardial functional and electrophysiological alterations after brief coronary artery occlusion in conscious dogs. J Clinical Invest 1975; 56: 978-85.
23. Sabbah HM, Marzilli M, Stein PD. The relative role of subendocardium and subepicardium in left ventricular mechanics. Am J Physiol 1981; 240: H920-6.
24. Oguma M, Tuiki K, Kaminishi T, Ohta I, Yasui S. Hyperkinetic contraction of a nonischemic segment of ischemic left ventricle in anesthetized dogs. Heart & Vessels 1985; 1: 145-51.
25. Theroux P, Ross J Jr, Franklin D, Kemper WS, Sasayama S. Regional myocardial function in the conscious dog during acute coronary occlusion and responses to morphine, propranolol, nitroglycerin, and lidocaine. Circulation 1987; 53: 302-14.
26. Gallagher KP, Kumada T, Koziol JA, McKnown MD, Kemper WS, Ross J Jr. Significance of regional wall thickening abnormalities relative to transmural myocardial perfusion in anesthetized dogs. Circulation 1980; 62: 1266-74.
27. Gallagher KP, Matsuzaki M, Osakada G, Kemper WS, Ross J Jr. Effect of exercise on the relationship between myocardial blood flow and

systolic wall thickening in dogs with acute coronary stenosis. Circ Res 1983; 52: 716-29.

28. Sabbah HN, Stein PD. Relation of intramyocardial and intracavitary pressure to regional myocardial asynergy in the canine left ventricle. Am Heart J 1983; 105: 380-6.

## CHAPTER V

### EFFECT OF DRIVE MODE OF LEFT VENTRICULAR ASSIST DEVICE

#### 5.1 INTRODUCTION

One of the important subjects to be studied is on the most effective drive mode of LVAD for the recovery of the left ventricle. Whether the synchronized drive with electrocardiogram (ECG) is essential and effective for reduction of the left ventricular work rather than the asynchronous pumping has not been documented well.

Although there are many reports on the bulk behavior of the left ventricle and the hemodynamics in the systemic circulation during cardiac assist (1-3), regional myocardial mechanics and bulk ventricular mechanics have not been studied well even in acute experiments on the normal heart. The regional mechanics of the myocardium is particularly important because the myocardial infarction often occurs locally.

This chapter primarily deals with influences of LVAD pumping modes on the bulk and regional cardiac mechanics. In order to find the best driving method of LVAD for the minimal left ventricular work with the acceptable systemic circulation and coronary blood flow, left ventricular dimensions and hemodynamic parameters were measured simultaneously during the LVAD pumping in various synchronous and asynchronous drive modes.

## 5.2 METHOD

### 5.2.1 Experimental Protocol

Seven mongrel dogs of both sexes weighing 15-27 kg (20 kg average) were anesthetized by the intravenous injection of pentobarbital sodium (25 mg/(kg body weight)), and maintained by the intermittent administration of this dose throughout the experiments. They were ventilated with room air and oxygen by a respirator (Mark-7, Bird, Palm Springs, California, U.S.A.). Left thoracotomy was performed at the 5th intercostal space, and the pericardium was widely open. Pneumatically driven, diaphragm-type LVAD pumps having a stroke volume of 40 ml (4) were implanted between the left atria and the descending aortae, as shown in Fig. 5.1. Newly designed tri-leaflet valves made of segmented polyether polyurethane (TM5, Toyobo, Osaka, Japan) (5) were used for the pump inflow and outflow (6). The diaphragm was made of the same polyurethane and was fabricated so as to be stable at the end-diastolic position.

Miniature ultrasonic sensors were embedded in the left ventricle while the LVAD was being pumped at the rate of 60 bpm with the systolic duration of 30 % to maintain the systemic circulation under good conditions. Three pairs of sensors were attached to the endocardium of the left ventricle for the measurements of a long-axis inner diameter (LD) and two short-axis inner diameters parallel and perpendicular to the septum (SDp and SDn, respectively) by the technique used by Goto et al. (7). Briefly, these sensors were inserted from the epicardium through small stab wounds and penetrated the myocardium. The sensors were then pulled back until they attached to the endocardium, and were

fixed by suturing their electrical wires to the epicardium. It took 3-8 min to attach a pair of sensors.

Two pairs of ultrasonic sensors were inserted in the same way as the diameter sensors, but embedded in the subendocardial muscle in the central region of the left ventricular free wall for the measurement of muscular length in the orthogonal (equatorial (SS) and meridian (LS)) directions, as shown in Fig. 5.1. The left ventricular diameter and segment length were measured by the eight-channel displacement meter described in CHAPTER IV (8,9).

Left atrial pressure (LAP) and aortic pressure (AoP) were monitored with fluid-filled catheter-type pressure transducers (P50, Gould, Oxnard, California, U.S.A.). Left ventricular pressure (LVP) was measured with an implantable wire strain gauge-type transducer (P6.5, Konigsberg, Pasadena, California, U.S.A.) to avoid the distortion and phase delay of the LVP signals. These transducers were calibrated prior to the experiments by measuring the pressure simultaneously with a mercury manometer.

Ascending aortic blood flow (AoFd) and pump bypass flow (BFd) were measured with electromagnetic flowmeters (MFV-2100 and -1100, Nihonkohden, Tokyo, Japan). A cuff-type and a cannulation-type probes were used to measure the AoFd and BFd, respectively. The AoFd and BFd were normalized by the animal body weight, which were denoted by AoF and BF, respectively. Total flow (TF) was calculated by adding AoF and BF. Total peripheral resistance was obtained by dividing the mean AoP by TF.

Five drive modes were used to study the mechanical effects of LVAD. In the synchronous modes, the pumps were counterpulsated synchronously with the electrocardiograms (ECGs) at three duty ratios: one pumping in a cardiac cycle (1:1 mode), one pumping in two cycles (2:1 mode), and

one pumping in for cycles (4:1 mode). The delay time of the start of the pump ejection from the R-wave of the ECG signal was adjusted so as to obtain the maximum pump bypass flow in each mode. In the 2:1 and 4:1 modes, the LVAD was held under the filling condition during the cardiac cycles without pumping. In the asynchronous modes, the LVADs were driven at two fixed rates: 60 bpm (I60 mode) and 80 bpm (I80 mode) with the systolic duration of 30 %.

Drive pressure and vacuum were controlled to obtain the maximum flow in each pumping mode (around 250 and -60 mmHg, respectively). Drive modes used in these experiments are summarized in Table V.I. The control data were obtained when the pumping was stopped temporarily, with its diaphragm being held at the end-systolic position.

All the dimensional and hemodynamic data were acquired when they became stable, usually around 30 min after all the sensors and devices were implanted. The first control data were obtained after acquiring the first pumped data arbitrarily selected among the five drive modes. The drive mode was then changed to one of the other four modes, and each series of data was recorded. Then, the third series of pumped data was obtained, followed by the acquisition of the second control data. The drive mode was then changed to one of the remaining two modes, and data were recorded. After the same procedure was taken for last pumping mode, the third series of control data was obtained. Thus, each series of pumping data was obtained before or after acquiring control data, which provides three control data for each animal. Each series of pumping data was recorded 2-5 min after changing the experimental conditions, when they seemed to be stable. Each series of data was acquired on magnetic tapes for around 15 seconds by a data recorder (XR-510, Teac, Tokyo, Japan) and on pen oscillographs (Recti-Horiz 8K23, and Polygraph 361,

NEC San-ei, Tokyo, Japan). It took about 30 min to obtain a series of the data on each animal.

After these experiments, the animals were killed by potassium chloride injection. During autopsies, their hearts were carefully examined to confirm the proper positioning of the ultrasonic sensors and Konigsberg's pressure transducers. Then, their left ventricular weights (LVWs) and the wall thickness (WT) at the position where the ultrasonic sensors for segment length were embedded were measured.

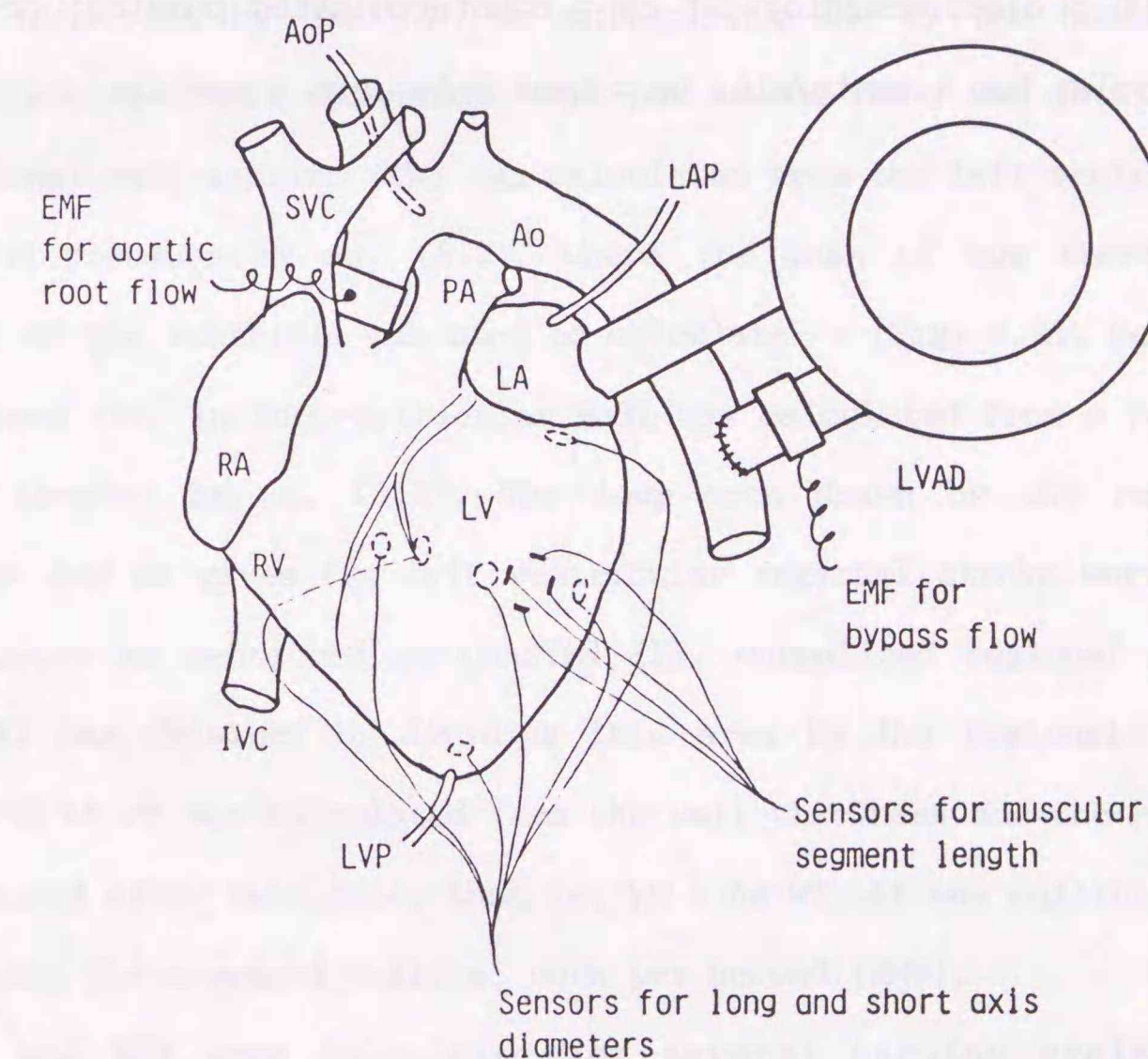


Fig. 5.1 Schematic diagram of the experimental arrangement for the implantation of ultrasonic sensors, hemodynamic transducers, and left ventricular assist device (LVAD). Ao, aorta; AoP, Ao pressure; EMF, electromagnetic flowmeter; IVC, inferior vena cava; LA, left atrium; LAP, LA pressure; LV, left ventricle; LVP, LV pressure; PA, pulmonary artery; RA, right atrium; RV, right ventricle; SVC, superior vena cava.

Table V.I Drive modes used for LVAD pumping.

Mode	Synchronous with ECG			Asynchronous	
	1:1	2:1	4:1	I60	I80
	1 cp	1 cp	1 cp	60 bpm br	80 bpm br
	in 1 cc	in 2 ccs	in 4 ccs	30 % sys	30 % sys

ECG = electrocardiogram; cp = counterpulsated pumping; cc = cardiac cycle; bpm = beats/min; br = beat rate; sys = systole.

### 5.2.2 Data analysis

All data recorded on magnetic tapes were fed off-line into a mini-computer system (PDP-11/44, DEC, Maynard, Massachusetts, U.S.A.) via 12-bit A/D converters at the 333 Hz sampling frequency (3 ms interval). Left ventricular volume (LVV) was calculated from the measured three inner diameters of the ventricular cavity by eq. (3.1).

The loop area of the trajectory of LVP versus LVW drawn in a cardiac cycle gives the left ventricular external stroke work as stated in CHAPTER III. Normalized bulk stroke work (BSW) was calculated by dividing this area by the LVW. By multiplying BSW by the heart rate (HR), the averaged bulk mechanical work per second (BMW) was obtained.

Regional wall tension ( $T_w$ ) was calculated from the left ventricular radius and pressure by eq. (3.2), where the mean of two short axis diameters of the ventricle was used to calculate  $r$  (Fig. 5.2). Regional rhombus area ( $A_m$ ) in the ventricular wall was calculated from a pair of muscular lengths by eq. (3.3). The loop area drawn by the relation between  $T_w$  and  $A_m$  gives the left ventricular regional stroke work in a cardiac cycle as mentioned in CHAPTER III. Normalized regional stroke work (RSW) was obtained by dividing this area by the regional muscle volume (VM) which was calculated from the wall thickness and the rhombus area measured after sacrifice, that is,  $VM = A_m \cdot WT$ . It was multiplied by HR to obtain the averaged regional work per second (RMW).

BSW and RSW were calculated for several cardiac cycles and averaged. For the synchronous pumping modes and the control condition, the data in four cardiac cycles were averaged to obtain the BSW and RSW in each dog. Thus obtained, three control data were averaged and finally used as the control data. In the asynchronous modes, the average was

carried out for four to eight cardiac cycles, according to the cyclic period of the beat frequency determined by the rates of the LVAD pumping and the natural heart.

All data were shown in mean $\pm$ SD. Statistical significance was evaluated by the paired t test, where the significant limit was taken at  $p = 0.05$ .

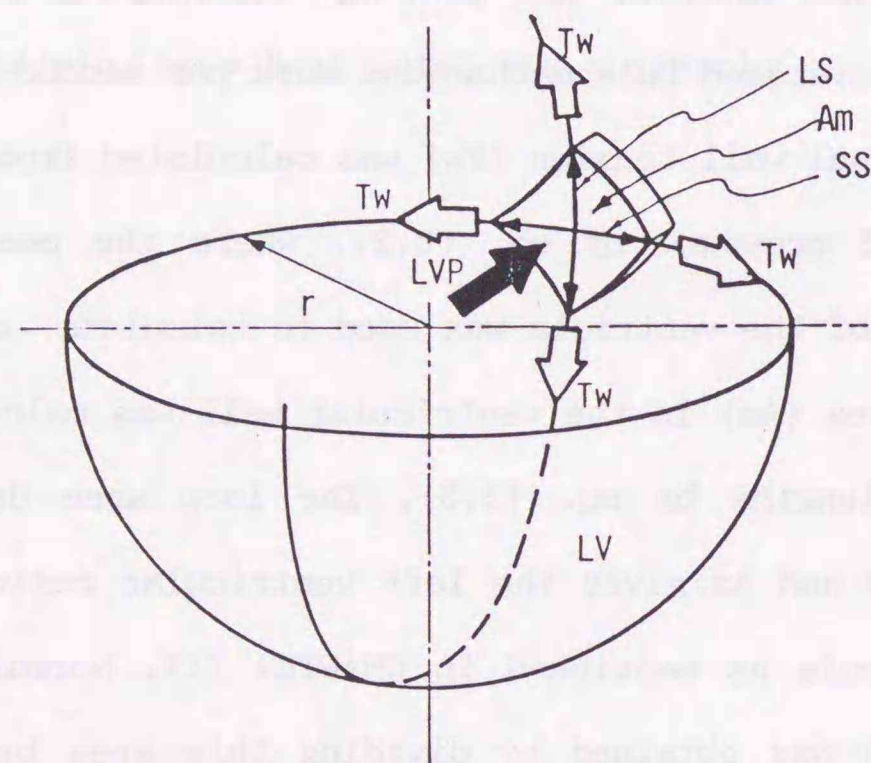


Fig. 5.2 Geometrical expression of regional wall tension ( $T_w$ ) and rhombus area ( $A_m$ ) of the left ventricle (LV). LS, meridian segment length; SS, equatorial segment length; LVP, left ventricular pressure; r, radius.

### 5.3. RESULTS

#### 5.3.1 Hemodynamic effect

An example of the phasic tracings (computer output) of the hemodynamic and dimensional parameters obtained during pumping in five modes and under the non-pumped, control condition are shown in Fig. 5.3.

Figure 5.4 summarizes the hemodynamic data. The heart rate (HR) seemed to be slightly higher under the control condition ( $148\pm 16$  bpm) than during pumping ( $143\pm 17$  to  $148\pm 19$  bpm) although the differences were not statistically significant. The mean AoP (mAoP) in the 1:1 pumping mode ( $97\pm 11$  mmHg) was significantly higher than those in the other modes ( $78\pm 9$  to  $89\pm 10$  mmHg). The mAoP during 4:1- and I60-mode pumping ( $78\pm 9$  and  $86\pm 10$  mmHg, respectively) were significantly lower than that observed under the control condition ( $91\pm 8$  mmHg). These results show that the 1:1 mode is most effective for maintaining the systemic circulation and coronary blood flow; the 4:1 and I60 modes are not preferred.

The variations of the peak LVP (pLVP) among the five modes were almost similar to those of the mAoP. This result might be partly attributed to the fact that the blood was withdrawn from the atrium by the LVAD, and partly to the fact that the LVAD was applied to the normal heart in these experiments. The normal left ventricle is powerful enough to suck the blood from the atrium and to eject it into the aorta even when the LVAD is inserted between the atrium and the aorta. Under the total bypass condition, the effect of LVAD on the pLVP would not be similar to that on the mAoP. All the pLVP except that measured during the 1:1-mode pumping were significantly lower ( $p < 0.01$ ) than the

control value. The pLVP in the 1:1-mode pumping was higher ( $p < 0.01$ ) than those in the other pumping modes. It might be ascribed to much more blood sucking into the left ventricle in the 1:1 mode due to the shortest period of the pump diastole.

The mean LAP (mLAP) under the pumping condition was between  $2 \pm 4$  (I80 mode) and  $3 \pm 3$  mmHg (4:1 mode). It increased significantly up to  $5 \pm 3$  mmHg by stopping the LVAD pumping (the control condition).

The total flow (TF) during the LVAD pumping ( $72 \pm 22$  to  $80 \pm 24$  ml/min/kg) was slightly less than the control value ( $85 \pm 34$  ml/min/kg) except that in the 1:1 mode ( $86 \pm 26$  ml/min/kg). However, the differences between them were not statistically significant, with only one exception observed between the 4:1 mode ( $72 \pm 22$  ml/min/kg) and the control condition. The bypass flow (BF) in the asynchronous modes ( $69 \pm 19$  and  $69 \pm 22$  ml/min/kg) were greater than those in the synchronous modes ( $32 \pm 14$  to  $61 \pm 24$  ml/min/kg). The BF during 2:1-mode pumping ( $61 \pm 24$  ml/min/kg) was highest in the synchronous modes. The averaged stroke volume of the natural heart under the control condition was calculated by dividing AoF by HR and was around 12 ml, which was large enough compared with the pump stroke volume (40 ml).

The total peripheral resistance under the pumping condition was between  $9.1 \times 10^4 \pm 2.3 \times 10^4$  (4:1 mode) and  $9.8 \times 10^4 \pm 3.5 \times 10^4$  dyn  $\cdot$  s  $\cdot$  cm $^{-5}$   $\cdot$  kg (I80 mode). It was not changed by stopping the pumping ( $9.5 \times 10^4 \pm 3.3 \times 10^4$  dyn  $\cdot$  s  $\cdot$  cm $^{-5}$   $\cdot$  kg).

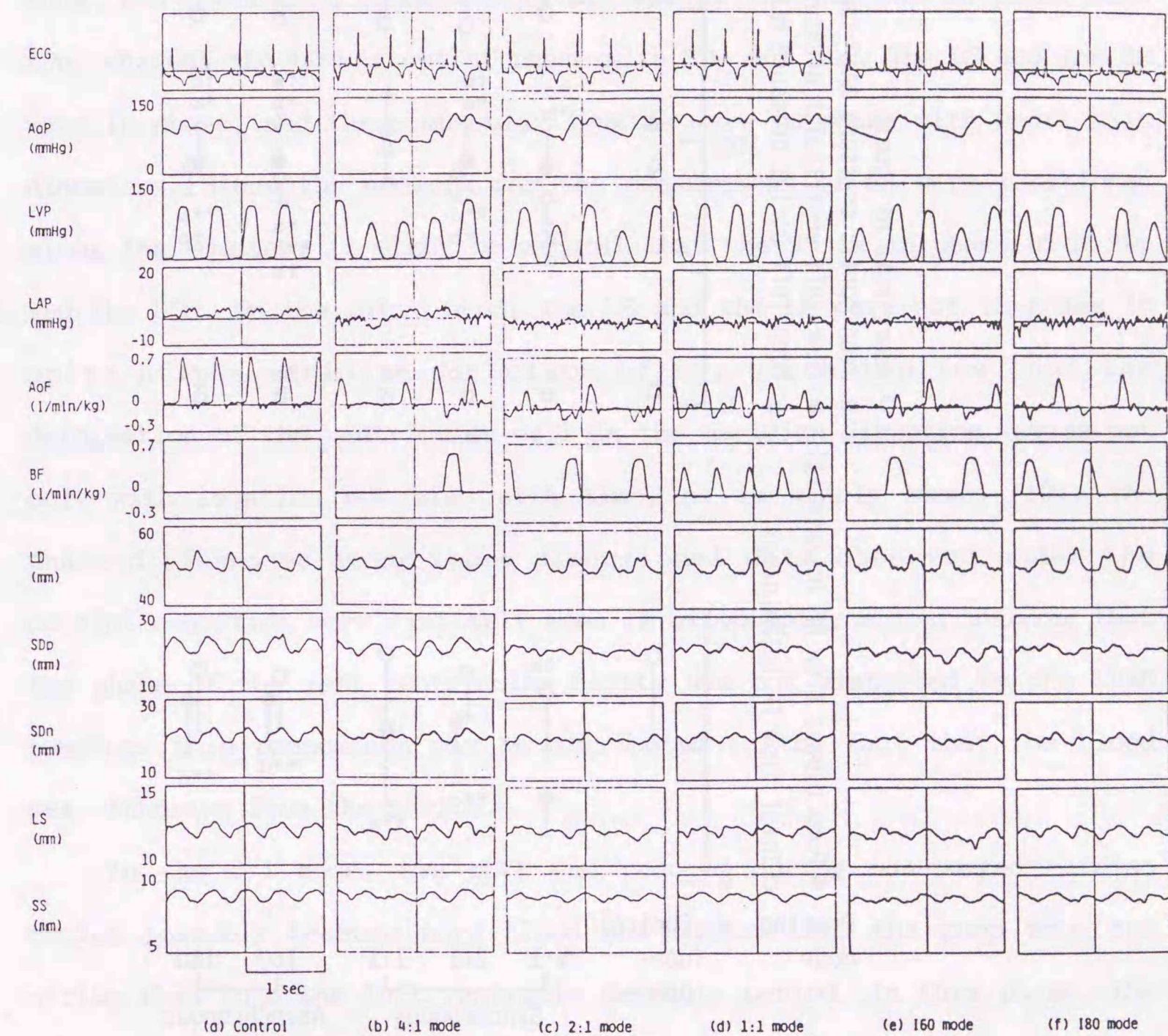


Fig. 5.3 Phasic tracings (computer output) of electrocardiogram (ECG), aortic pressure (AoP), left ventricular pressure (LVP), left atrial pressure (LAP), aortic root flow (AoF), pump bypass flow (BF), long-axis diameter of the left ventricle (LD), short-axis diameter parallel (SDp) and perpendicular (SDn) to the septum, meridian (LS) and equatorial (SS) segment length of the left ventricular free wall.

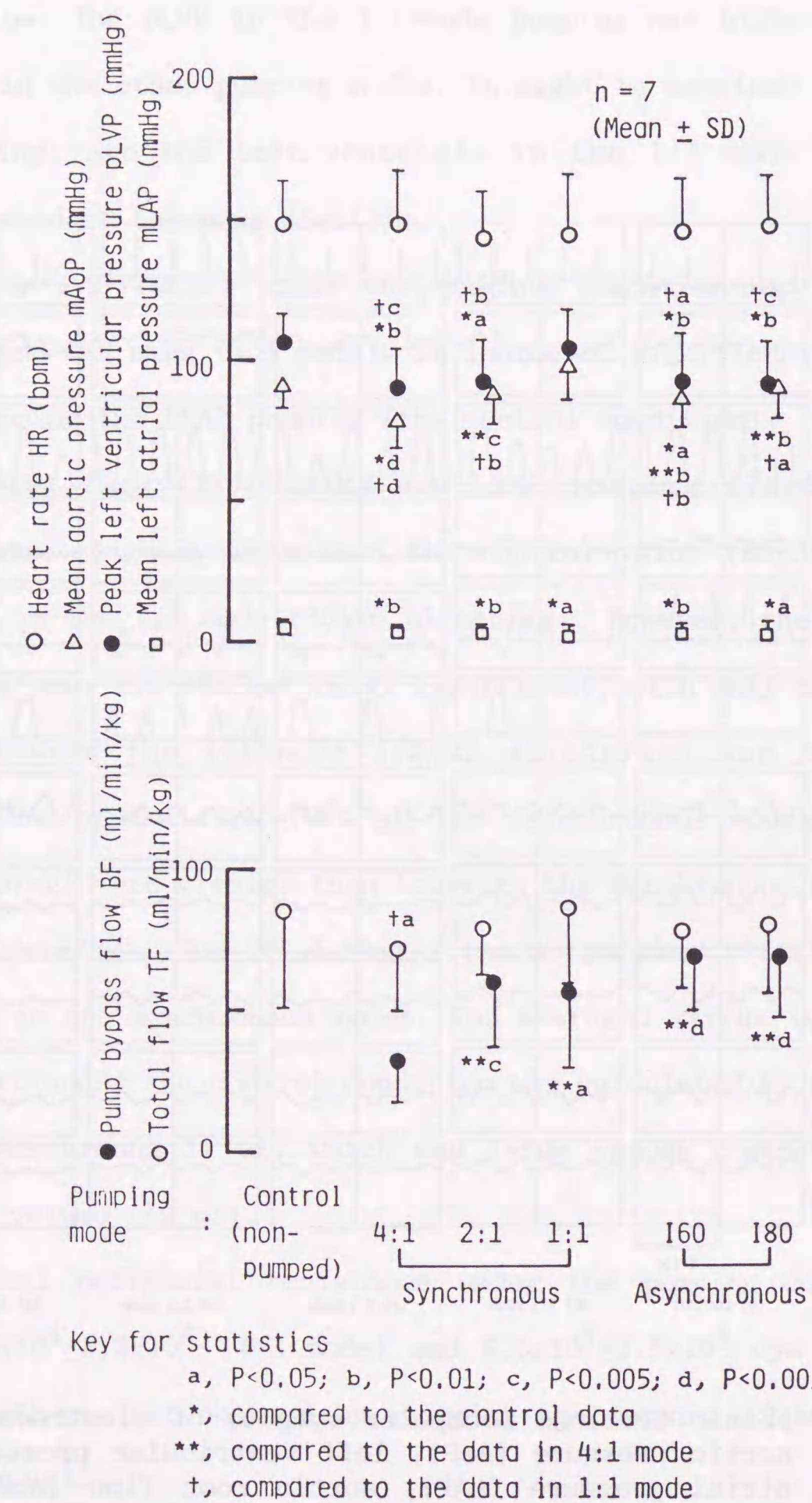


Fig. 5.4 Hemodynamic effects of LVAD pumping with various synchronous and asynchronous modes.

### 5.3.2 Mechanical effect

As shown in Fig. 5.3, large phase shifts were observed between the long- and short-axis diameters in all cases. The SDp was in phase with SDn, whereas the LD was out of phase with SDp and SDn. The LS and the SS were in phase, and these muscular lengths were in phase with short axis diameters. Since the sensors for the measurement of SS were positioned along the equator, it might be natural that the SS is in phase with SDp and the SDn. On the other hand, the LS and the LD were not in phase in spite of the meridian direction of LS, which implies that the deformation of the ventricular wall in the meridian direction varies not only with location but also with time, as is widely known (10). The phase differences among these dimensional data observed under the control condition were similarly seen in all pumping modes, showing that the shape of the left ventricular cavity was not distorted by the LVAD pumping. This phenomenon may be attributed to the fact that the blood was withdrawn from the atrium.

In the 2:1 mode, the pLVP was reduced during non-pumped cardiac cycles possibly because more blood was sucked into the pump from the atrium than into the left ventricle for this period. In this phase, the natural left ventricle frequently could not eject much blood and did very little mechanical work, as will be described later. In the cardiac cycle with the LVAD pumping, the blood is mainly sucked into the left ventricle, and then ejected against the high systemic blood pressure developed by the preceding LVAD pumping. This might be one of the reasons why the BF in the 1:1 mode is lowest (Fig. 5.3).

In the 4:1 mode, the pump diaphragm reaches the full end-diastolic position in the first to second non-pumped cardiac cycles, and the pump

is filled with blood during this period. In the third non-pumped cycle, the blood is all sucked into the left ventricle from the atrium. For this reason, the pLVP and the AoF in the last non-pumped cycle were highest among three non-pumped cycles (Fig. 5.3). However, the pLVP could not be as high in this phase as the control value because the circulatory blood volume was reduced by the blood being temporarily stored in the LVAD pump until the next pumping out.

Phasic tracings of the LVV and the Am, calculated from the dimensional data by eqs. (3.1) and (3.3), respectively, are shown in Fig. 5.5. The LVV was closely in phase with the Am in each case. The difference of the average values of the LVV between pumping and non-pumping (control) conditions were not so large. This result is attributed to the fact that much blood could not be sucked from the atrium because the LVAD sucking pressure had to be maintained at moderate levels in order to avoid the collapse of the flexible atrium.

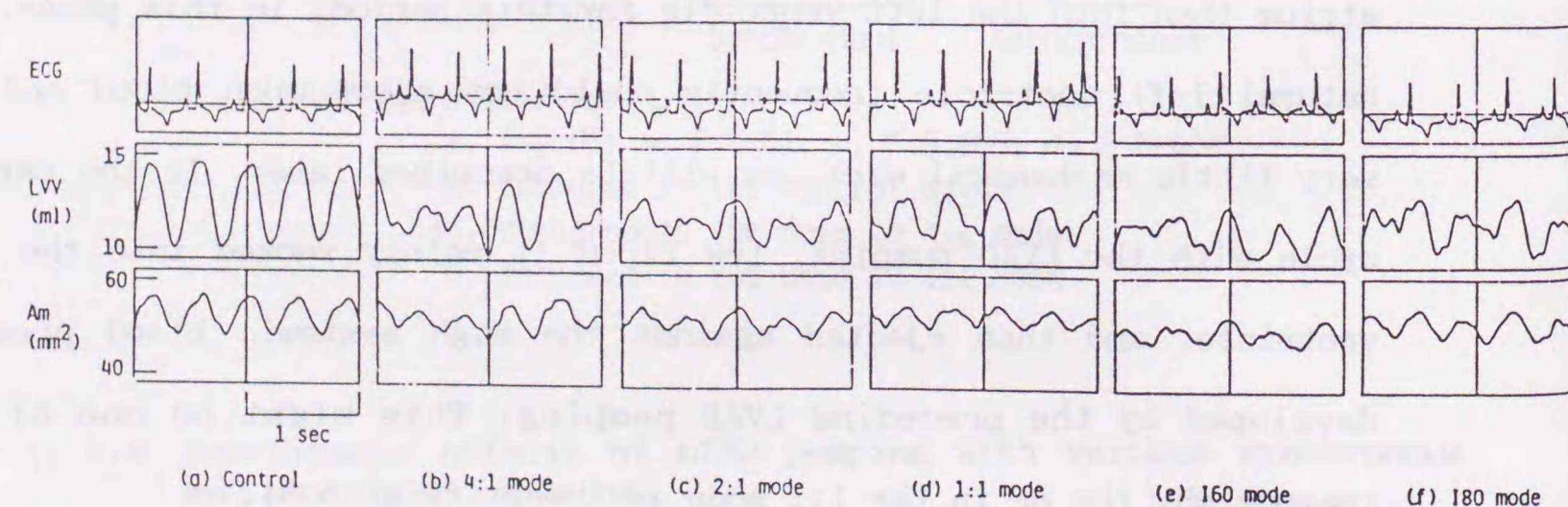


Fig. 5.5 Phasic tracings (computer output) of the left ventricular volume (LVV) and subendocardial regional muscular rhombus area (Am) calculated from the data shown in Fig. 5.3. ECG, electrocardiogram.

### 5.3.3 Bulk mechanical work of the left ventricle

Figure 5.6a shows LVP-LVW loops depicted from the 2:1-mode and control data. The loops in the 2:1-mode pumping were obtained from the successive two cardiac cycles: the smaller loop was obtained in the non-pumped cardiac cycle, and the larger one in the pumped cycle. The summarized data of the bulk mechanical work are shown in Fig. 5.7a. Since the HRs did not change so much among five pumping modes, the BMW showed similar variations to the BSW.

As expected from the hemodynamic data, the BSW done during the LVAD pumping ( $27 \pm 21$  to  $47 \pm 31$  mJ/(100 g LVW)) was significantly smaller ( $p < 0.01$ ) than that performed under the control condition ( $88 \pm 42$  mJ/(100 g LVW)): the former was 30-50 % of the latter. The BSW in the 2:1, I60, and I80 modes ( $36 \pm 27$ ,  $27 \pm 24$ , and  $27 \pm 21$  mJ/(100 g LVW), respectively) were lower ( $p < 0.05$ ) than those in the 4:1 and 1:1 modes ( $46 \pm 30$  and  $47 \pm 31$  mJ/(100 g LVW), respectively).

Similar to the BSW, the BMW observed during the LVAD pumping ( $61 \pm 52$  to  $110 \pm 63$  mW/(100 g LVW)) was significantly smaller ( $p < 0.01$ ) than the control value ( $216 \pm 97$  mW/(100 g LVW)): the former was 30-50 % of the latter. The BMW in the 2:1, I60, and I80 modes ( $81 \pm 56$ ,  $61 \pm 52$ , and  $64 \pm 51$  mW/(100 g LVW), respectively) were lower ( $p < 0.05$ ) than those in the 1:1 and 4:1 modes ( $109 \pm 64$  and  $110 \pm 63$  mW/(100 g LVW), respectively). In the synchronous modes, the BSW and BMW were lowest in the 2:1 pumping mode.

In the asynchronous modes, the rate of the natural heart was often around twice or three times as much as the LVAD pumping rate. In such a case, a quasi-synchronous pumping might occur, which could reduce the BSW and the BMW, as in the synchronous modes.

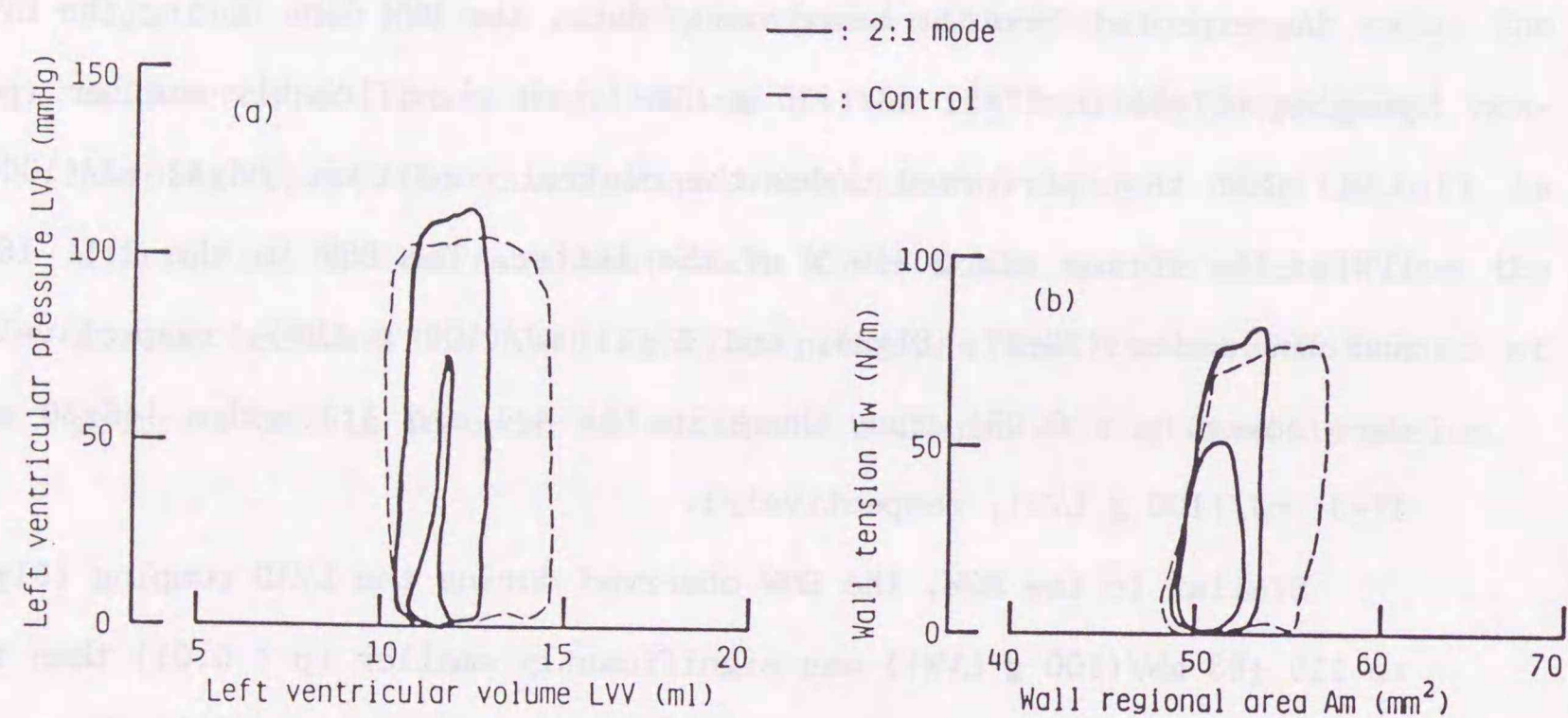
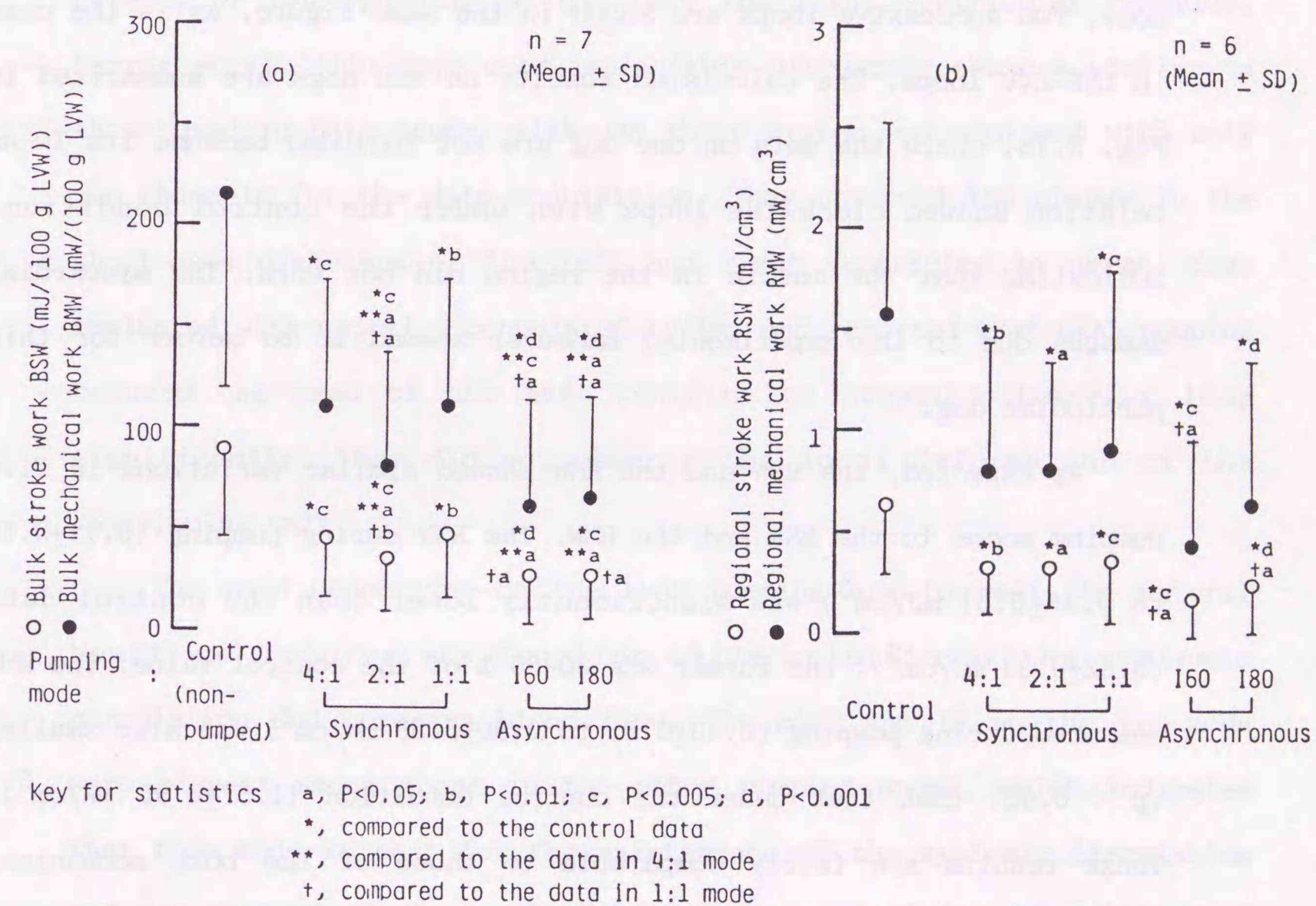


Fig. 5.6 Left ventricular pressure-volume loops (a) and regional wall tension-area loops (b) in the 2:1 pumping mode and under the non-pumped, control condition. These loops were obtained from the data shown in Figs. 5.3 and 5.5. Two successive cardiac cycles are shown for the 2:1 mode.



Key for statistics a,  $P < 0.05$ ; b,  $P < 0.01$ ; c,  $P < 0.005$ ; d,  $P < 0.001$   
 \*, compared to the control data  
 \*\*, compared to the data in 4:1 mode  
 †, compared to the data in 1:1 mode

Fig. 5.7 (a) Bulk stroke work (BSW) and averaged bulk mechanical work per second (BMW), and (b) regional stroke work (RSW) and averaged regional work per second (RMW) in various synchronous and asynchronous pumping modes.

#### 5.3.4 Regional mechanical work of the left ventricle

Figure 5.6b shows examples of the Tw-Am loops observed during the 2:1-mode pumping and under the control condition. In the 2:1 pumping mode, two successive loops are shown in the same figure, as is the case in LVP-LVV loops. The calculated results on six dogs are summarized in Fig. 5.7b, where the data on one dog are not included because its Tw-Am relation showed clockwise loops even under the control condition, indicating that the muscle in the region did not work. The myocardial damages due to the experimental maneuver seemed to be severe for this particular dog.

As expected, the RSW and the RMW showed similar variations in five pumping modes to the BSW and the BMW. The RSW during pumping ( $0.17 \pm 0.19$  to  $0.36 \pm 0.31$   $\text{mJ}/\text{cm}^3$ ) was significantly lower than the control data ( $0.62 \pm 0.33$   $\text{mJ}/\text{cm}^3$ ): the former was 30-60 % of the control value. The RMW measured during pumping ( $0.43 \pm 0.51$  to  $0.90 \pm 0.89$   $\text{mW}/\text{cm}^3$ ) was also smaller ( $p < 0.05$ ) than that under the control condition ( $1.57 \pm 0.95$   $\text{mW}/\text{cm}^3$ ). These results are fairly comparable to those of the bulk mechanical work.

#### 5.4 DISCUSSION

The mechanical effect of the LVAD pumping on the natural heart has not been fully studied yet even on the normal heart. To study the effects of LVAD pumping on the left and right ventricular behavior, Farrar et al. (11) have used implantable ultrasonic sensors similar to those used in this study, although their system was equipped with only two channels for the data acquisition. They observed the change in the short-axis diameters of the left and right ventricles in normal dogs implanted with apically cannulated LVADs, and reported that LVAD pumping reduced the area of the left ventricular pressure-diameter loop significantly. They did not observe the local deformation of the ventricular wall.

The main objectives of the LVAD pumping are to rest the natural heart and recover its function while maintaining the systemic circulation and coronary blood flow. The mAoP and TF in the 1:1 mode were highest among those in the other pumping modes, which indicates that this mode is best for the maintenance of the systemic circulation and coronary blood flow. If the LVAD was applied to the debilitated heart rather than to the normal heart, the blood might be sucked into the LVAD pump more easily, and the total bypass would be brought about due to the degraded function of the natural heart. The differences of the bypass flow among drive modes might be smaller.

It has been expected that the LVAD reduces the bulk and regional mechanical work of the left ventricle to rest it although there have been few detailed studies about the ventricular mechanics during the cardiac assist. It has been proven in this study that the BSW, BMW, RSW, and RMW in each pumping mode are significantly lower than those under

the control condition.

In the ECG synchronous pumping modes, the timing of the pump ejection must be determined carefully. The counterpulsation method utilized here has been widely used because the diastolic augmentation in the aortic pressure obtained by this method improves the coronary blood flow. In this study, the delay time of the start of the pump ejection from the R-wave of the ECG signal was set so as to obtain the maximum pump bypass flow.

The 2:1 mode was most effective for reducing the mechanical work in the synchronous pumping modes. As mentioned above, the blood did not enter the left ventricle so much during the non-pumped cardiac cycles because the pump diaphragm was held at the diastolic position, and the blood was sucked into the pump. As the result, the left ventricular stroke volume was fairly small, as shown in the second and fourth cardiac cycles in Fig. 5.5c and as demonstrated by the smaller loop in Fig. 5.6a. In the pumped cardiac cycles, on the other hand, the left ventricle could suck much blood, especially during the LVAD ejection period, resulting in large stroke volume, as shown in the first, third, and fifth cardiac cycles in Fig. 5.5c and as demonstrated by the larger loop in Fig. 5.6a. Therefore, the average blood volume sucked into the left ventricle, i.e. the average stroke volume, in the 2:1 pumping mode was less than that in the 1:1 mode (Fig. 5.5c and d). This is one of the main reasons why the left ventricular mechanical work in the 2:1 mode is lower than that in the 1:1 mode.

In the 4:1 pumping mode, the LVAD could not sufficiently unload the left ventricle, resulting in larger left ventricular mechanical work than that in the 2:1 mode.

The mechanical work of the left ventricle done in the asynchronous

pumping modes was similar to or slightly lower than that in the 2:1 synchronous mode. In the asynchronous modes, the LVAD pump ejects the blood regardless of the systolic or diastolic phase of the natural heart. When the blood is ejected during the diastole, the similar effect to that observed in the synchronous pumping modes occurs. As stated above, the LVAD pumping rates used for the asynchronous modes in this study (60 and 80 bpm) were very often around one-half and one-third of the pulse rates of the natural hearts, which brought about a kind of quasi-synchronous pumping. The LVAD pumping during the systolic phase of the natural heart, on the other hand, elevates the afterload pressure, which reduces the stroke volume of the natural heart. This phenomenon is observed in the second cardiac cycle in Figs. 5.3e and 5.5e. As a result, the mechanical work of the left ventricle was significantly lowered in the asynchronous modes.

From the results obtained in this study, it is suggested that the drive mode should be carefully selected considering the condition of the patients. To maintain the systemic circulation and coronary blood flow, the 1:1 mode is best; the 2:1 mode might be effective to rest the heart. When the LVAD pump is weaned off, the duty ratio is usually decreased step by step in order to gradually load the natural heart. A lower duty ratio such as 4:1 is useful for this purpose because the decrease in the ratio increases the load exerted on the left ventricle, and the heart would gradually adapt to the non-pumping condition.

The full stroke volume of the pump (around 40 ml) used in this chapter was large enough compared with that of the natural heart (around 12 ml). If we use a pump having a larger stroke volume, the blood staying in the pump would decrease the circulatory blood volume, especially in the 2:1 and 4:1 modes, and would cause the decrease in the

afterload. Besides, thrombus formation might occur inside the pump due to the low blood velocity in the large pump. A smaller pump having a stroke volume less than that of the natural heart could not unload the left ventricle well. Therefore, the stroke volume of the pump should be chosen carefully (4).

The high filling capability is one of the most important performances required of the pump, especially when the blood is sucked from the flexible atrium. If the blood filling was not very smooth in the pump diastole, the effect of the LVAD pumping on the natural heart would not be very good because much blood would be sucked into the left ventricle. The diaphragm of the pump used here was fabricated so as to be stable at the end-diastolic position to make the blood filling smooth.

In these experiments, the blood was withdrawn from the atrium and bypassed to the descending aorta. Total bypass was hardly brought about by this arrangement because the left ventricle competed with the pump for blood suction. The rate of the blood entering the pump is determined by both the LVAD pump performance and the left ventricular function. If the blood was withdrawn from the apex, the total bypass would be obtained easily because the whole blood is sucked into the pump, and the results might have changed. For example, the LVP during pumping would be much smaller and the BMW and the RMW would be much less compared with those observed in the case of atrium-aorta bypass, dealt with in these experiments.

The bulk and regional behavior of the ischemic ventricle implanted with LVAD is very important for the effective application of the LVAD to clinical cases. Because the myocardial infarction is usually of a local nature, regional behavior of the ventricular muscle should be studied in

both the normal and ischemic areas. For this purpose, the method used here is very useful. Bulk and regional mechanical effects of LVAD pumping on the ischemic heart are shown in the next chapter.

## 5.5 SUMMARY

Pneumatically driven left ventricular assist devices (LVADs) were acutely implanted between the left atria and the descending aortas of dogs, and were driven in five pumping modes: electrocardiogram synchronous modes with the duty factors of 1:1, 2:1, and 4:1, and asynchronous modes with the pulse rates of 60 and 80 beats/min. The ventricular diameter and myocardial segment length were measured by the ultrasonic displacement meter and implantable miniature sensors. Bulk mechanical work of the left ventricle and regional mechanical work of the myocardium were calculated from these dimensions and the left ventricular pressure.

LVAD reduced the bulk mechanical work of the left ventricle by 30-50 % and the regional work by 30-60 %. The mean aortic pressure and total flow (= aortic flow + pump bypass flow) were highest in the 1:1 synchronous pumping mode, which indicates that this mode is most effective to maintain the systemic circulation and coronary blood flow. Asynchronous pumping and synchronous pumping with 2:1 duty factor were most useful to reduce the mechanical work of the left ventricle.

## REFERENCES

1. Norman JC. Partial artificial hearts: mechanical cloning of the ventricle. *Artif Organs* 1978; 2: 235-43.
2. Mitamura Y, Takahashi M, Mikami T, Yamamoto K, Nakamura T, Nishiura K, Onuma T, Takahashi E. Effects of left ventricular bypass rate on myocardial cellular viability after coronary occlusion. *Trans Am Soc Artif Intern Organs* 1979; 25: 216-9.
3. Nakatani T, Takano H, Taenaka Y, Umezu M, Tanaka T, Yutani C, Matsuda T, Iwata H, Noda H, Nakamura T, Takatani S, Seki J, Hayashi K, Akutsu T, Manabe H. Therapeutic effect of left ventricular assist device on induced profound left ventricular failure. -Evaluation by left ventriculography-. *Trans Am Soc Artif Intern Organs* 1984; 30: 533-9.
4. Taenaka Y, Takano H, Nakatani T, Umezu M, Tanaka T, Akutsu T, Naito Y, Manabe H. Ventricular assist device (VAD) for children: in vitro and in vivo evaluation. *Trans Am Soc Artif Intern Organs* 1984; 30: 155-8.
5. Hayashi K, Matsuda T, Nakamura T, Umezu M, Takano H. Mechanical and ESCA studies of segmented polyether polyurethanes with various molecular weights for blood pump application. *Progress in Artif Organs-1985*, ISAO Press, 1986; 989-93.
6. Umezu M, Tanaka T, Tsuchiya K. Water hammer phenomenon observed in the artificial heart. *Proc 1st Symp on Fluid Control, Tokyo, 1986*; 163-8.
7. Goto Y, Yamamoto J, Saito M, Haze K, Sumiyoshi T, Fukami K, Hiramori K. Effects of right ventricular ischemia on left ventricular geometry and the end-diastolic pressure-volume relationship in the

dog. Circulation 1985; 72: 1104-14.

8. Nakamura T, Hayashi K, Seki J, Nakatani T, Noda H, Fukuda S, Takano H, Akutsu T. Eight-channel ultrasonic displacement meter for the measurement of myocardial dimensions during cardiac assist. Proc IEEE 1985 Ultrasonics Symp, San Francisco, 1986: 860-3.
9. Nakamura T, Hayashi K, Seki J. Eight-channel ultrasonic displacement meter for implantable miniature sensors. Med & Biol Eng & Comput 1987; 25: 355-8.
10. Goldman MJ. Principles of clinical electrocardiography. Tokyo: Maruzen Co, Ltd, 1976.
11. Farrar DJ, Compton PG, Herson JJ, Foner JD, Hill JD. Right ventricular pressure-dimension relationship during left ventricular assistance in dogs. Trans Am Soc Artif Intern Organs 1984; 30: 121-3.

## CHAPTER VI

### ACUTE EFFECT OF LEFT VENTRICULAR ASSIST DEVICE ON THE ISCHEMIC HEART

#### 6.1 INTRODUCTION

In the preceding chapters, an 8-channel ultrasonic displacement meter was developed and applied to the study on the effects of LVAD drive modes on the left ventricular bulk and regional mechanical work as well as on the hemodynamics in the dogs having the normal heart (1).

This chapter is devoted to the analysis of the mechanical and hemodynamic effects of LVAD pumping on the failing heart in acute animal experiments. LVADs were implanted in dogs with induced myocardial ischemia. The regional mechanical work done in the ischemic myocardial area of the failing heart was compared with that in the normal area (2).

## 6.2 METHOD

### 6.2.1 Experimental Protocol

Eight mongrel dogs of both sexes weighing 15-29 kg (average 20 kg) were anesthetized by the intravenous injection of pentobarbital sodium (25 mg/(kg body weight)), and maintained by the occasional administration of this dose throughout the experiments. They were ventilated with room air and oxygen gas by a respirator (Mark-7, Bird, Springs Farm, California, U.S.A.). The left thoracotomy was performed at the 5th intercostal space, and the pericardium was opened widely.

The same LVAD pump as that described in CHAPTER V, that is a pneumatically driven diaphragm-type LVAD pump having the stroke volume of 40 ml (3), was implanted between the left atrium and the descending thoracic aorta, as shown in Fig. 6.1.

The left ventricular diameter and myocardial segment length were measured by the 8-channel ultrasonic displacement meter (4,5). Miniature ultrasonic sensors were embedded in the left ventricle while the LVAD was being pumped under conditions of 60 bpm pumping rate and 30 % systolic duration to maintain the systemic circulation in a good state.

Three pairs of sensors were attached to the LV endocardium for the measurement of a long axis inner diameter (LD) and two short axis inner diameters parallel and perpendicular to the septum (SDp and SDn, respectively) according to the procedure mentioned in CHAPTER V.

Four pairs of ultrasonic sensors were used to measure the myocardial segment length. They were embedded in the subendocardium in the same way as that explained in CHAPTER V. Two pairs were implanted in the central region of the left ventricular free wall for the measurement

of muscular length in the orthogonal (equatorial (SSn) and meridian (LSn)) direction. Since this area was kept normal even after local ischemia was induced, it was called the 'normal' region.

The other two pairs were positioned in the distributing area of the left anterior descending coronary artery (LAD) in the same manner as that used for the implantation in the 'normal' area. Ischemia was induced in this area by the ligation of the LAD, and this area was called the 'ischemic' region. The equatorial and meridian segment lengths in the 'ischemic' region were denoted by SSi and LSi, respectively.

Left atrial pressure (LAP), aortic pressure (AoP), and left ventricular pressure (LVP) were monitored with the same pressure transducers as stated in CHAPTER V. These transducers were calibrated with a mercury manometer prior to each experiment.

The blood flow in the ascending thoracic aorta (AoFd) and pump bypass flow (BFd) were measured by the same method described in CHAPTER V. The AoFd and BFd were normalized by the animal body weight, which were denoted by AoF and BF, respectively. Total blood flow (TF) was calculated by adding AoF and BF. Total peripheral resistance (TPR) was obtained by dividing the mean AoP by TF.

The pump was counterpulsated synchronously with the ECG signal at two duty ratios: one pumping in a cardiac cycle (1:1 mode) and one pumping in two cycles (2:1 mode). These drive modes were selected according to the results obtained from the experiments described in CHAPTER V, which indicated that the 1:1 mode was useful to maintain the systemic and coronary circulation and the 2:1 mode was effective to rest the left ventricle (1). The systolic duration of the pumping (around 30 % of the cardiac cycle), the pressure of compressed air (around 250

mmHg) and vacuum (around -60 mmHg) for driving the pump, and the delay time from the R-wave of the ECG signal for the pump ejection were controlled so that the maximum pump flow was obtained.

The pump was driven in the 2:1 pumping mode through the experiments except when it was stopped to obtain non-pumping data and was being pumped in the 1:1 mode to record the data in this mode. A series of data was acquired (before the induction of local ischemia) as follows when all dimensional data became stable, usually around 30 minutes after all sensors and devices were implanted. The data in the 2:1 pumping mode were recorded first. Then, the pumping was stopped temporarily, with the pump diaphragm being held at the end-systolic position to prevent the decrease in the circulatory blood volume. The non-pumping data were recorded 2 to 5 minutes after stopping the pumping, when they seemed to be stable. Then the pumping was started again in the 1:1 mode, and the drive condition was tuned to obtain the maximum BF. After all parameters seemed to be stable, the data in this mode were acquired. Then, the pumping mode was returned to the 2:1 mode and the drive condition was tuned again. All data were recorded on magnetic tapes and on pen oscillographs in the same way as stated in CHAPTER V.

After collecting these data, the LAD was ligated at the proximal position to the 1st diagonal branch, as shown in Fig. 6.1. In the first 4 experiments, data were obtained 0.5, 1, 2, and 3 h after the ligation in order to observe the time course of cardiac and hemodynamic parameters. The data at each time were obtained in the same manner as that used before the LAD ligation. As will be mentioned later, the results obtained from these experiments showed that all parameters became stable around 2 h after the LAD ligation. Therefore, in the other 4 dogs which were used to study the effects of the local ischemia, all

data were acquired around 2 h after the ligation.

After the experiments, the animals were sacrificed by the injection of potassium chloride. During autopsies, their hearts were carefully examined to confirm the proper positioning of the ultrasonic sensors and Konigsberg's pressure transducers. To calculate the regional wall tension in the 'normal' and 'ischemic' myocardium, the angle of each sensor for the segment length was measured on the equatorial plane (see APPENDIX A.2 for detail). The left ventricular weight (LVW) and the wall thickness at the ultrasonic sensors for the segment length were measured.

Two more experiments were performed to confirm the severity of the left ventricular damage caused by the LAD ligation. In these cases, the LVAD was not applied. In the first dog, ventricular fibrillation occurred around 2 minutes after the LAD ligation, and the heart did not recover in spite of the electrical defibrillation procedure and the injection of an anti-arrhythmic drug (lidocaine hydrochloride). In the other dog, ventricular fibrillation and tachycardia continued for 20 minutes after the LAD ligation. Although the anti-arrhythmic drug was administered throughout the experiment, the hemodynamic condition did not become stable for over 3 h, and ventricular tachycardia occurred many times. No inotropic drugs were used in these experiments in order not to change the myocardial contractility. These results indicate that the ischemia induced by the maneuver used in these experiments was too severe for the hearts to maintain their function without the LVAD application.

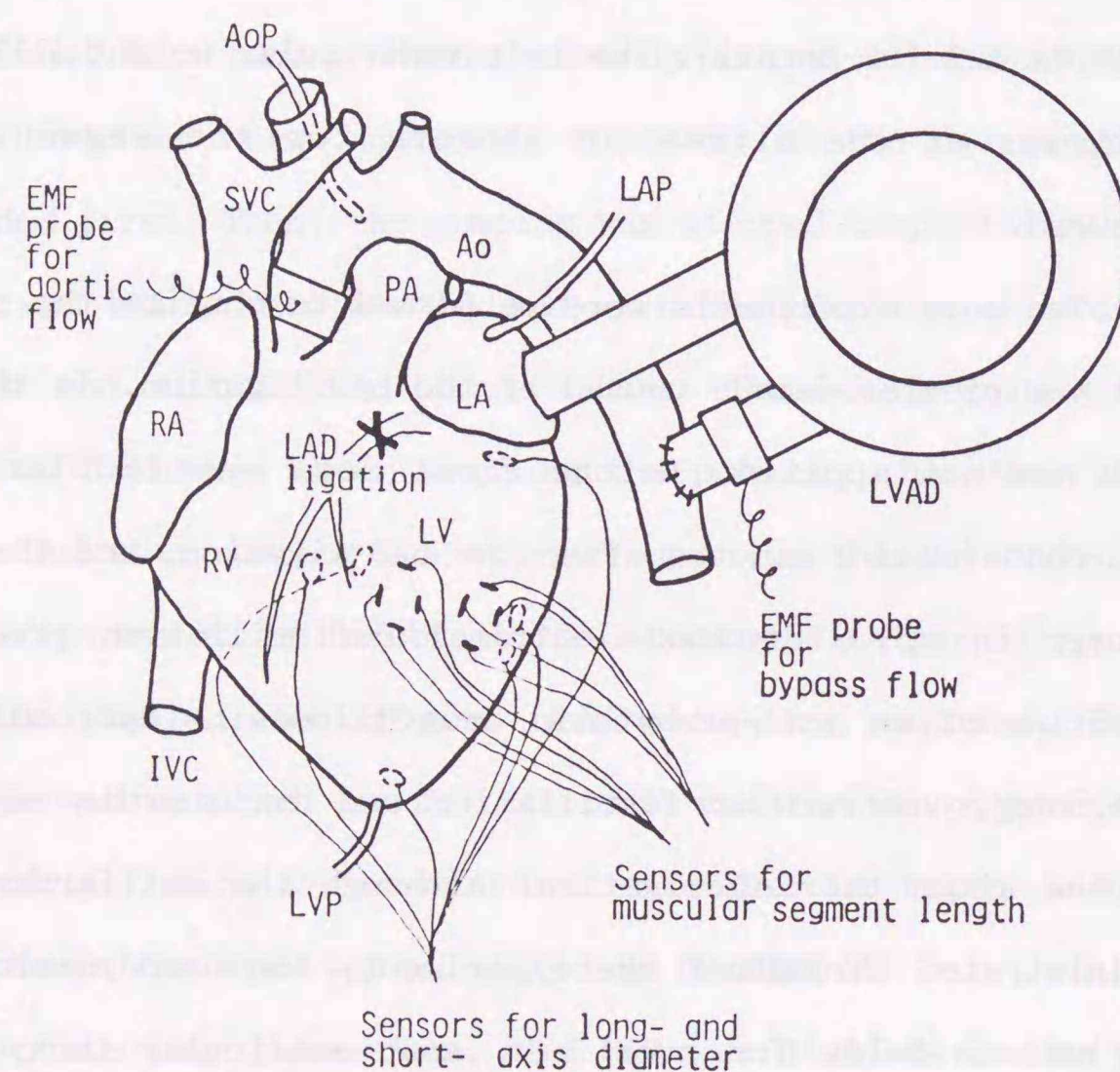


Fig. 6.1 Schematic diagram of the experimental arrangement for the implantation of ultrasonic sensors, hemodynamic transducers and left ventricular assist device (LVAD). Ischemia was induced by the ligation of the left anterior descending coronary artery (LAD). Ao, aorta; AoP, aortic pressure; EMF, electromagnetic flowmeter; IVC, inferior vena cava; LA, left atrium; LAP, left atrial pressure; LV, left ventricle; LVP, left ventricular pressure; PA, pulmonary artery; RA, right atrium; RV, right ventricle; SVC, superior vena cava.

### 6.2.2 Data Analysis

The data were analyzed by almost the same methods as those described in CHAPTER V (1).

Left ventricular volume (LVV) was calculated by eq. (3.1). The external stroke work of the left ventricle was obtained from the relation between the LVP and LVV as described in CHAPTER III. The stroke work was normalized by the LVW and multiplied by the heart rate (HR) to obtain the averaged bulk mechanical work per second (BMW).

Regional wall tensions ( $T_{w_n}$  and  $T_{w_i}$  in the 'normal' and 'ischemic' regions, respectively) were calculated from the LV diameters and pressure, and the angle of the each local area, using eq. (3.2). They are given by:

$$T_{w_k} = \frac{r_k}{2} P, \quad (k = n \text{ and } i) \quad (6.1)$$

where  $r_k$  was calculated by the method mentioned in APPENDIX A.2.

Local rhombus areas in the 'normal' and 'ischemic' regions of the LV free wall ( $A_{m_n}$  and  $A_{m_i}$ , respectively) were calculated by eq. (3.3), which are given by:

$$A_{m_k} = \frac{1}{2} L_{Sk} \cdot S_{Sk}. \quad (k = n \text{ and } i) \quad (6.2)$$

Regional stroke work of the left ventricle was obtained from the relation between the wall tension and area as stated in CHAPTER III. It was normalized by the regional muscular volume, calculated by multiplying the wall thickness and rhombus area measured after sacrifice. The averaged regional work per second were derived by multiplying the normalized stroke work by HR. The regional work in the 'normal' and 'ischemic' areas were denoted by RMWn and RMWi,

respectively.

The bulk and regional work of the left ventricle done during LVAD pumping were compared to those obtained without pumping, and the regional work in the 'ischemic' area of the ischemic heart was compared to that in the 'normal' area. Statistical significance was evaluated by paired t test, where the significant limit was taken at  $p = 0.05$ .

### 6.3 RESULTS

Examples of the phasic change (computer output) in the hemodynamic and dimensional data observed before and 2 h after the LAD ligation are shown in Fig. 6.2. The left atrial pressure (LAP) elevated by the LAD ligation was reduced to the normal level by the LVAD pumping. All the left ventricular diameters were elongated by the LAD ligation (20 % increase in LD, 37 % increase in SDp, and 41 % increase in SDn under pump-off condition), which shows that the left ventricular cavity was enlarged to do the demanded work with lower contractility. The left ventricular diameters in the ischemic heart were shortened by 4 % ( $p < 0.05$ ) by the LVAD pumping. The regional myocardial segment lengths in the 'normal' region (LSn and SSn) were not changed by the LAD ligation, whereas the segment length in the 'ischemic' area (SSi) was elongated to 172 % of that measured before the ligation.

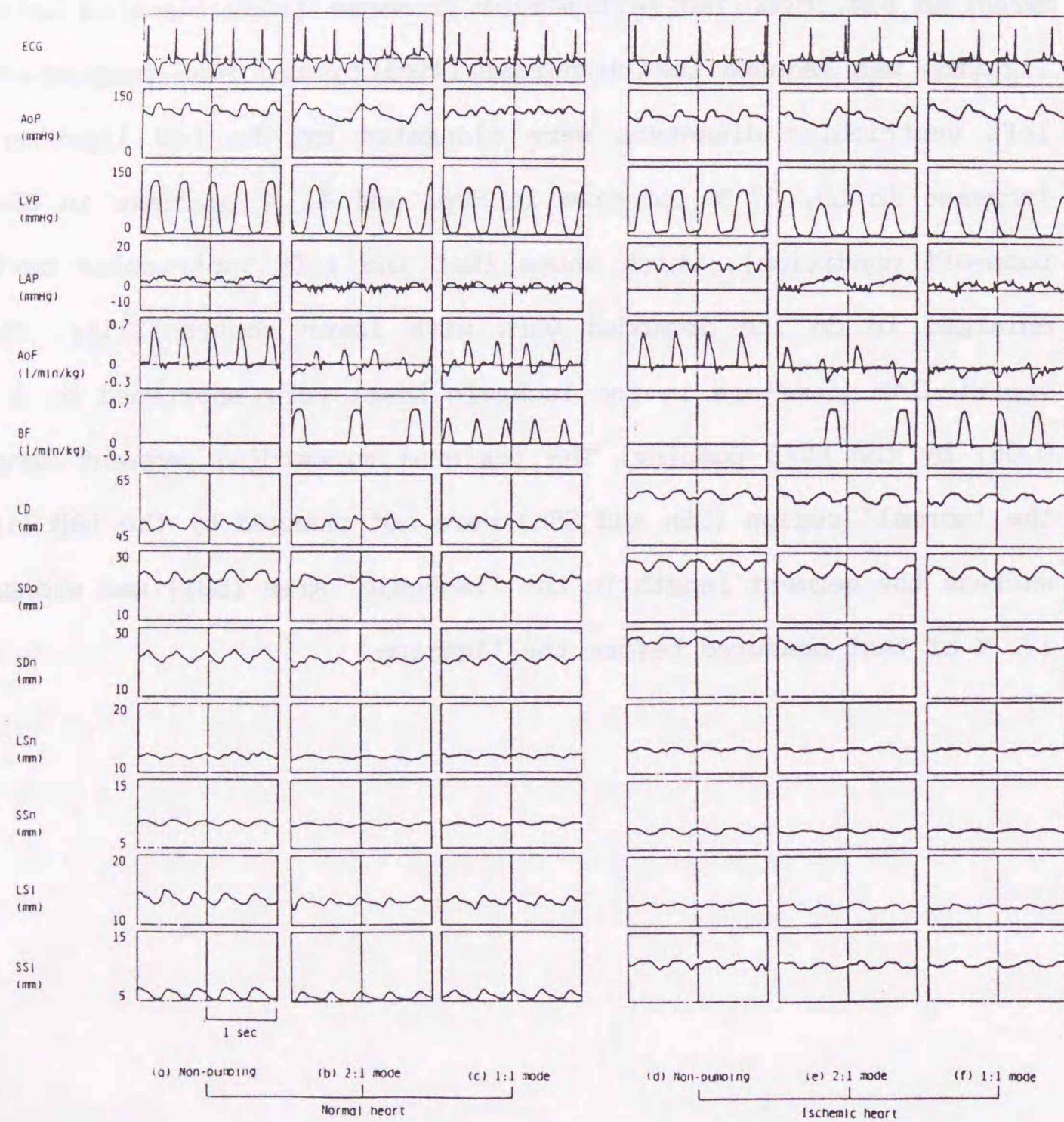


Fig. 6.2 Phasic tracings (computer output) of electrocardiogram (ECG), aortic pressure (AoP), left ventricular pressure (LVP), left atrial pressure (LAP), aortic root flow (AoF), pump bypass flow (BF), long axis diameter of the left ventricle (LD), short axis diameter perpendicular (SDn) and parallel (SDp) to the septum, meridian (LSn) and equatorial (SSn) segment length in the central region ('normal' area) of the left ventricular free wall, and meridian (LSi) and equatorial (SSi) segment length in the distributing area of the left anterior descending coronary artery (LAD) ('ischemic' region). Waves in (a), (b) and (c) were obtained before the LAD ligation, and (d), (e) and (f) were done 2 hours after ligation.

### 6.3.1 Hemodynamic effect

Figure 6.3 summarizes the time course of the hemodynamic data. The heart rate (HR) was almost unchanged for 3 h after the LAD ligation. The peak LV pressure (pLVP), mean aortic pressure (mAoP), and total blood flow (TF) measured under pump-off condition were decreased to 84, 85, and 87 %, respectively, by the myocardial dysfunction. All data obtained during the 1:1 pumping mode were similar to those in the 2:1 mode, except that pLVP and mAoP were 8 % higher in the 1:1 pumping mode. The pump bypass flow (BF) decreased to 87 % after the LAD ligation, possibly because of the decrease in the circulatory blood volume. The mean left atrial pressure (mLAP) measured under pump-off condition increased very slightly after the ligation. Although the total peripheral resistance (TPR) under pump-off condition was not changed by the LAD ligation, that obtained during pumping was increased gradually. All of these data became stable 1 to 2 h after the LAD ligation except HR, which increased slightly between 2 and 3 h. Because the LV mechanical work also became stable around 2 h after ligation, as shown later, hemodynamic and cardiac data were procured before and 2 h after ligation in the following four experiments.

The hemodynamic data obtained from 8 dogs before and 2 h after the LAD ligation are summarized in Table VI.I. The heart rate, HR, was slightly higher under non-pumping condition ( $149 \pm 17$  and  $147 \pm 19$  bpm before and after the LAD ligation, respectively) than during 2:1 pumping ( $146 \pm 18$  and  $141 \pm 16$  bpm) and 1:1 pumping ( $143 \pm 20$  bpm after the ligation). The heart rate measured under pump-off condition was not changed by the LAD ligation.

In the non-pumping state, the peak left ventricular pressure, pLVP,

obtained after the LAD ligation ( $100 \pm 12$  mmHg) was lower ( $p < 0.05$ ) than that obtained before ligation ( $113 \pm 15$  mmHg). The pLVP during pumping ( $95 \pm 16$  and  $107 \pm 17$  mmHg before ligation, and  $84 \pm 20$  and  $88 \pm 25$  mmHg after ligation) were lower than those obtained when the pumping was temporarily stopped ( $p < 0.05$ ). Although the pLVP observed during the 2:1 pumping in the normal heart was significantly lower than that in the 1:1 mode, it was not significant in the failing heart. In two dogs, the pLVP was lower than the minimum AoP after the LAD ligation, which indicates that the blood was totally bypassed by the LVADs in these cases.

Under pump-off condition, the mean aortic pressure, mAoP, obtained after the LAD ligation ( $87 \pm 11$  mmHg) was significantly lower than that observed before ligation ( $98 \pm 16$  mmHg). The mAoP during the 1:1 mode pumping ( $100 \pm 15$  and  $90 \pm 16$  mmHg before and after ligation, respectively) were not significantly different from those measured under pump-off condition ( $98 \pm 16$  and  $87 \pm 11$  mmHg). The mAoP in the 2:1 mode ( $92 \pm 15$  and  $84 \pm 12$  mmHg before and after ligation, respectively) were lower ( $p < 0.05$ ) than those in the non-pumping and 1:1 modes.

The mean left atrial pressure, mLAP, in the non-pumping mode was elevated from  $6 \pm 3$  to  $8 \pm 4$  mmHg by the LAD ligation. Irrespective of the LAD ligation, the mLAP was increased by stopping the pumping.

The total blood flow, TF, under pump-off condition, i.e. AoF, was significantly decreased from  $93 \pm 36$  to  $82 \pm 28$  ml/min/kg by the LAD ligation ( $p < 0.05$ ). There were no significant differences in the TF between the 1:1 mode ( $94 \pm 35$  and  $76 \pm 32$  ml/min/kg before and after ligation, respectively) and the 2:1 mode ( $88 \pm 40$  and  $73 \pm 24$  ml/min/kg). Under the ischemic condition, pumping seemed to decrease the TF, although the change was not statistically significant.

The bypass flow, BF, was slightly decreased by the myocardial dysfunction (from  $75 \pm 43$  to  $65 \pm 25$  ml/min/kg in the 2:1 mode and from  $61 \pm 29$  to  $58 \pm 32$  in the 1:1 mode), possibly due to the lower circulatory blood volume. These values measured after the LAD ligation were around 87 and 95 % in the 2:1 and 1:1 pumping modes, respectively, of those before ligation. The ischemia decreased the TF obtained under pump-off condition by around 12 %, which is fairly close to the percentages of the decrease in BF.

The TPR in the non-pumping state was not changed by the LAD ligation ( $9.6 \pm 3.6$  and  $9.4 \pm 3.5 \times 10^4$  dyn $\cdot$ s $\cdot$ cm $^{-5}$  $\cdot$ kg before and after ligation, respectively). Under the ischemic condition, it was slightly higher during pumping than in the non-pumping state, but the differences were not significant.

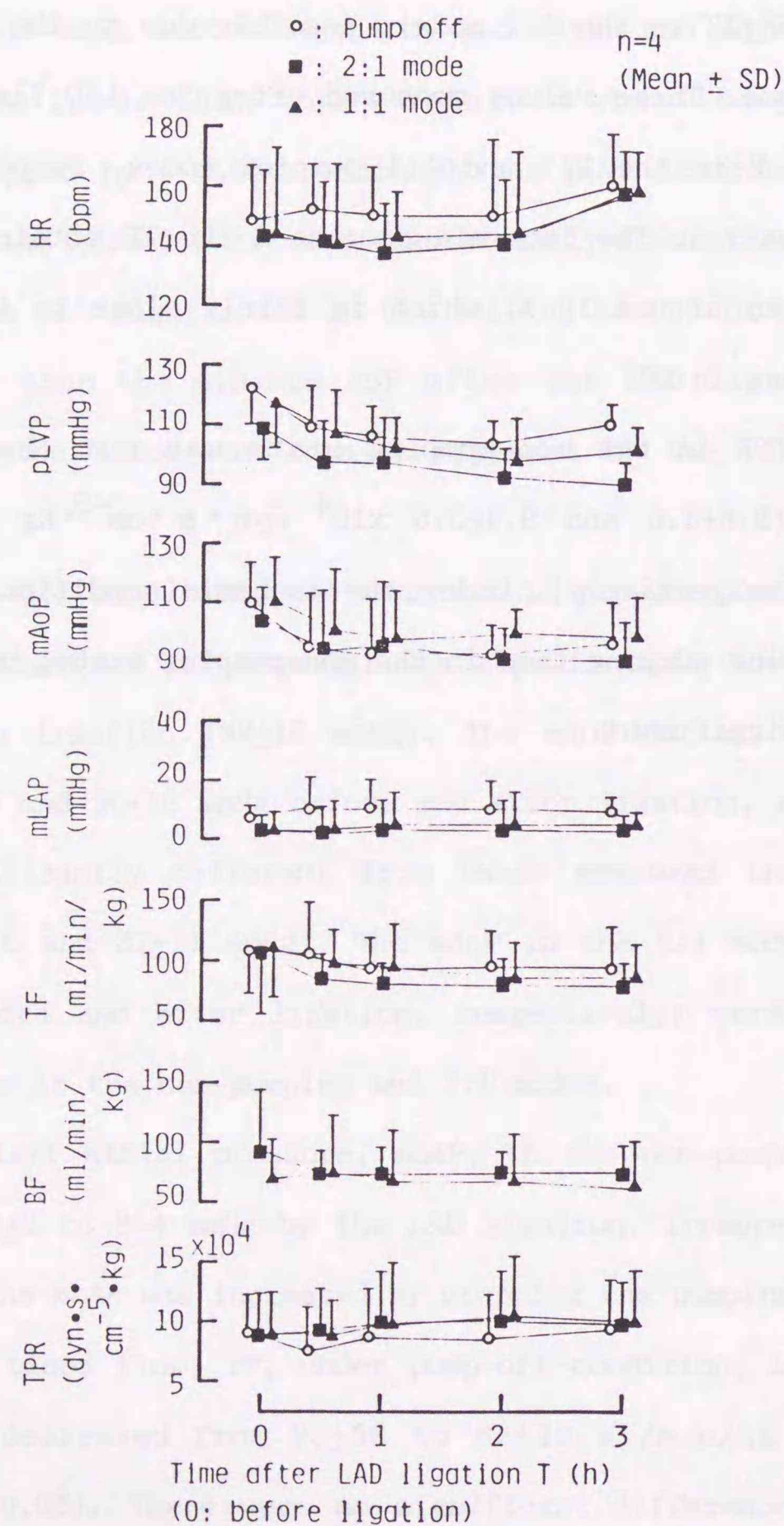


Fig. 6.3 Hemodynamic change after the ligation of the left anterior descending coronary artery. HR, heart rate; pLVP, peak left ventricular pressure; mAoP, mean aortic pressure; mLAP, mean left atrial pressure; TF, total flow (= aortic root flow + pump bypass flow (BF)); TPR, total peripheral resistance.

Table VI.1 Hemodynamic data obtained before and 2 h after LAD ligation (n=8, Mean $\pm$ SD).

LAD ligation	LVAD	HR (bpm)	pLVP (mmHg)	mAoP (mmHg)	mLAP (mmHg)	TF (ml/min/kg) ( $\times 10^4 \text{ dyn} \cdot \text{s} \cdot \text{cm}^{-5} \cdot \text{kg}$ )	BF	TPR
Before	Off	149 $\pm$ 17	113 $\pm$ 15	98 $\pm$ 16	6 $\pm$ 3	93 $\pm$ 36	-	9.6 $\pm$ 3.6
	2:1	146 $\pm$ 18* <sup>a</sup>	95 $\pm$ 16*c	92 $\pm$ 15*c	3 $\pm$ 3*c	88 $\pm$ 40	75 $\pm$ 43	9.4 $\pm$ 3.1
	1:1	147 $\pm$ 22	107 $\pm$ 17** <sup>a</sup>	100 $\pm$ 15** <sup>c</sup>	3 $\pm$ 4*c	94 $\pm$ 35	61 $\pm$ 29	9.5 $\pm$ 3.5
After	Off	147 $\pm$ 19	100 $\pm$ 12* <sup>a</sup>	87 $\pm$ 11* <sup>a</sup>	8 $\pm$ 4* <sup>a</sup>	82 $\pm$ 28* <sup>a</sup>	-	9.4 $\pm$ 3.5
	2:1	141 $\pm$ 16* <sup>a</sup>	84 $\pm$ 20* <sup>c</sup>	84 $\pm$ 12* <sup>a</sup>	4 $\pm$ 3* <sup>c</sup>	73 $\pm$ 24	65 $\pm$ 25	10.2 $\pm$ 4.1
	1:1	143 $\pm$ 20* <sup>a</sup>	88 $\pm$ 25* <sup>a</sup>	90 $\pm$ 16* <sup>a</sup>	4 $\pm$ 4* <sup>c</sup>	76 $\pm$ 32	58 $\pm$ 32	11.2 $\pm$ 5.2* <sup>a</sup>

Key:

BF, pump bypass flow; HR, heart rate; LAD, left anterior descending coronary artery; LVAD, left ventricular assist device; mAoP, mean aortic pressure; mLAP, mean left atrial pressure; pLVP, peak left ventricular pressure; TF, total flow (= aortic root flow + pump bypass flow (BF)); TPR, total peripheral resistance.

Key for statistics:

a,  $p < 0.05$ ; b,  $p < 0.01$ ; c,  $p < 0.005$ ;

\*, compared to the pump-off data obtained before the LAD ligation;

\*\* , compared to the data obtained in the 2:1 mode before the LAD ligation;

# , compared to the pump-off data obtained after the LAD ligation;

## , compared to the data obtained in the 2:1 mode after the LAD ligation.

### 6.3.2 Mechanical effect

Figure 6.4 exhibits phasic tracings of the left ventricular volume (LVV) and local myocardial areas ( $Am_n$  and  $Am_i$ ) calculated from the dimensional data shown in Fig. 6.2 by using eqs. (3.1) and (6.2). The LVV was closely in phase with the  $Am_n$  and  $Am_i$  in the normal heart, whereas in the case of ischemic heart, it was in phase with the  $Am_n$ , but out of phase with the  $Am_i$ .

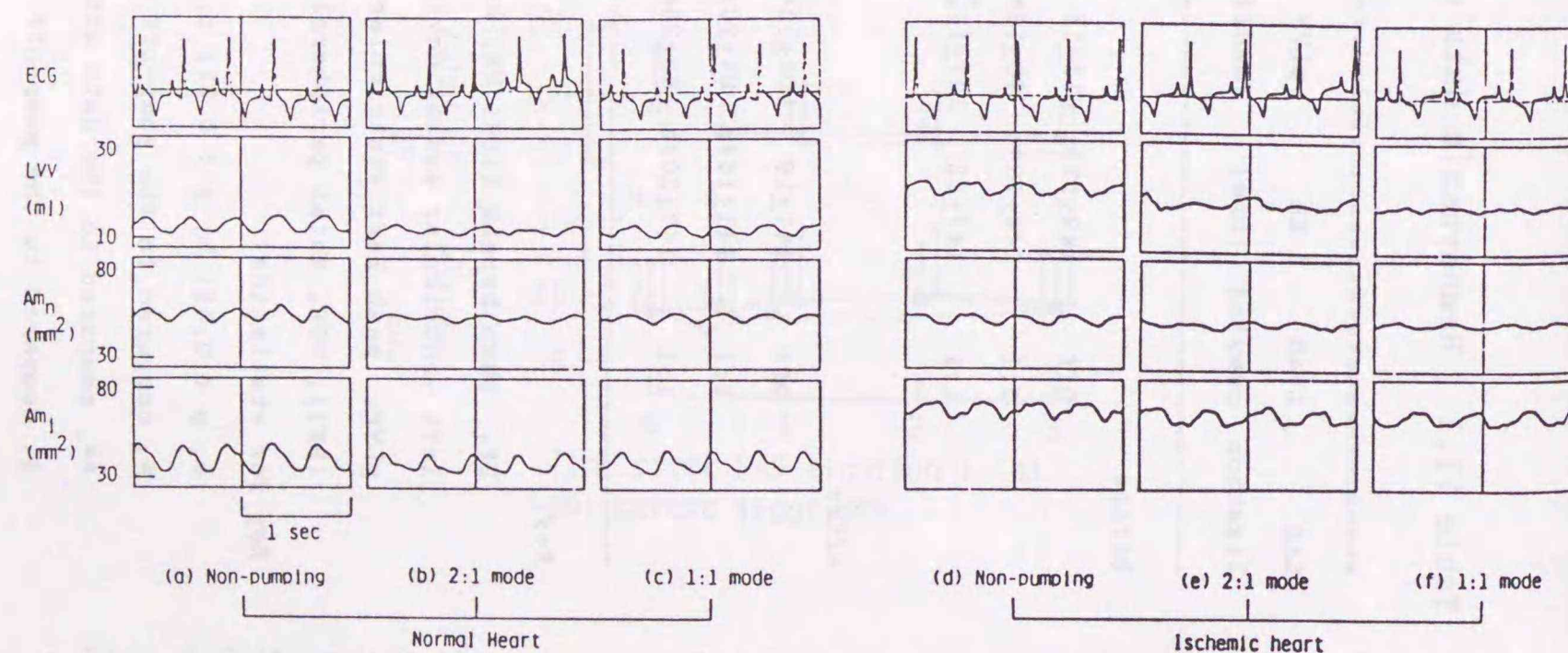


Fig. 6.4 Phasic tracings (computer output) of the left ventricular volume (LVV) and subendocardial regional rhombus areas in the 'normal' ( $Am_n$ ) and 'ischemic' ( $Am_i$ ) regions calculated from the data shown in Fig. 6.2. ECG denotes electrocardiogram.

#### 6.3.2.1 Bulk mechanical work of the left ventricle

Examples of the left ventricular pressure-volume relations during a cardiac cycle are shown in Fig. 6.5. In each case, a counterclockwise loop was drawn in a cardiac cycle. As shown in Fig. 6.5 (b-1), two different but successive loops were depicted in the 2:1 pumping mode. The loops moved towards right and their areas increased when stopping the LVAD pumping. They were also shifted to right by the LAD ligation.

Figure 6.6 (a) shows the time course of the left ventricular bulk work (BMW) obtained in 4 dogs. The bulk work obtained under intermittent pump-off condition decreased gradually until around 2 h after the LAD ligation. The work in the pumping modes decreased rather rapidly for the first 30 minutes and, then, became stable. The decreases of BMW in these cases were smaller than that obtained under pump-off condition. Before the LAD ligation (i.e. in the normal heart), the bulk work in the 2:1 mode was smaller than that in the 1:1 mode. However, the difference seemed to be reduced after the induction of myocardial dysfunction.

Table VI.II summarizes the bulk mechanical work obtained in 7 dogs before and 2 h after the LAD ligation. The data obtained of one out of 8 dogs were omitted and are not included in the table because of the malposition of an ultrasonic sensor for the measurement of the left ventricular long axis diameter in this animal.

The BMW obtained under pump-off condition was significantly decreased from  $0.27 \pm 0.16$  to  $0.16 \pm 0.11$  W/(100 g LVW) by the LAD ligation ( $p < 0.01$ ). The BMW was significantly increased ( $p < 0.005$ ) by stopping the LVAD pumping, regardless of the normal or ischemic heart. The difference of the BMW between the 2:1 and 1:1 modes was smaller in the ischemic heart than in the normal one.

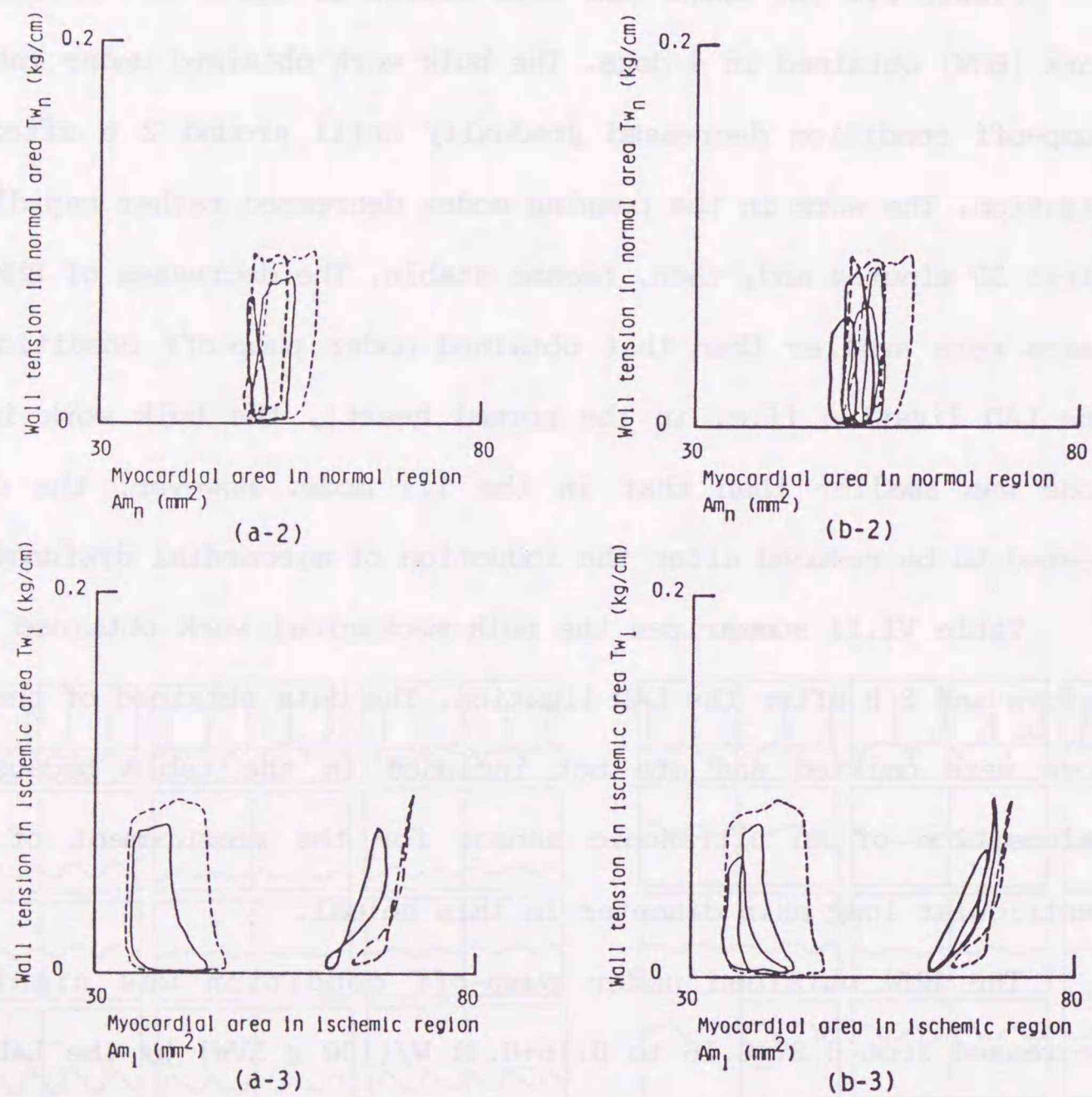
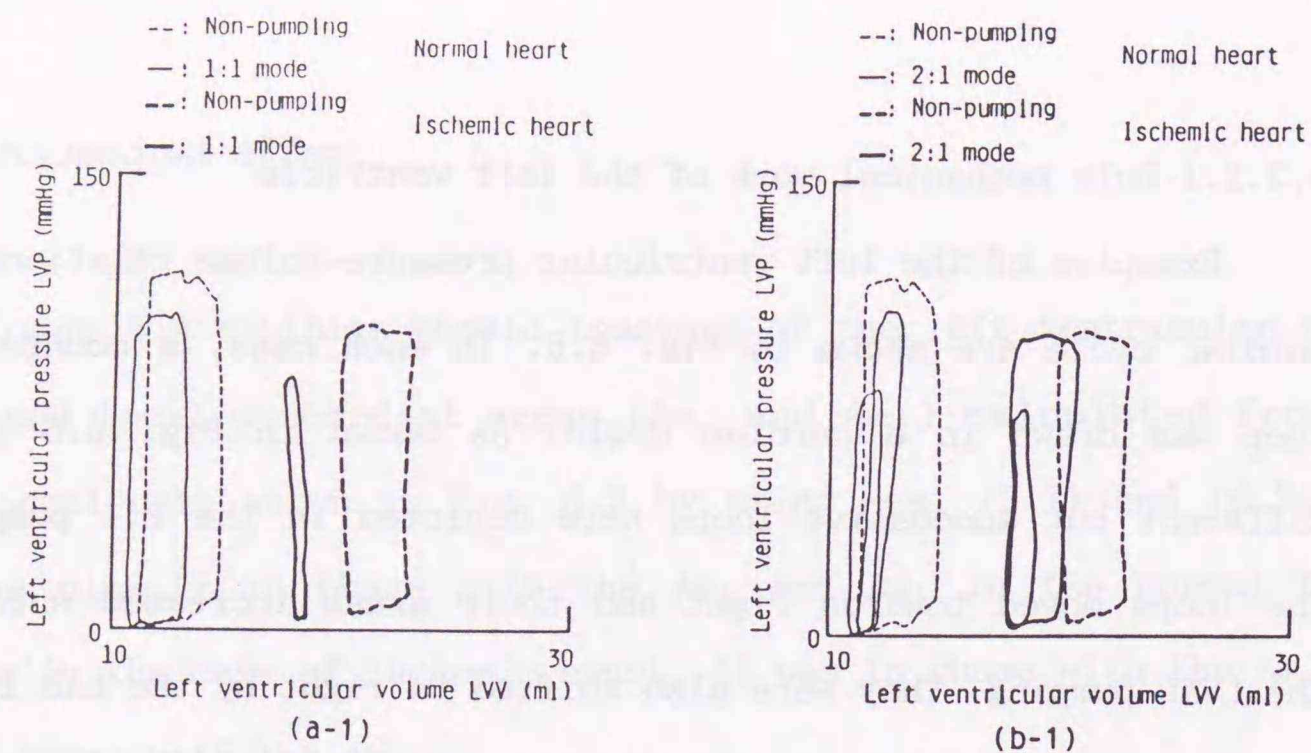


Fig. 6.5 Left ventricular pressure-volume loops ((a-1) and (b-1)) and regional wall tension-area loops in the 'normal' ((a-2) and (b-2)) and 'ischemic' areas ((a-3) and (b-3)). The loops obtained before and 2 h after the ligation of the left anterior descending coronary artery are shown by the thin and thick lines, respectively. Two successive loops are depicted for the 2:1 mode. These loops were obtained from the data shown in Figs. 6.2 and 6.4.

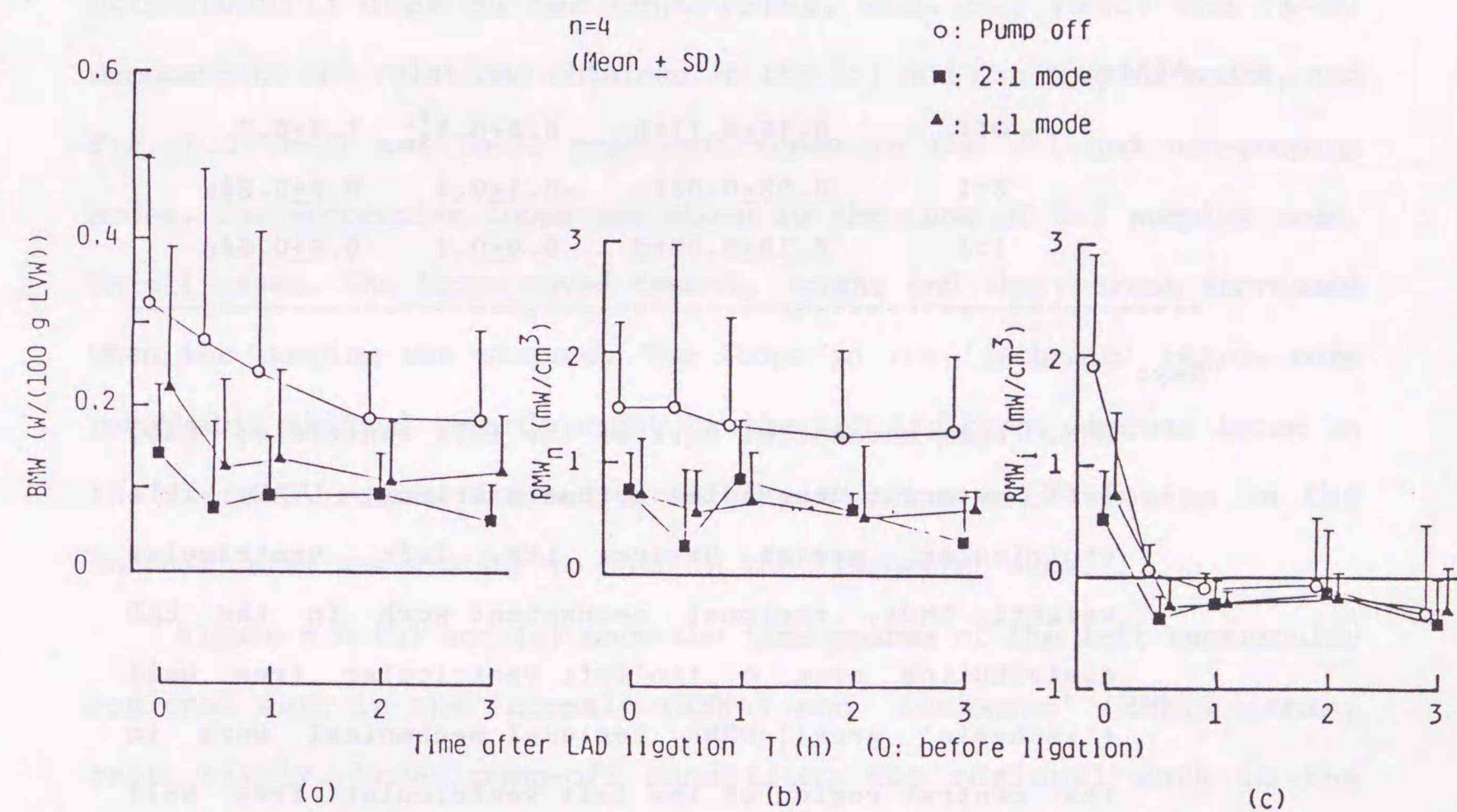


Fig. 6.6 Time course of (a) bulk mechanical work of the left ventricle (BMW) and (b) regional work in the 'normal' area (RMW<sub>n</sub>) and (c) that in the 'ischemic' region (RMW<sub>i</sub>) of the left ventricular free wall.

Table VI.II Effect of the LAD ligation and LVAD pumping on the left ventricular mechanical work (n=7, Mean±SD).

LAD ligation	LVAD pumping	BMW (W/(100 g LVW))	RMWi (mW/cm <sup>3</sup> )	RMWn (mW/cm <sup>3</sup> )
-----				
Before				
	Off	0.27±0.16	2.0±1.0	1.6±1.2
	2:1	0.10±0.09*d	0.6±0.4*c	0.8±0.5*a
	1:1	0.15±0.15*c	0.9±0.7*d	0.8±0.6*a
After				
	Off	0.16±0.11*b	0.2±0.5 <sup>*c</sup> <sub>\$a</sub>	1.2±0.7
	2:1	0.08±0.08#c	-0.1±0.4	0.5±0.2#a
	1:1	0.10±0.08#d	0.0±0.4	0.6±0.6#c

Key:

BMW, bulk mechanical work of the left ventricle; LAD, left anterior descending coronary artery; LVAD, left ventricular assist device; LVW, left ventricular weight; RMWi, regional mechanical work in the LAD distributing area of the left ventricular free wall ('ischemic' area); RMWn, regional mechanical work in the central region of the left ventricular free wall ('normal' area).

Key for statistics:

a, p < 0.05; b, p < 0.01; c, p < 0.005; d, p < 0.001;  
 \*, compared to the pump-off data obtained before the LAD ligation;  
 #, compared to the pump-off data obtained after the LAD ligation;  
 \$, compared to the pump-off data obtained in the 'normal' region after the LAD ligation.

### 6.3.2.2 Regional mechanical work of the left ventricle

Examples of the wall tension-area relations during a cardiac cycle are also shown in Fig. 6.5. Fig. 6.5 (a-2) and (b-2) demonstrate the results obtained at the central position of a left ventricular free wall ('normal' region), which gave counterclockwise loops. Fig. 6.5 (a-3) and (b-3) show the loops obtained of a LAD distributing area ('ischemic' region). These loops in the 'ischemic' areas were not always counterclockwise, indicating that the work in these regions were occasionally done on the ventricles. Fig. 6.5 (a-2) and (a-3) demonstrate the relations obtained in the 1:1 and non-pumping modes, and Fig. 6.5 (b-2) and (b-3) represent those in the 2:1 and non-pumping modes. Two successive loops are shown in the case of 2:1 pumping mode. In all cases, the loops moved towards right and their areas increased when the pumping was stopped. The loops in the 'ischemic' region were remarkably shifted towards right by the LAD ligation, whereas those in the 'normal' region did not move. The maximum wall tension in the 'normal' area was similar to that in the 'ischemic' area.

Figure 6.6 (b) and (c) show the time course of the left ventricular regional work in the 'normal' (RMWn) and 'ischemic' (RMWi) areas, respectively. Under pump-off condition, the regional work in the 'normal' area was not changed by the LAD ligation. The regional work in the 'ischemic' region, however, dropped to near zero within 0.5 h after ligation and was maintained at that level for at least 2.5 h.

Table VI.II summarizes the regional mechanical work obtained of 7 dogs before and 2 h after the LAD ligation. The data on one dog are not included in this table because its myocardial wall tension-area relation showed clockwise loops even under the non-pumping condition with the normal heart, indicating that the muscle in the region did not work.

Experimental maneuver might have induced unusually severe myocardial damages in this dog. This particular animal is different from the dog whose BMW data were omitted.

The RMWn and RMWi in the normal heart gave similar values in each pumping mode, and they were significantly increased ( $p < 0.005$ ) by stopping the LVAD pumping. After the LAD ligation, the RMWn under pump-off condition slightly decreased, whereas the RMWi dropped to near zero ( $0.2 \pm 0.5 \text{ mW/cm}^3$ ). The latter result indicates that the myocardium in the 'ischemic' region turned out to do no mechanical work. The LVAD pumping reduced the RMWn by around 55 %, but did not change the RMWi.

#### 6.4 DISCUSSION

Kresh et al. (6) measured the regional intra-myocardial pressure in the failed left ventricles of dogs during LVAD pumping, and concluded that the intra-myocardial pressure was not reduced by the mechanical assist device. However, they did not measure the LV dimension. Since the LVAD is often used for volume unloading, the LV dimensional change is important to evaluate the mechanical effect of the LVAD.

Farrar et al. (7,8) measured the short axis diameters of the non-ischemic left and right ventricles in the dogs implanted with LVADs by apical cannulation, and reported that the LVAD significantly reduced the left ventricular pressure-diameter loop area. However, they did not study the local deformation of ventricular wall. Since the heart failure induced by ischemia is generally of local nature, it is required to study the regional behavior of myocardium for the detailed analysis of the mechanical effects of LVAD and the mechanism of the recovery of failing heart.

In the present experiments, ischemia was induced locally by ligating the left anterior descending coronary artery (LAD) which provides the blood flow in the anterior region of the left ventricular wall. The ischemia was so severe that the heart could not stably maintain its function without the aid of LVAD. The regional myocardial behavior in the 'ischemic' area was compared with that observed in the 'normal' central region.

In clinical cases, the LVAD is usually applied a fairly long time after the development of myocardial infarction. The ischemic model used in this chapter is different from the clinical cases because the ischemia was induced at the time of the onset of LVAD pumping. However,

pertinent and valuable insights could be obtained from the present study for the clinical application of LVAD.

It has been anticipated that the LVAD reduces the bulk and regional mechanical work of the failing heart, although there have been few direct studies on the mechanical effects. This study proved that the LVAD decreases the mechanical work in the 'normal' region of the left ventricle, and exerts no load to the 'ischemic' myocardium, and reduces the bulk mechanical work. By virtue of the LVAD, the blood circulation was maintained well in spite of the severely damaged natural ventricle.

In these experiments, the author applied the left atrial cannulation technique, which has been widely used in clinical cases. If the blood is sucked from the left ventricle by the apical cannulation, a greater reduction of LVP and increase in the pump bypass flow might be expected compared with the case of atrial cannulation.

In two dogs, the blood was totally bypassed through LVADs after the LAD ligation. In the normal heart, the blood cannot be totally bypassed because the natural heart is powerful enough to suck the blood from the atrium (1) as seen in CHAPTER V. In such a case, the drive mode and condition of LVAD are important for the reduction of the ventricular mechanical work. This is not the case for the debilitated ventricle. As the result, the difference of pLVP between the 1:1 and 2:1 pumping mode was statistically significant before the LAD ligation, but not after ligation. In addition, the difference between the bulk mechanical work done during the 1:1 and 2:1 pumping was smaller in the ischemic heart than in the normal heart.

The myocardium in the 'ischemic' region became to do no external work within 0.5 h after the LAD ligation, while the mechanical work in the 'normal' area remained unchanged during the experimental period

(Fig. 6.6). The total blood flow (TF) and bulk mechanical work (BMW) measured under pump-off condition decreased gradually until 1 to 2 h after ligation and did not change thereafter, whereas those obtained during pumping greatly decreased within 0.5 h. Considering that the BMW in the pump-off state is dependent on the local myocardial contractility in the normal area, the passive mechanical properties of the severely damaged myocardium in the ischemic area, and the behavior of the border region, the results shown in Fig. 6.6 indicate that the myocardial damage gradually extends into the 'normal' region within 1 to 2 h after ligation. If there was no aid of LVAD, the damaged area would extend more rapidly and continuously, resulting in the failure of the whole heart. In fact, this episode was confirmed by the additionally performed non-LVAD experiments. These results imply that the LVAD unloads the myocardium and also supplies enough oxygen to the myocardium possibly by the increased blood flow in the co-lateral coronary arteries. That is, the LVAD is useful not only to rest the severely damaged natural heart but also to maintain the viability of ischemic myocardium.

Although the LVAD unloads and rests the damaged myocardium, the regional mechanical work in the 'ischemic' area (RMWi) remained at near zero until 3 h after the LAD ligation. This result indicates that the ischemic myocardium did not recover. Although some part in the ischemic area was necrotized and infarcted by the ligation, other part of the ischemic myocardium might not have been completely infarcted, having the possibility of recovery by the longer-time LVAD pumping if a sufficient amount of co-lateral coronary flow was retained. To clarify whether the ischemic myocardium can recover its mechanical function by the LVAD pumping or not, and to know the mechanism of recovery process of the bulk and regional left ventricular function, a series of chronic animal

experiments were performed and the details are stated in CHAPTER VIII. Before going those experiments, another series of chronic experiments were preliminary conducted to confirm the feasibility of long-term use of the sonomicrometer and to know the effect of long-term pumping on the left ventricular mechanics in the normal heart. The method for these experiments and the results obtained are described in the next chapter.

## 6.5 SUMMARY

Pneumatically driven left ventricular assist devices (LVADs) were implanted between the left atria and the descending thoracic aortas of dogs and were counterpulsated synchronously with the electrocardiogram at 1:1 and 2:1 duty ratios. Seven pairs of miniature sonomicrometers were implanted into the left ventricle (LV) to measure the LV muscular length and diameter. Ischemia was induced by the ligation of the left anterior descending coronary artery (LAD). Bulk and regional mechanical work were calculated from these dimensions and the left ventricular pressure.

LVAD reduced the bulk work in the ischemic and normal hearts not only in the 1:1 but also in the 2:1 pumping modes. The left ventricular bulk work measured under pump-off condition decreased progressively until around 2 h after the LAD ligation, and thereafter it became constant. The regional myocardial work in the normal area of the ischemic heart was significantly decreased by the LVAD pumping (by 55%), whereas that in the ischemic area remained at near zero level regardless of pumping or non-pumping.

The results obtained indicated that LVAD is useful not only to rest the severely damaged natural heart, but also to maintain the viability of ischemic myocardium.

REFERENCES

1. Nakamura T, Hayashi K, Seki J, Nakatani T, Noda H, Takano H, Akutsu T. Effect of drive mode of left ventricular assist device on the left ventricular mechanics. *Artif Organs* 1988; 12: 56-66.
2. Nakamura T, Hayashi K, Seki J, Nakatani T, Noda H, Fukuda S, Takano H, Akutsu T. Bulk and regional mechanical work of ischemic heart during left ventricular assistance. *Progress in Artif Organs-1985*, ISAP Press, 1986: 447-51.
3. Taenaka Y, Takano H, Nakatani T, Umezu M, Tanaka T, Akutsu T, Naito Y, Manabe H. Ventricular assist device (VAD) for children: in vitro and in vivo evaluation. *Trans Am Soc Artif Intern Organs* 1984; 30: 155-8.
4. Nakamura T, Hayashi K, Seki J, Nakatani T, Noda H, Fukuda S, Takano H, Akutsu T. Eight-channel ultrasonic displacement meter for the measurement of myocardial dimensions during cardiac assist. *Proc IEEE 1985 Ultrasonics Symp, San Francisco*, 1986: 860-3.
5. Nakamura T, Hayashi K, Seki J. Eight-channel ultrasonic displacement meter for implantable miniature sensors. *Med & Biol Eng & Comput* 1987; 25: 355-8.
6. Kresh JY, Kerkhof PLM, Goldman SM, Brockman SK. Heart-mechanical assist device interaction. *Trans Am Soc Artif Intern Organs* 1986; 32: 437-43.
7. Farrar DJ, Compton PG, Herson JJ, Foner JD, Hill JD. Right ventricular pressure-dimension relationship during left ventricular assistance in dogs. *Trans Am Soc Artif Intern Organs* 1984; 30: 121-3.
8. Farrar DJ, Chow E, Wood JR, Hill D. Anatomic interaction between the

right and left ventricles during univentricular and biventricular circulatory support. *Trans Am Soc Artif Intern Organs* 1988; 34: 235-40.

## CHAPTER VII

### EFFECT OF LONG-TERM APPLICATION OF LEFT VENTRICULAR ASSIST DEVICE

#### ON THE NORMAL HEART

##### 7.1 INTRODUCTION

As described in the previous chapters, the following results were obtained from acute animal experiments:

- (i) in the normal heart model, LVAD pumping in the electrocardiogram (ECG) synchronous mode at the duty ratio of 2:1 (one counterpulsated pumping in two cardiac cycles) was most effective to reduce the left ventricular mechanical work, whereas that of 1:1 (one pumping in a cardiac cycle) was best to maintain the systemic circulation (1),
- (ii) in the induced ischemic heart model, LVAD reduced the regional mechanical work done in the normal area, keeping the work in the ischemic myocardium at near zero level, and decreased the mechanical work of the bulk left ventricle (2).

From these acute experiments, however, still unclear are the effects of long-term pumping of LVAD on the myocardial mechanics. For example, long-term unloading, particularly excessive unloading may cause myocardial atrophy. Very few reports have been published on the effects of long-term LVAD pumping on the ventricular and myocardial mechanics.

This chapter is devoted to describing the results of the studies carried out aiming: (i) to confirm the feasibility of chronic application of the ultrasonic miniature sensors used in the acute

experiments, and (ii) to know the effects of long-term LVAD pumping on the bulk and regional mechanics of the normal left ventricle.

## 7.2 METHOD

### 7.2.1 Experimental procedure

Three goats of both sexes weighing 29 (experiment no. P8520), 34 (P8613) and 28 kg (P8620) were used for this study. Each goat was anesthetized with the gas mixture of fluothane and oxygen after the administration of ketamine hydrochloride. The ventilation was maintained by a positive pressure respirator (Servo Ventilator 900C, Siemens-Elma, Sweden). The left thoracotomy was performed at the 5th intercostal space, and the pericardium was widely opened.

A pneumatically driven, diaphragm type LVAD pump having a stroke volume of 70 ml (3) was implanted between the left atrium (LA) and the descending thoracic aorta (Ao) as shown in Fig. 7.1. The pump was fabricated of a segmented polyether polyurethane (TM3, Toyobo, Osaka, Japan). Bjork-Shiley disc valves of 23ABP and 21ABP were used for the inflow and outflow, respectively. Polyvinyl chloride tubes coated with the same polyurethane as used for the pump were utilized for the inflow and outflow cannulae. The inflow cannula was inserted into LA from its appendage. Cooley low porosity woven Dacron vascular graft (Meadox, Oakland, New Jersey, U.S.A.) was attached to one end of the outflow cannula and was used for the end-to-side anastomosis with Ao.

Six pairs of miniature ultrasonic sensors (2 mm in diameter) (4) were implanted in the left ventricle (Fig. 7.1) to measure the left ventricular diameter, segment length, and wall thickness with the 8-channel ultrasonic displacement meter (4).

Three pairs of them were attached to the endocardial surface of the left ventricle for the measurements of the long axis diameter (LD) and

two short axis diameters parallel (SDp) and perpendicular (SDn) to the septum. Two pairs of sensors were positioned in the central area of the left ventricular free wall. They were embedded in the subendocardium to measure the segment length in the orthogonal (equatorial (SS) and meridian (LS)) direction. The technique used for the implantation of these five pairs of sensors was the same as that applied to the acute experiments (1,2) described in the previous chapters.

The remaining one pair of sensors were implanted close to the sensors for the segment length, and were used for the measurement of left ventricular wall thickness (WT): one of the sensors was inserted into the subendocardium obliquely, while the counterpart was attached to the epicardium using a Dacron velour backing of the sensor.

Left atrial pressure (LAP) and aortic pressure (AoP) were measured with extracorporeal, fluid-filled catheter-type pressure transducers (P50, Gould, Oxnard, California, U.S.A.) which were calibrated prior to each experiment. These transducers were periodically calibrated during the experiments.

Left ventricular pressure (LVP) was measured by a wire-strain-gauge type pressure transducer of high fidelity (P6.5, Konigsberg, Pasadena, California, U.S.A.) to avoid the distortion and delay of the signal, which was inserted into the left ventricular cavity through the apex. This transducer was calibrated prior to each experiment. The long-term stability was tested in vitro prior to the series of experiments, which showed that the drift of the output for the atmospheric pressure at 37 °C temperature was less than 1.8 mmHg for 1 month.

Pulmonary arterial blood flow (PAFd) and pump bypass flow (BFd) were monitored by electromagnetic flowmeters (EMFs) (MFV-2100 and -1200, respectively, Nihonkohden, Tokyo, Japan) and perivascular probes. Since

it was very difficult to attach the EMF probes to the anatomically very short ascending aorta in the goat, PAFd was measured for the total systemic blood flow. BFD was measured on the vascular graft attached to the pump outflow conduit. PAFd and BFD were normalized by dividing them by the body weight measured during the autopsy, and denoted by PAF and BF, respectively.

During the implantation of these sensors and probes, the LVAD pump was driven in the asynchronous mode (30 %-systole at the 60 bpm pumping rate) to maintain the systemic circulation well.

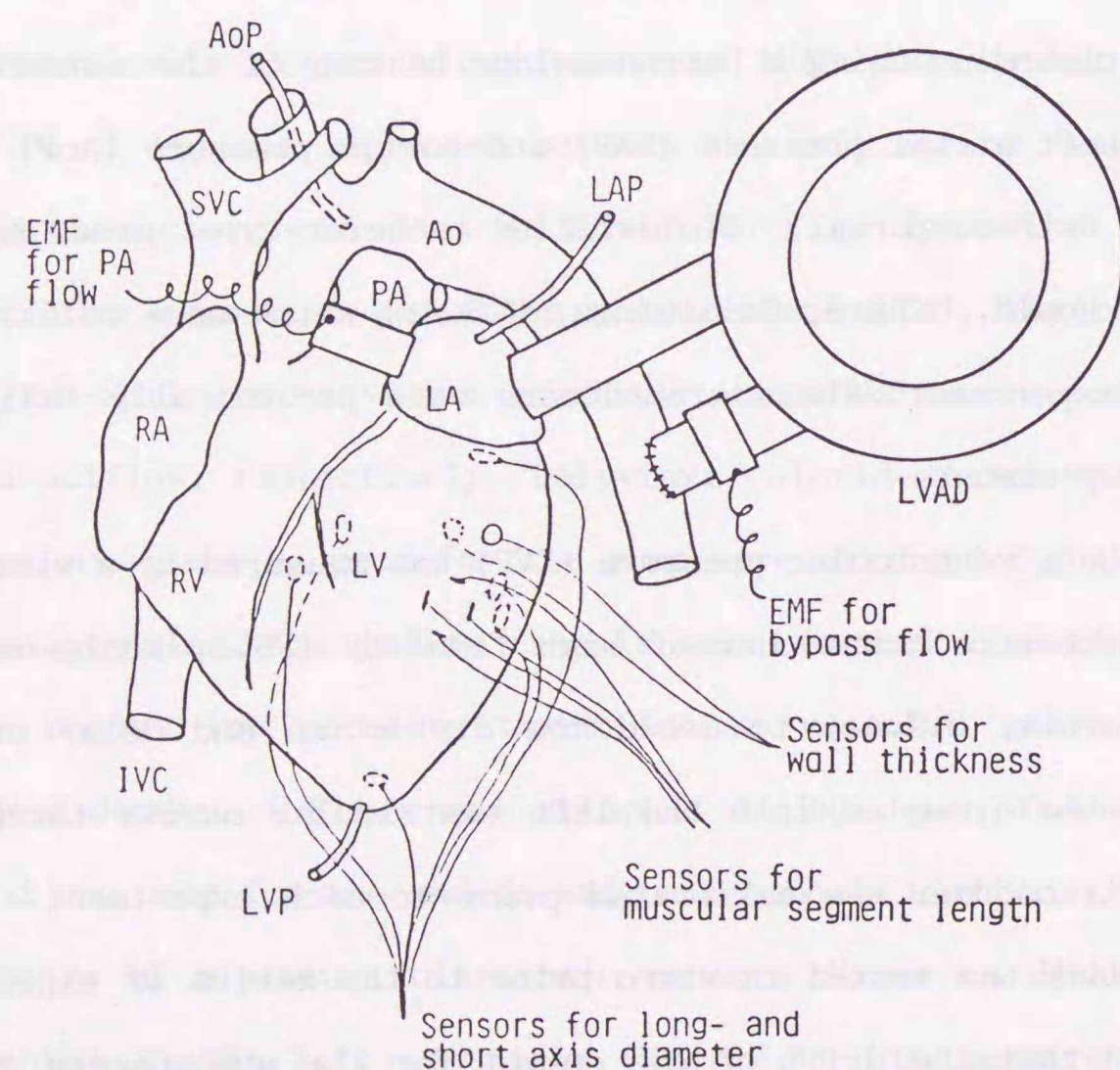


Fig. 7.1 Schematic diagram of the experimental arrangement. Ao, aorta; AoP, Ao pressure; EMF, electromagnetic flowmeter; IVC, inferior vena cava; LA, left atrium; LAP, LA pressure; LV, left ventricle; LVAD, LV assist device; LVP, LV pressure; PA, pulmonary artery; RA, right atrium; RV, right ventricle; SVC, superior vena cava.

### 7.2.2 Post-operative care and data acquisition

Each animal was kept alive for around 1 month after operation. In a goat (P8620), the LVAD was removed on the 1st post-operative day to obtain the control data. In the remaining two goats (P8520 and P8613), the LVAD was counterpulsated synchronously with the ECG at the duty ratio of 2:1 through the experiments. Because heart rate (HR) was very high for one week after the operation as shown later, the duty ratio was set at 2:1 and was not changed through each experiment, although pumping was stopped temporarily while the pump-off data were acquired, and also temporarily pumped in the 1:1 pumping mode while the data in this mode were recorded. The pump driving conditions, namely the drive pressure (around 200 mmHg), drive vacuum (around -60 mmHg), systolic duration, and delay from the R-wave of the ECG signal were often set carefully to obtain the maximum pump bypass flow.

Hemodynamic and cardiac data were acquired once a day, and recorded on magnetic tape for around 15 sec using a data recorder (XR-510, Teac, Tokyo, Japan) and on pen oscillographs (Polygraph 361 and Recti-Horiz 8K23, NEC San-ei, Tokyo, Japan).

In the animals implanted with LVADs, pumping conditions were tuned to obtain a maximum bypass flow before acquiring data. After all the hemodynamic and dimensional data became stable (usually within several minutes), they were recorded while being pumped in the 2:1 mode. Then, pumping was stopped temporarily, and non-pumping data were acquired after all parameters became stable again. Pumping was then restarted in the 1:1 mode, and pumping conditions were tuned again. The data in this mode were acquired after all parameters became stable. The pumping mode was then returned to 2:1 mode, and the drive conditions were tuned up.

Around 1 month after the operation, these animals were sacrificed. The heart was carefully resected and the positioning of the implanted sensors and probes was checked. The body weight and left ventricular weight (LVW) were measured. The myocardial thickness of the left ventricular free wall where the ultrasonic sensors for the measurement of segment length were embedded was also measured.

### 7.2.3 Data analysis

Method of data analysis used for this study is the same as that mentioned in detail in CHAPTER V (1). A mini-computer system (PDP-11/44, DEC, Maynard, Massachusetts, U.S.A.) was used to analyze the data recorded on magnetic tape.

Left ventricular volume, LVV, was calculated from the three diameters by eq. (3.1), as described in CHAPTER III. The maximum and minimum LVV in a cardiac cycle were regarded as the end-diastolic (EDV) and end-systolic volume (ESV), respectively.

The bulk external mechanical stroke work done by the left ventricle was obtained from the left ventricular pressure-volume relation as mentioned in CHAPTER III. This stroke work was normalized by the left ventricular weight (LVW) measured during autopsy, and multiplied by the heart rate (HR) to obtain the bulk mechanical work per second (BMW).

The left ventricular wall tension,  $T_w$ , was calculated by eq. (3.2). The subendocardial rhombus area,  $A_m$ , surrounded by two pairs of sensors for the measurement of segment length was calculated by eq. (3.3). The end-diastolic and end-systolic myocardial area (EDA and ESA, respectively) were determined at the same time as the EDV and ESV were obtained, respectively.

From a relation between  $T_w$  and  $A_m$ , the regional external mechanical stroke work done by the local myocardium was obtained as stated in CHAPTER III, and was normalized in the same way as that used in CHAPTER V (1) to obtain the regional mechanical work per second (RMW), where the regional myocardial volume was calculated multiplying the rhombus subendocardial area by the wall thickness measured during autopsy.

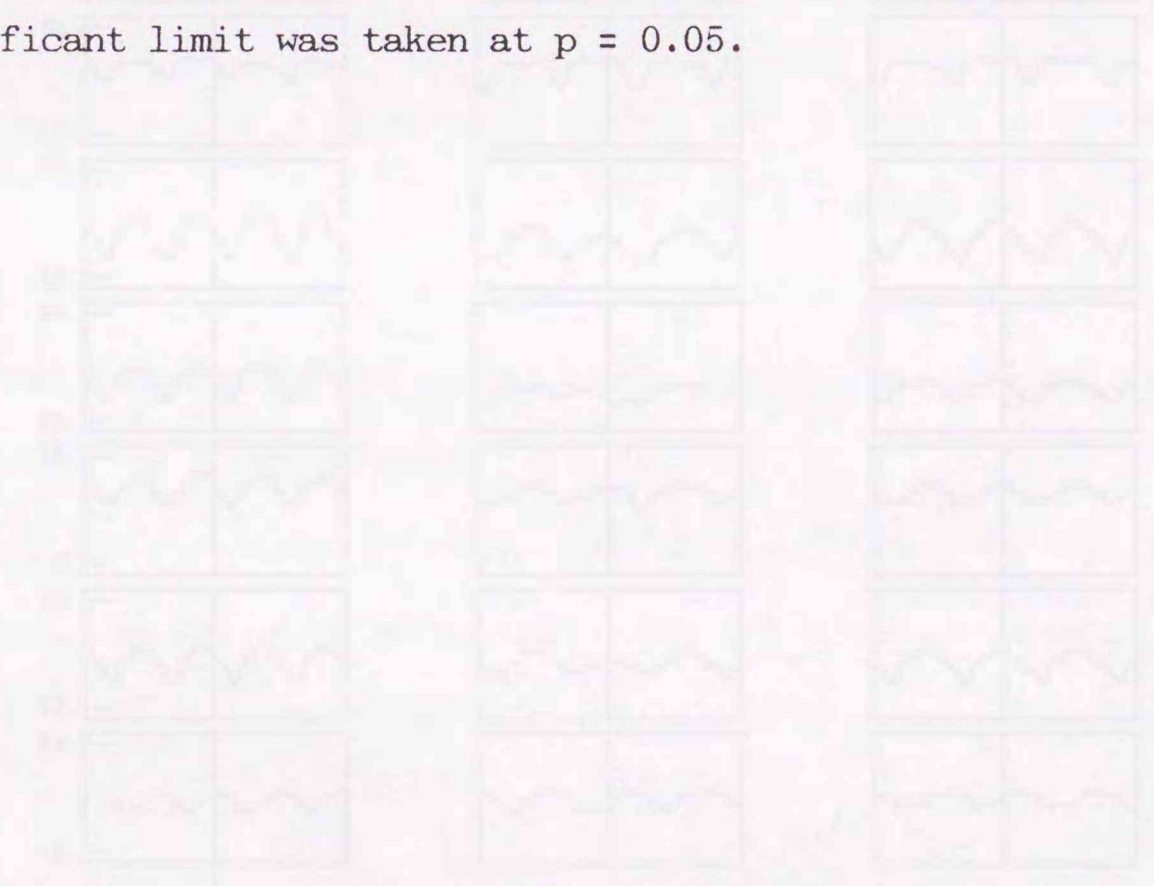
All data shown in this chapter are expressed as mean values  $\pm$  one

standard deviations (SD) except for the data expressed by %. The percentage data are shown by mean values only.

#### 7.2.4 Histology

Myocyte diameter was used as a histological parameter. The myocardium located at the central part of the left ventricular free wall was cut out and used to make histological specimens stained with hematoxylin-eosin. To avoid the influence of cutting angle against the axis of myocyte, the shortest diameter of each myocyte containing cellular nucleus was measured using microscopic photographs of the endocardial one-third, middle, and epicardial one-third layers, assuming that the cross section of myocardial filament is round.

Statistical significance was evaluated by the standard t test, where significant limit was taken at  $p = 0.05$ .



7.3 RESULTS

Figure 7.2 shows the waveforms of hemodynamic and cardiac parameters measured on the 10th post-operative day in the P8613 experiment. The peak-to-peak value of each left ventricular dimension in a cardiac cycle measured during LVAD pumping was generally smaller than that obtained under pump-off condition, showing unloading effect of LVAD.

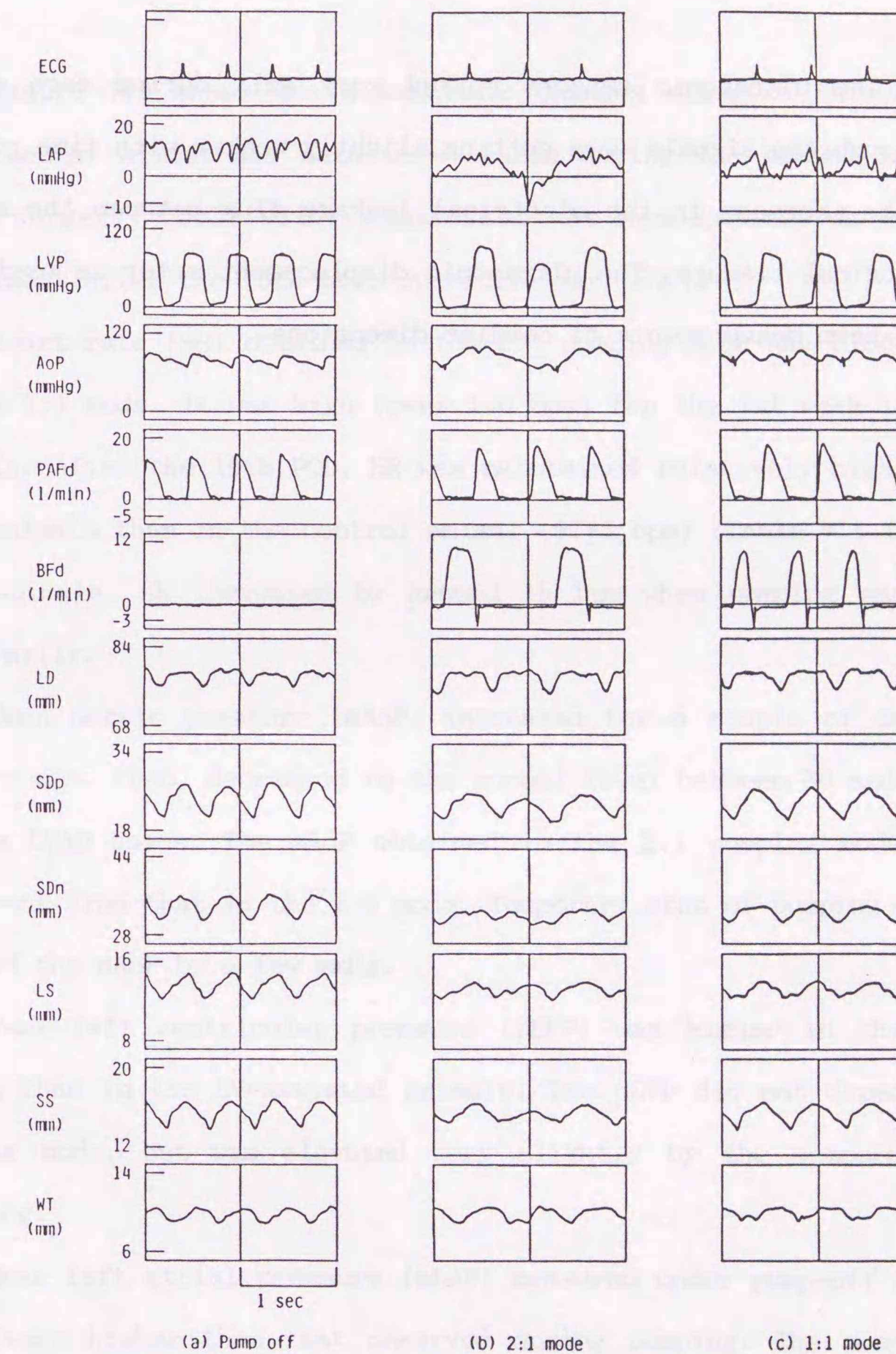


Fig. 7.2 Phasic tracings (computer output) of electrocardiogram (ECG), left atrial pressure (LAP), left ventricular pressure (LVP), aortic pressure (AoP), pulmonary arterial flow (PAFd), pump bypass flow (BFd), long axis diameter of the left ventricle (LD), short axis diameter parallel (SDp) and perpendicular (SDn) to the septum, meridian (LS) and equatorial (SS) segment length of the left ventricular free wall, and wall thickness (WT). Data were obtained on the 10th post-operative day in the P8613 experiment.

### 7.3.1 Feasibility of the long-term ultrasonic measurements

The ultrasonic sensors worked very well during each experiment, although the signals were getting slightly weaker with time possibly due to the increase in the electrical leakage flux between the sensors and biological tissues. The ultrasonic displacement meter is useful for the long-term measurements of cardiac dimensions.

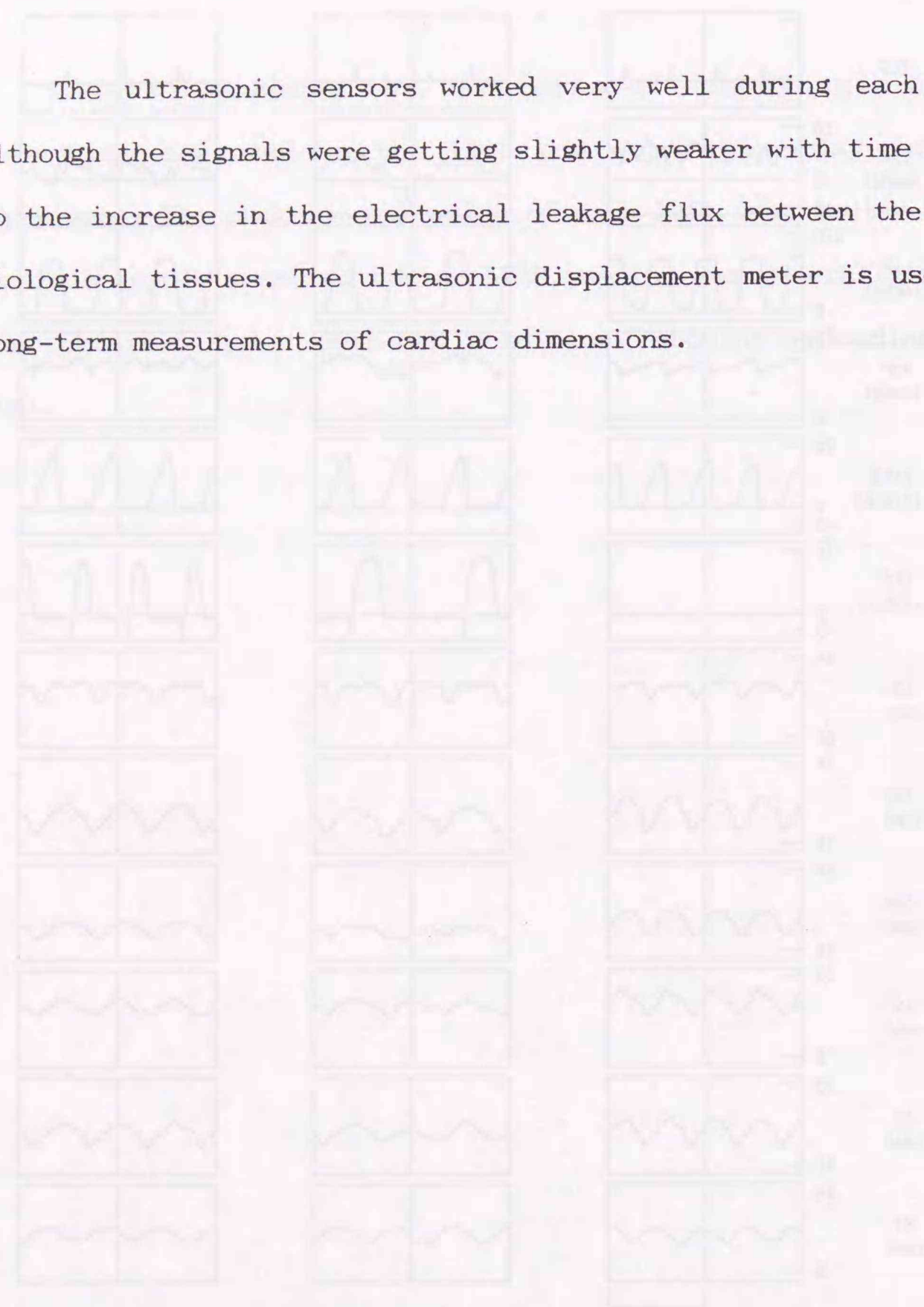


Fig. 7.3. Ultrasonic measurements of cardiac dimensions. The traces show the displacement of the ultrasonic sensor over time. The traces are arranged in three columns, with eight traces per column. The traces show a series of peaks and troughs, representing cardiac dimensions over time.

### 7.3.2 Hemodynamics

Figure 7.3 shows the hemodynamic changes observed throughout the experiments. Almost all data were stable during the second half month after surgery. Table VII.I summarizes the hemodynamic data in each experiment after the 15th post-operative day (POD).

Heart rate (HR) obtained in the 2:1 pumping mode was close to that in the 1:1 mode. It was high (over 140 bpm) for the 1st week in all the animals. After the 15th POD, HR was maintained relatively higher in the LVAD animals than in the control animal ( $97 \pm 5$  bpm) (Table VII.I). In the LVAD animals, HR increased by around 15 bpm when pumping was stopped temporarily.

Mean aortic pressure (mAoP) increased for a couple of days after surgery and, then, decreased to the normal level between 80 and 100 mmHg in the LVAD cases. The mAoP obtained in the 2:1 pumping mode was not different from that in the 1:1 mode. Temporary stop of pumping sometimes reduced the mAoP by a few mmHg.

Peak left ventricular pressure (pLVP) was higher in the control animal than in the LV-assisted animals. The pLVP did not depend on the pumping mode, but was elevated very slightly by the temporary pump-stopping.

Mean left atrial pressure (mLAP) measured under pump-off condition was always higher than that observed during pumping. The pumping mode did not much affect the mLAP.

Pulmonary arterial flow (PAF) decreased by 8 and 6 % in P8520 and P8613, respectively, when pumping was stopped temporarily. Again, PAF was not affected by the drive mode.

Pump bypass flow in the 2:1 pumping mode was higher than that in

the 1:1 mode by around 20 ml/min/kg in each animal. After the 15th POD, the bypass ratio (BF/PAF) was 68 and 96 % in the 2:1 mode for P8520 and P8613, respectively, and 55 and 78 %, respectively, in the 1:1 mode. Almost total bypass was observed in P8613 under the 2:1-mode drive condition.

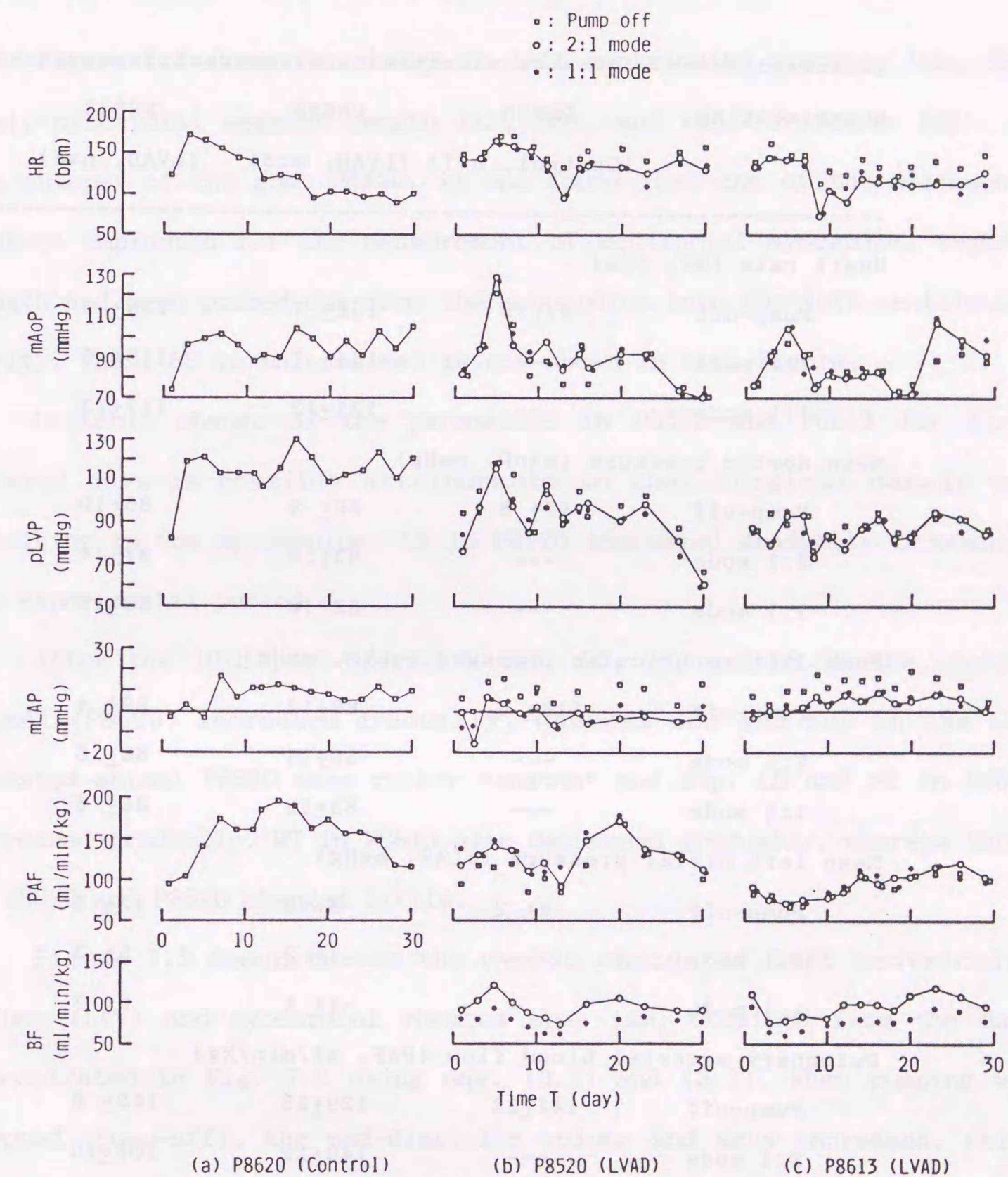


Fig. 7.3 Change in the hemodynamic parameters. HR, heart rate; mAoP, mean aortic pressure; pLVP, peak left ventricular pressure; mLAP, mean left atrial pressure. The other abbreviations are the same as those in Fig. 7.2.

Table VII.I Hemodynamic data (Mean±SD) obtained after the 15th post-operative day when the animal condition became stable.

Experiment no.	P8620 (Control, n=7)	P8520 (LVAD, n=5)	P8613 (LVAD, n=6)
Heart rate (HR, bpm)			
Pump-off	97± 5	152± 7	136± 9
2:1 mode	---	134± 7	116± 6
1:1 mode	---	131±12	117±13
Mean aortic pressure (mAoP, mmHg)			
Pump-off	97± 6	80± 9	85±10
2:1 mode	---	83±10	87±14
1:1 mode	---	82±10	88±15
Peak left ventricular pressure (pLVP, mmHg)			
Pump-off	116± 6	89±14	89± 4
2:1 mode	---	86±16	88± 5
1:1 mode	---	83±16	86± 6
Mean left atrial pressure (mLAP, mmHg)			
Pump-off	8± 2	8± 5	13± 5
2:1 mode	---	-4± 2	5± 3
1:1 mode	---	-1± 4	6± 3
Pulmonary arterial blood flow (PAF, ml/min/kg)			
Pump-off	147±22	129±25	100± 8
2:1 mode	---	140±22	106±10
1:1 mode	---	141±26	105± 9
Bypass flow (BF, ml/min/kg)			
2:1 mode	---	95± 6	102±11
1:1 mode	---	78± 3	82± 7

### 7.3.3 Left ventricular dimension

Figure 7.4 shows the change in left ventricular diameter (LD, SDp, SDn), myocardial segment length (LS, SS), and wall thickness (WT). At the autopsy of the goat P8520, it was found that one of the ultrasonic sensors implanted for the measurement of equatorial myocardial segment length had been pushed out from the myocardium into the left ventricular cavity. Thus, SS in this animal is not shown in this figure.

Unstable change of the parameters in P8520 and P8613 for first several days is possibly attributable to that surgical damage was remaining in the myocardium. LS in P8520 increased gradually throughout the experimental period.

After the 10th post-operative day, LD, SDp and LS in the control animal (P8620) increased gradually, whereas SDn and SDp in the LV-assisted animal P8520 were rather constant and SDp, LS and SS in P8613 decreased gradually. WT in P8613 also decreased gradually, whereas those in P8620 and P8520 changed little.

Figure 7.5 demonstrates the cyclic change of left ventricular volume (LVV) and myocardial rhombus area (Am) obtained from the data demonstrated in Fig. 7.2 using eqs. (3.1) and (3.3). When pumping was stopped (pump-off), the end-diastolic volume and area increased, while the systolic volume and area did not change much.

Figure 7.6 shows the change in the end-diastolic and end-systolic left ventricular volume (EDV and ESV, respectively), and end-diastolic and end-systolic regional myocardial area (EDA and ESA, respectively). EDV and ESV in the control animal increased gradually from 30 and 20 ml to 50 and 30 ml, respectively. EDA and ESA were smaller for the first several days than those obtained thereafter, possibly due to the

myocardial local damage caused by surgical maneuvers.

EDV and ESV in the LV-assisted animal P8613 showed little change throughout the experiment. EDV obtained during pumping was smaller than that recorded under temporary pump-off condition, whereas ESV was not affected by pump-off nor by pumping condition. EDA and ESA observed in the same animal showed some irregular changes for the first 10 days, although EDA became fairly stable thereafter and ESA gradually decreased. The effects of the change in the pumping mode and temporary pumping-off on EDA and ESA were the same as those on EDV and ESV, respectively. In the experiment P8520, EDV and ESV showed a tendency of a slight increase throughout the experiment. EDA and ESA were not shown for this animal because of the reason mentioned above. The stroke volume (EDV-ESV) during pumping was slightly smaller than that obtained under pump-off condition.

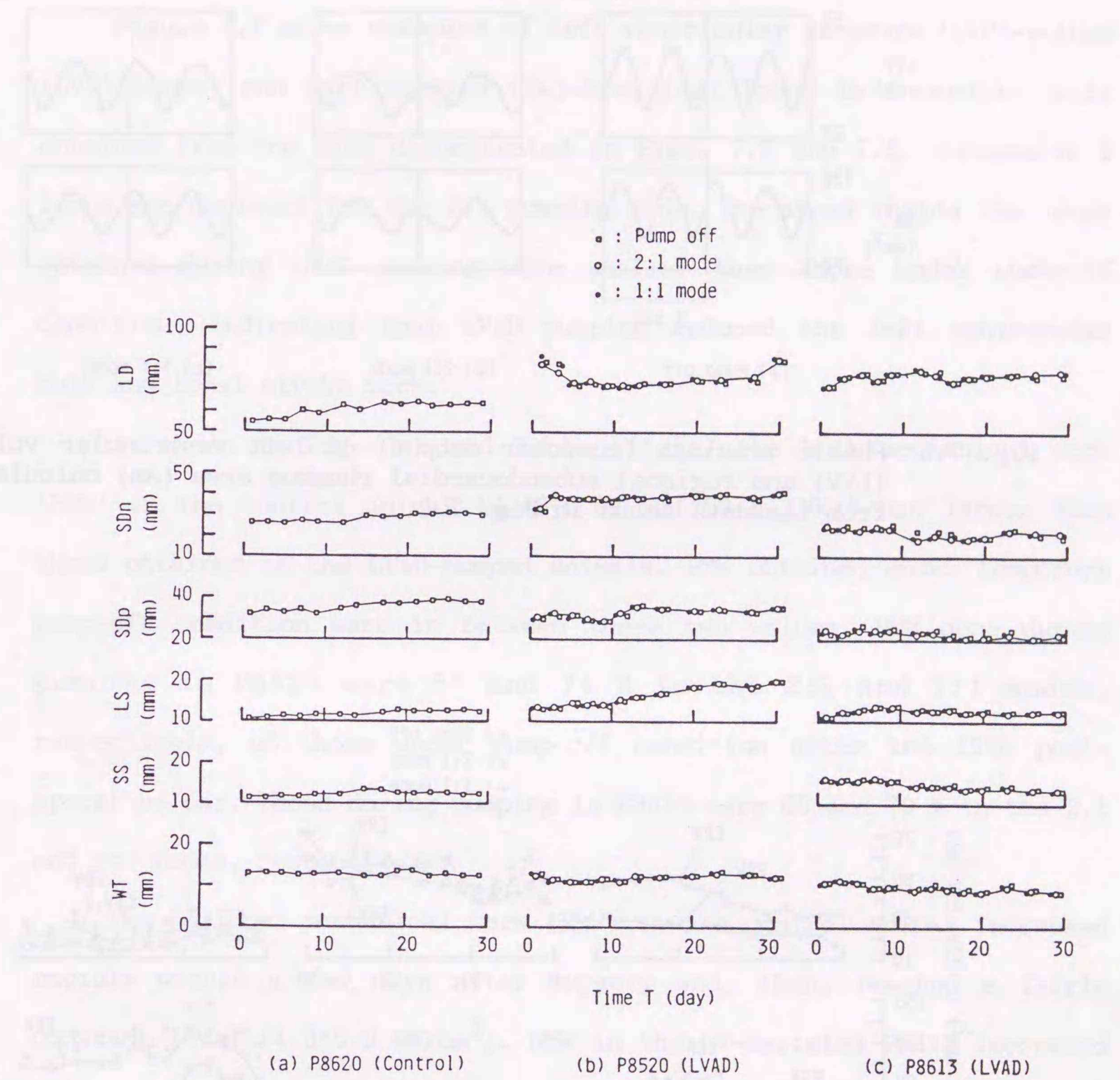


Fig. 7.4 Change in the averaged cardiac dimensions. The abbreviations are the same as those in Fig. 7.2.

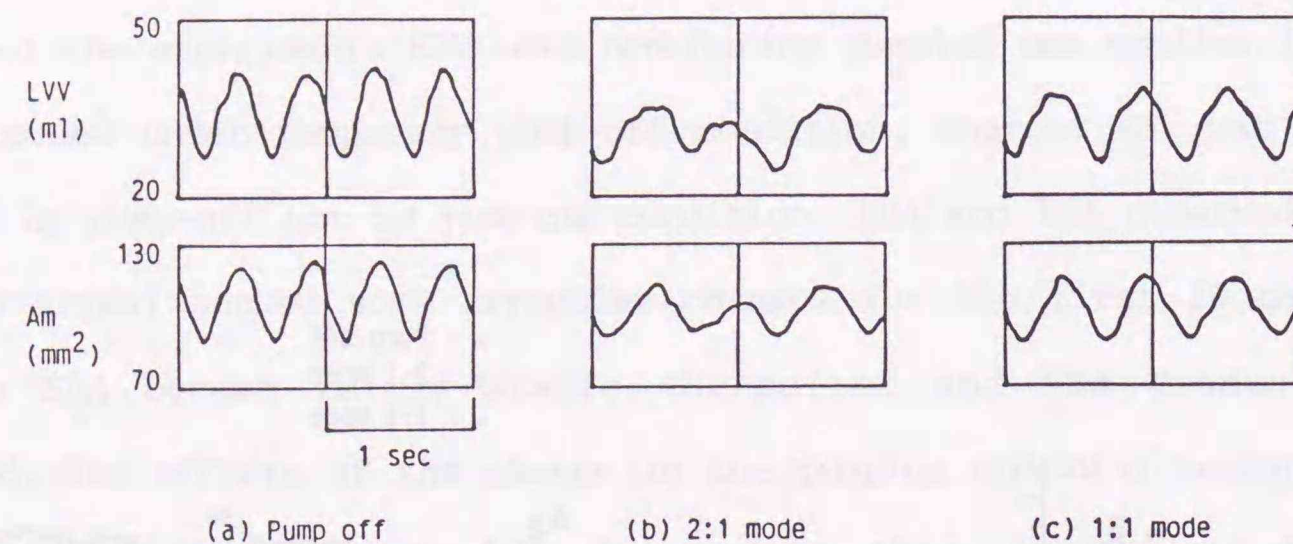


Fig. 7.5 Phasic tracings (computer output) of left ventricular volume (LVV) and regional subendocardial rhombus area (Am) calculated from the data shown in Fig. 7.2.

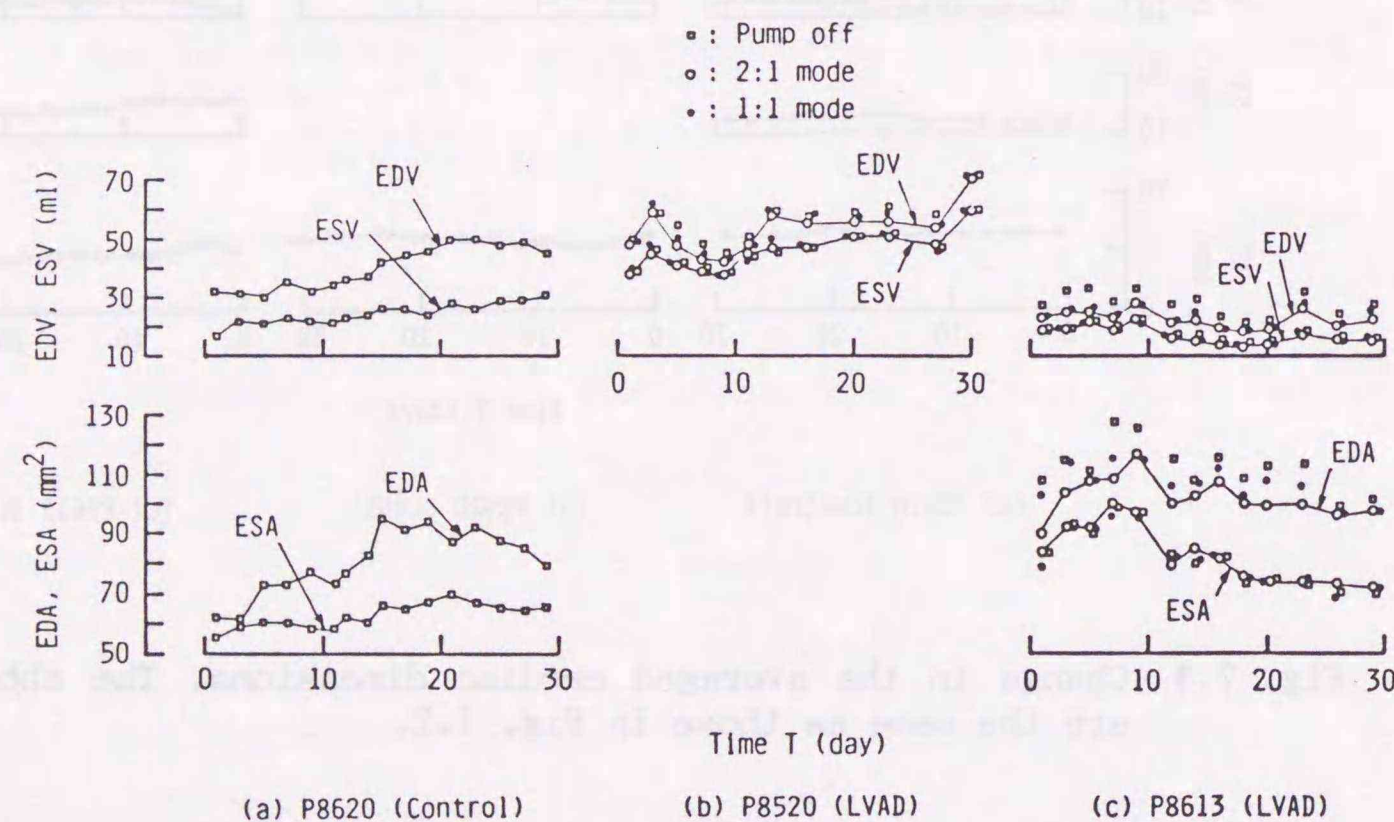


Fig. 7.6 Change in the left ventricular end-diastolic (EDV) and end-systolic (ESV) volume, and end-systolic (EDA) and end-diastolic (ESA) subendocardial rhombus area.

#### 7.3.4 Bulk and regional mechanical work

Figure 7.7 shows examples of left ventricular pressure (LVP)-volume (LVV) loops, and wall tension (Tw)-area (Am) loops in a cardiac cycle obtained from the data demonstrated in Figs. 7.2 and 7.5. Successive 2 loops are depicted for the 2:1 pumping mode. The areas inside the loops obtained during LVAD pumping were smaller than those under pump-off condition, indicating that LVAD pumping reduced the left ventricular bulk and local stroke work.

As shown in Fig. 7.8 and Table VII.II, the bulk mechanical work (BMW) in the control animal ( $0.43 \pm 0.07$  W/(100 g LVW)) was larger than those obtained in the LVAD-pumped animals. BMW obtained under temporary pump-off condition were in between these two values. BMW done during pumping in P8520 were 57 and 74 % in the 2:1 and 1:1 modes, respectively, of those under pump-off condition after the 15th post-operative day. Those during pumping in P8613 were 60 and 70 % in the 2:1 and 1:1 modes, respectively.

The regional mechanical work (RMW) in the control animal increased rapidly within a few days after surgery and, then, reached a fairly constant level ( $4.3 \pm 0.9$  mW/cm<sup>3</sup>). RMW in the LV-assisted P8613 increased gradually for 2 weeks after surgery and, then, reached constant levels of  $6.2 \pm 0.7$ ,  $4.3 \pm 0.5$  and  $4.6 \pm 0.8$  mW/cm<sup>3</sup> under the pump-off, 2:1-mode and 1:1-mode conditions, respectively. RMW done during pumping were 69 and 74 % in the 2:1 and 1:1 modes, respectively, of those obtained under pump-off condition. RMW obtained under pump-off condition during the last 15 days was somewhat larger than that in the control animal.

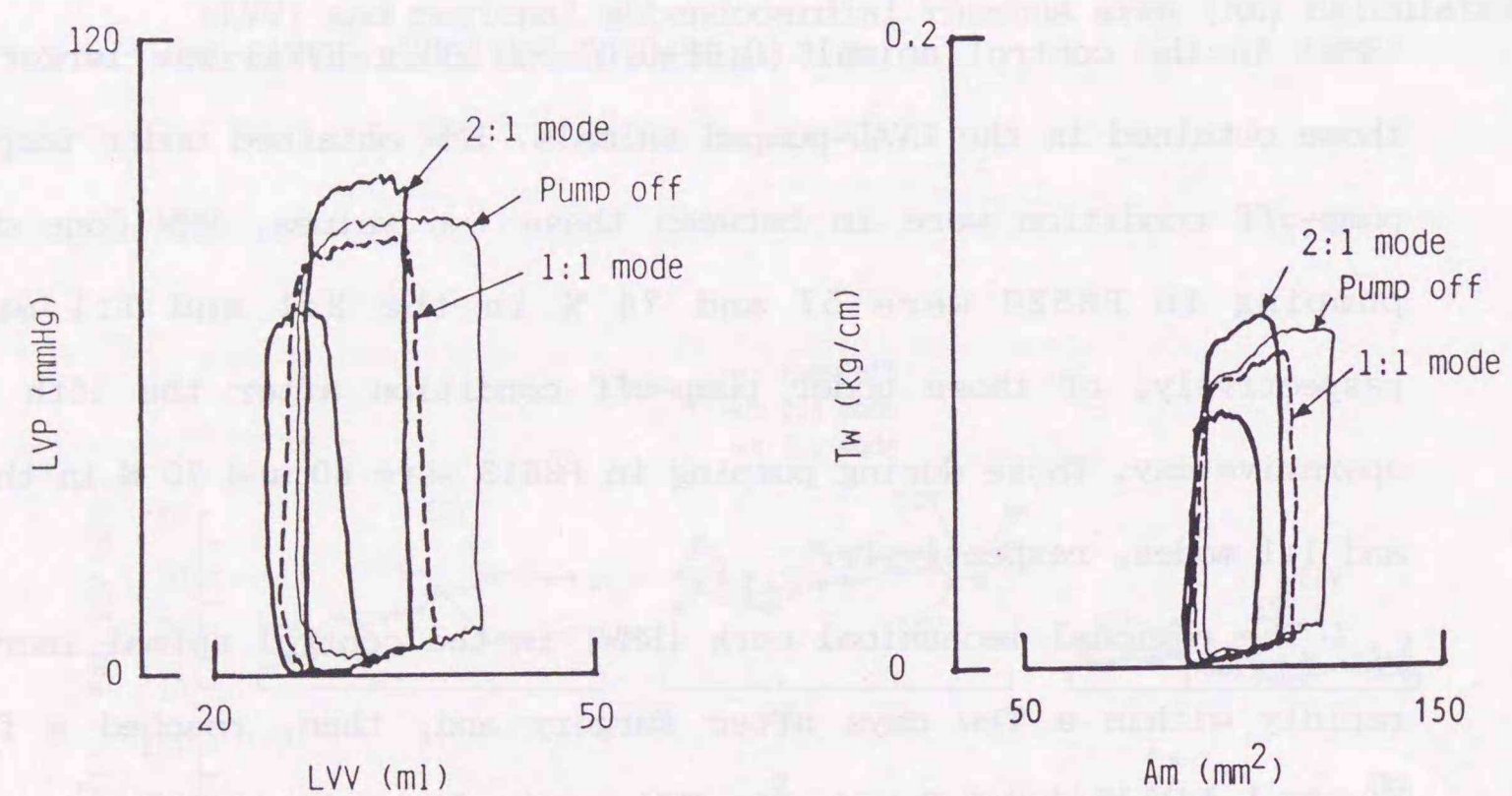


Fig. 7.7 Relationships between the left ventricular pressure (LVP) and volume (LVV) (left figure), and between the regional wall tension (Tw) and area (Am) (right figure) in a cardiac cycle obtained from the data shown in Figs. 7.2 and 7.5.

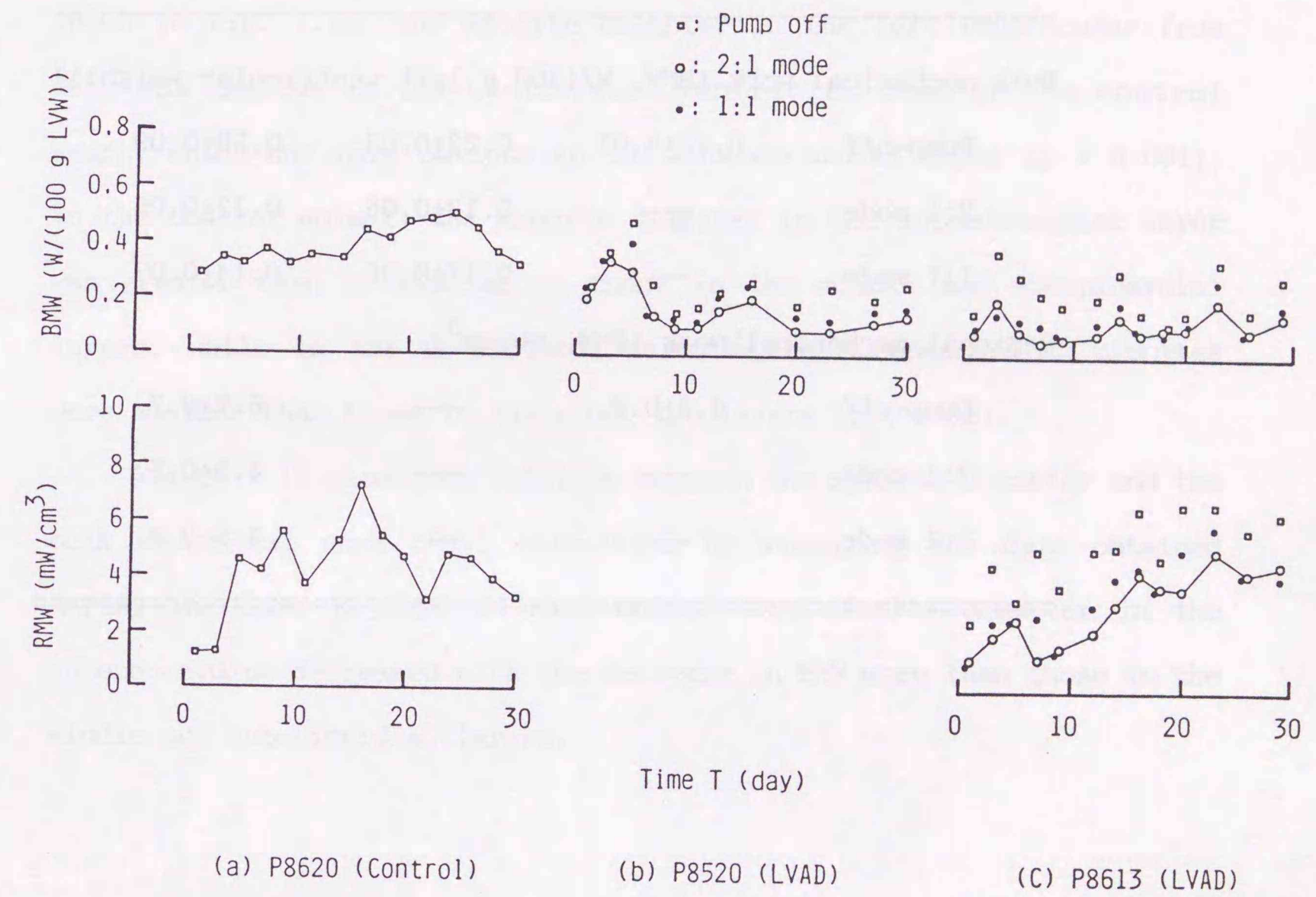


Fig. 7.8 Change in the bulk and regional mechanical work (BMW and RMW, respectively).

Table VII.II Cardiac data (Mean±SD) after the 15th post-operative day when the animal condition became stable.

Experiment no.	P8620 (Control, n=7)	P8520 (LVAD, n=5)	P8613 (LVAD, n=6)
Bulk mechanical work (BMW, W/(100 g left ventricular weight))			
Pump-off	0.43±0.07	0.23±0.03	0.20±0.09
2:1 mode	---	0.13±0.05	0.12±0.05
1:1 mode	---	0.17±0.05	0.14±0.07
Regional mechanical work (RMW, mW/cm <sup>3</sup> )			
Pump-off	4.3±0.9	---	6.2±0.7
2:1 mode	---	---	4.3±0.5
1:1 mode	---	---	4.6±0.8

### 7.3.5 Histological Study

Figure 7.9 shows photographs of the histological specimens obtained from subepicardium (a), middle myocardium (b) and subendocardium (c) of the control and LV-assisted animals (P8620 and P8613, respectively). As shown in Fig. 7.10, the myocyte diameter in the left ventricular free wall was smaller in the LV-assisted ventricles than in the control heart, which was more obvious in the subendocardial layer ( $p < 0.001$ ). In the control animal, the myocyte diameter in the subendocardial layer was greater than or similar to those in the middle and subepicardial layers, while in the LV-assisted animals the subendocardial myocytes were smaller than those in the other two layers ( $p < 0.02$ ).

Figure 7.11 shows the relation between the myocyte diameter and the bulk mechanical work (BMW) calculated by averaging the data obtained during the last 10 days in each animal. The myocyte diameter in the subendocardium decreased with the decrease in BMW more than those in the middle and subepicardial layers.

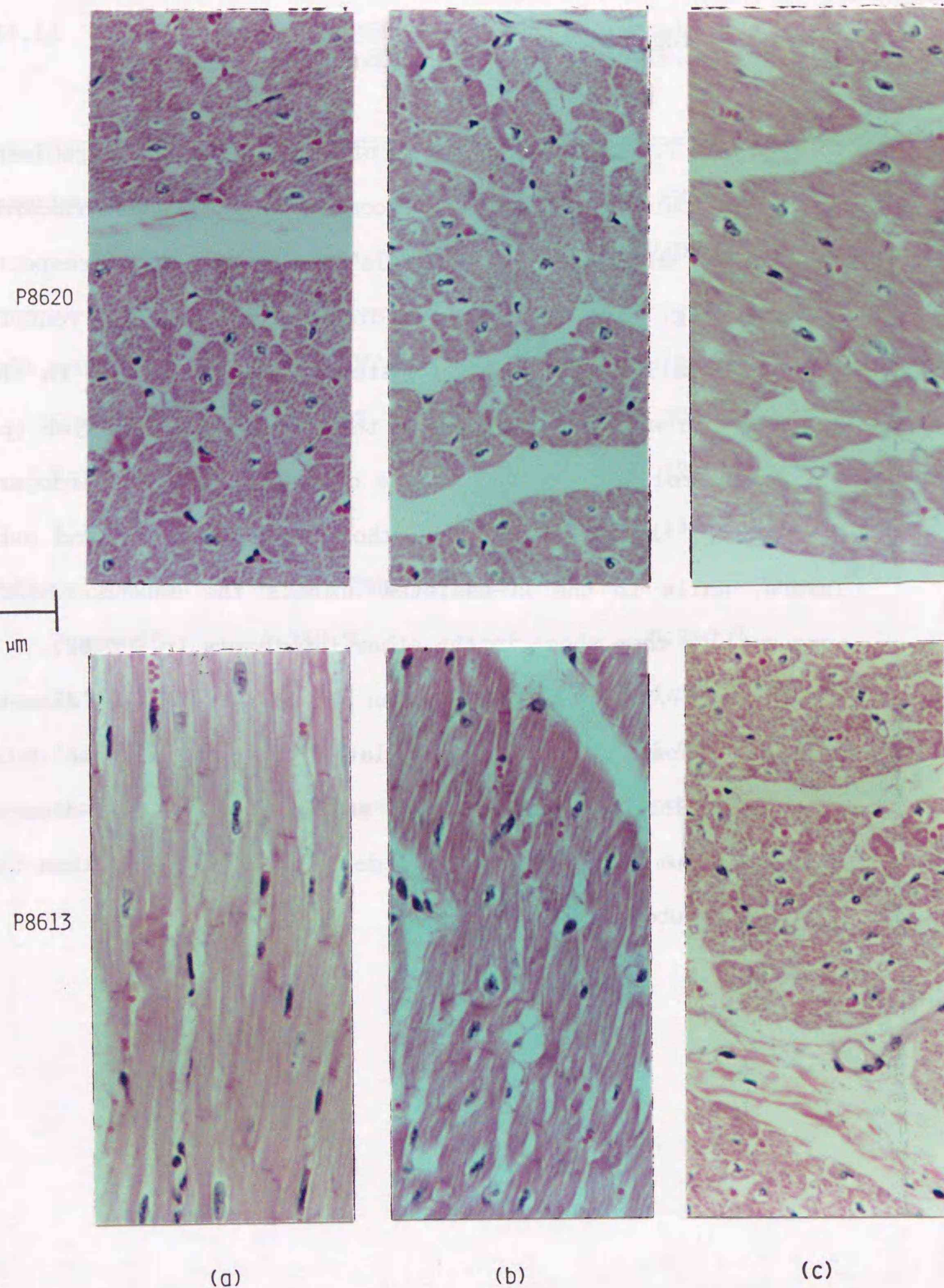


Fig. 7.9 Photographs of histological specimens obtained from subepicardium (a), middle myocardium (b), and subendocardium (c) stained with hematoxylin-eosin, obtained from the control (P8620) and LV-assisted (P8613) animals.

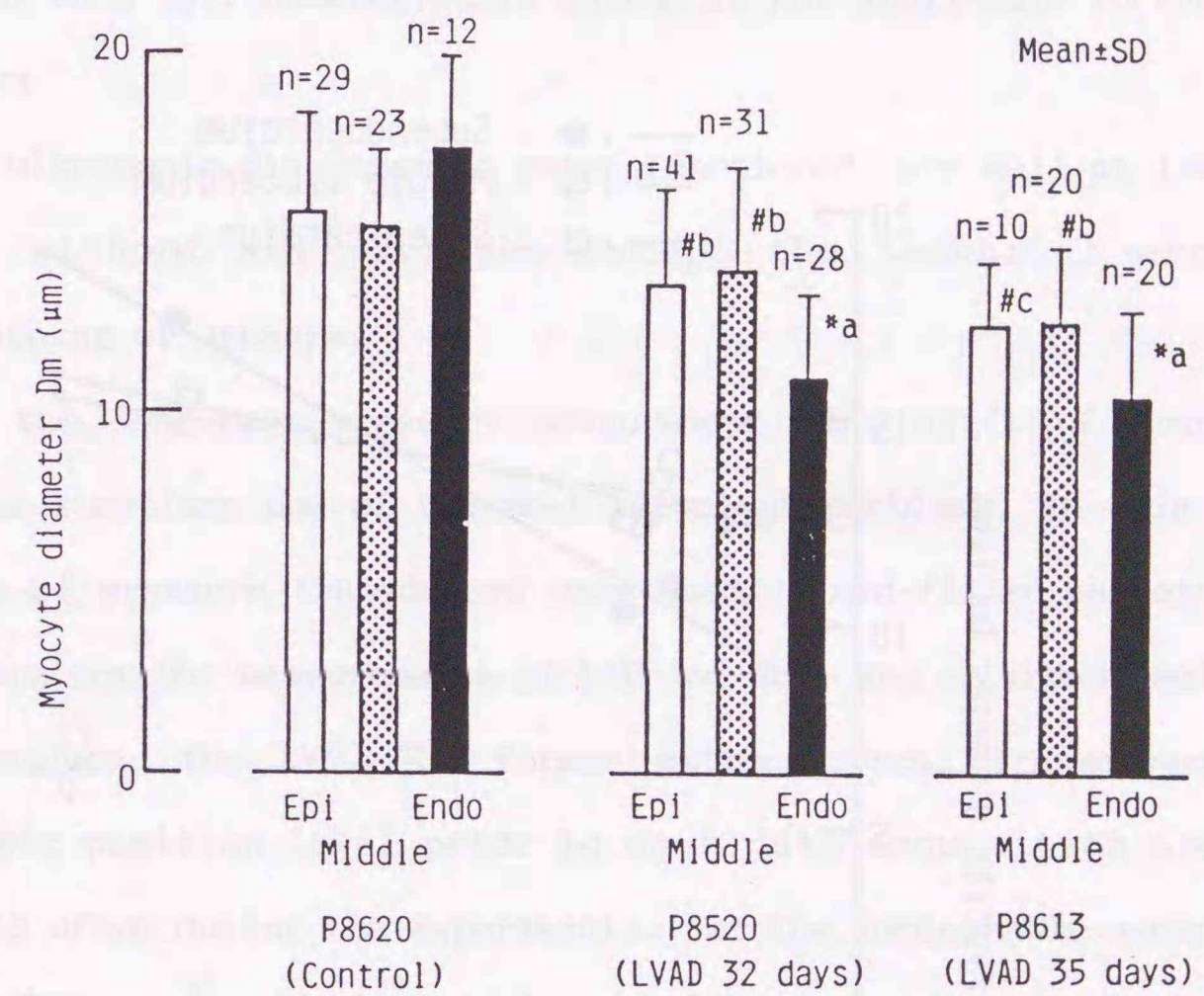


Fig. 7.10 Myocyte diameter (Dm) in the subepicardial, middle and subendocardial one-third layers (Epi, Middle and Endo, respectively) of the left ventricular free wall. Key: a,  $p < 0.001$ ; b,  $p < 0.005$ ; c,  $p < 0.02$ ; \*, compared to the subendocardial data of control animal; #, compared to the subendocardial data of each animal.

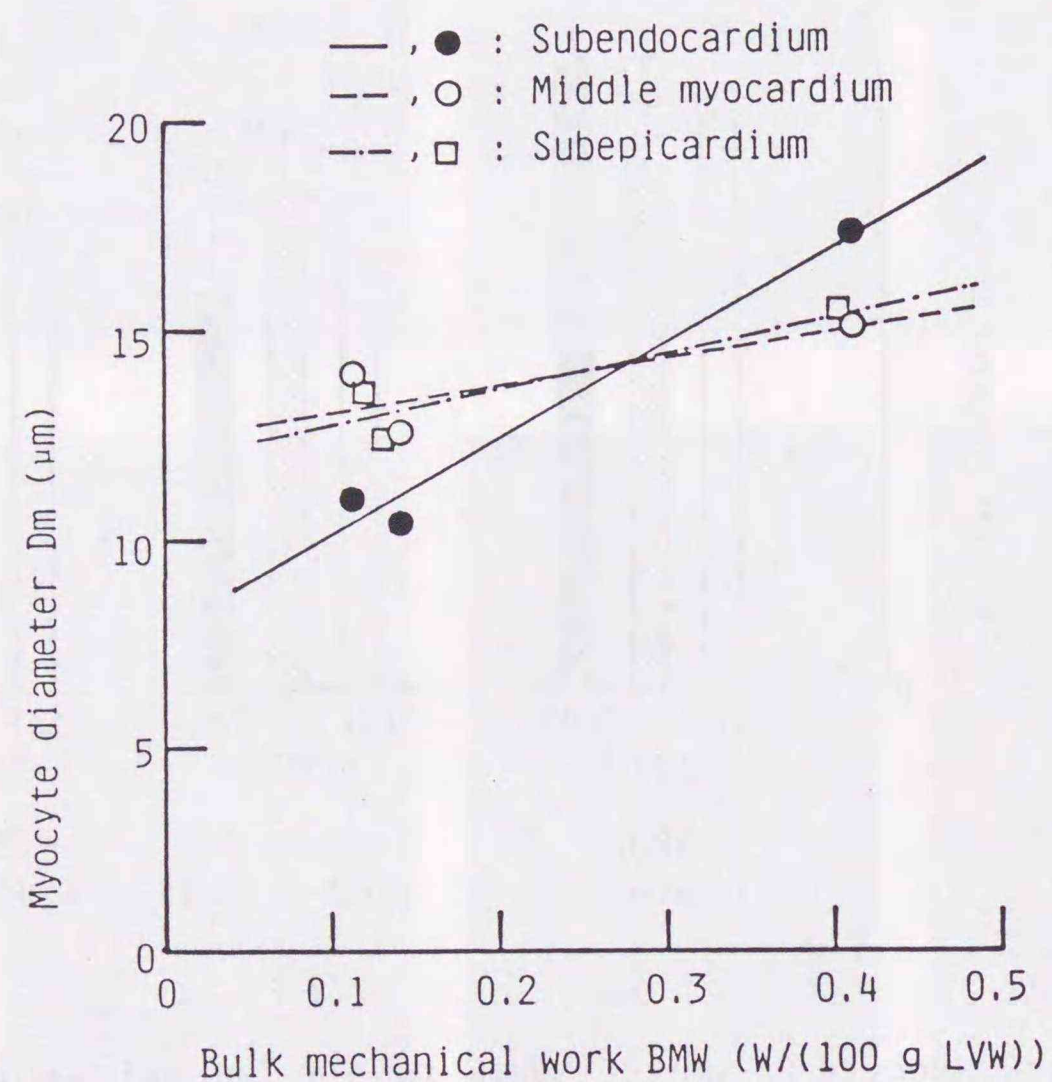


Fig. 7.11 Relationships between the myocyte diameter (Dm) and bulk mechanical work (BMW). Three regression lines were calculated by a least squares method for each layer.

By chronic animal experiments, Nakatani et al. obtained the left ventricular volume by means of the left ventriculography to depict the LVP-LVV loop, and showed that LVAD pumping reduces the left ventricular mechanical work (9). However, this method is not applicable to the local myocardium.

The ultrasonic displacement meter functioned very well at least for a month without any problems except the technical error of malpositioning of sensors.

For the long-term pressure measurement, the drift of transducer signals is sometimes one of the most important problems. In this study, two types of pressure transducers were used: fluid-filled catheter-type transducers for the measurements of LAP and AoP, and an indwellable tip-type transducer for LVP. The former extracorporeal transducers were reset their position level prior to each data acquisition and were calibrated often during the experiments. For the implantable sensor, the drifts of signals were measured prior to these experiments, which showed that the drifts for a month are as quite small as less than 1.8 mmHg.

Based on the results described in CHAPTER V (1), ECG synchronous pumping modes with the duty ratios of 2:1 and 1:1 were selected for this study. The drive pressure, drive vacuum, pumping delay from the onset of cardiac cycle, and %-systole of the pumping were manually adjusted several times everyday to obtain the maximum pump bypass flow.

The hemodynamic parameters were almost stable after around the 10th post-operative day (POD): surgical effects seemed to remain for a week or 10 days. The differences in the hemodynamic data between the 2:1 and 1:1 modes were very little except the bypass flow (Fig. 7.3 and Table

VII.I). These results are different from those obtained in the acute experiments (CHAPTER V) (1), where the 1:1 mode was superior to the 2:1 mode for maintaining the circulatory condition well. The main reason for the difference might be attributable to the difference in the metabolism between the anesthetized animals in the former acute experiments and the conscious ones in the present experiments.

The left ventricular dimensional data, which are affected by surgical damage, ventricular contractility, stroke volume (circulatory blood volume), pump-on or -off, and so on, were also stable during the last half period of the experiments. LD and SDp in the control animal (P8620) increased gradually, whereas those in the LV-assisted animals did not change much (P8520) or rather decreased (SDp in P8613)(Fig. 7.4). Although the reason for the increase in these diameter is not known well, the phenomena observed in the assisted ventricles may show their morphological adaptation caused by the unloading effect of LVAD: the assisted ventricles do not need to have large diameter.

WT in P8613 also decreased gradually, whereas those in P8620 and P8520 changed little. This phenomenon could be related to the fact that almost all the blood was bypassed in this particular animal P8613. Such a great unloading might have reduced the wall thickness.

As shown in Fig. 7.6, the differences between EDV and ESV, i.e. stroke volume, in the LV-assisted animals were similar to each other but significantly smaller than those in the control animal, which means that the stroke volume in the assisted ventricle is less than in the control heart. EDV was increased much more than ESV by the temporary pump-off maneuver, which possibly causes the small stroke volume during pumping.

The bulk and regional mechanical work done during pumping were

smaller than those observed under pump-off condition (Fig. 7.8), which was brought about by such a decrease in the end-diastolic volume and area during pumping as stated above. These results are consistent with those obtained in the acute experiments shown in the previous chapters (1,2).

BMW in the 2:1 and 1:1 pumping modes were 59 (57 % for P8520 and 60 % for P8613) and 72 % (74 % for P8520 and 70 % for P8613), respectively, of those obtained under pump-off condition. The regional mechanical work in the 2:1 and 1:1 modes were 69 and 74 %, respectively. These results show that the 2:1 mode is more useful for the reduction of the left ventricular mechanical work, which is consistent to such a result obtained by acute experiments as described in CHAPTER V (1).

Kinoshita et al. reported that the myocardial histological change observed after the 3-month implantation of LVAD was atrophic, although little change was observed after 1-month pumping (10). Since the normal natural heart was very powerful before the LVAD implantation and had enough cardiac reserve to tolerate even against such a high load condition as exercise, the 1-month LVAD pumping should have reduced only the myocardial reserve.

In the histological observation, the myocardium was divided into 3 parts: subendocardial, middle and subepicardial layers. There were no large differences in the myocyte diameter in the middle and subepicardial layers between the LV-assisted and non-pumped myocardia, which is a similar finding to that reported by Kinoshita et al. (10). However, the subendocardial myocytes in the LV-assisted ventricles were thinner than those in the control heart. Since the subendocardium is more highly stressed and contributes more to the left ventricular mechanical work than the subepicardium, it is reasonable that the

subendocardial myocyte diameter was somewhat greater than that in the middle and subepicardial layers in the control animal, and that the decreased load by the LVAD pumping reduced the myocyte dimension in the subendocardial layers more than those in the middle and subepicardial layers.

As shown in Fig. 7.11, the subendocardial myocyte diameter was closely related to the left ventricular bulk work, although the number of data was not satisfactory. This relation might result from the adaptation of myocardial fiber to the mechanical loading, which is often observed in the skeletal muscle. Longer pumping period than 1 month or larger amount of unloading even for shorter period causes the reduction of left ventricular work and may lead to the more atrophic change of the myocardium.

In the severely failed hearts experienced in clinical cases, the normal cardiac muscle is generally mixed with the damaged one especially in border zone. In those cases, the left ventricular load must be reduced much in order to rest the damaged myocardium and/or to avoid the ventricular rupture. However, the similar phenomena of myocardial atrophy to that observed here in the normal heart might appear in the normal part of the infarcted heart: excessive unloading may cause the atrophy of the normal myocardium even of failing heart at the same time and might result in slow recovery. Therefore, the pump-weaning timing and bypass rate are very important for the recovery of the damaged myocardium and the recovery process of the failed heart should be documented well for more effective use of this powerful mechanical means and, then, the optimal drive method and condition should be established.

Based on the results shown in this chapter, chronic animal experiments were conducted to study the effects of LVAD pumping on the

myocardial mechanics in the infarcted hearts, particularly to know the recovery mechanisms of the left ventricular function. The experimental method and the results are described in the next chapter.

## 7.5 SUMMARY

Pneumatically driven, diaphragm type left ventricular assist devices (LVADs) were implanted for around 1 month into 2 goats having normal hearts to study the effects of long-term pumping of LVAD on the cardiac mechanics. One sham operated goat was used to obtain control data. Diameters, and myocardial segment lengths of the left ventricle were measured with the ultrasonic displacement meter to obtain the bulk mechanical work (BMW) and regional myocardial mechanical work (RMW), respectively. LVAD was pumped in the 2:1 drive mode (one counterpulsated pumping in two cardiac cycles), and was driven temporarily in the 1:1 mode (one pumping in a cardiac cycle) or stopped to obtain the data under these conditions.

During the second half of the post-operative period while the animal condition was stable, BMW in the 2:1 and 1:1 modes were around 59 and 72 % of that observed under the temporary pump-off condition (0.22 W/(100 g)), respectively. RMW in the 2:1 and 1:1 modes were 69 and 74 % of that obtained during pump-off ( $6.2 \text{ mW/cm}^3$ ), respectively. The myocyte diameter in the subendocardial layer was reduced by unloading effect of one-month pumping, whereas those in middle and subepicardial layer showed little change.

## REFERENCES

1. Nakamura T, Hayashi K, Seki J, Nakatani T, Noda H, Takano H, Akutsu T. Effect of drive mode of left ventricular assist device on the left ventricular mechanics. *Artif Organs* 1988; 12: 56-66.
2. Nakamura T, Hayashi K, Seki J, Nakatani T, Noda H, Fukuda S, Takano H, Akutsu T. Effects of cardiac assist on the bulk and regional mechanics of the ischemic left ventricle in dogs. *Artif Organs* 1990; 14: 57-68.
3. Takano H, Taenaka Y, Nakatani T, Akutsu T, Fujita T, Manabe H. Circulation control of experimental and clinical profound left ventricular failure by automatic left ventricular assist system. *Jap Circ J* 1984; 48: 302-11.
4. Nakamura T, Hayashi K, Seki J. Eight-channel ultrasonic displacement meter for implantable miniature sensors. *Med & Biol Eng & Comput* 1987; 25: 355-8.
5. Little WC, Freeman GL, O'Rourke RA. Simultaneous determination of left ventricular end-systolic pressure-volume and pressure dimension relationships in closed-chest dogs. *Circulation* 1985; 71: 1301-8.
6. Suga H. Total mechanical energy of a ventricle model and cardiac oxygen consumption. *Am J Physiol* 1979; 236: H498-505.
7. Sugawara M, Tamiya K, Nakano K. Regional work of the ventricle: Wall tension-area relation. *Heart and Vessels* 1985; 1: 133-44.
8. Goto Y, Suga H, Yamada O, Igarashi Y, Saito M, Hiramori K. Left ventricular regional work from wall tension-area loop in canine heart. *Am J Physiol* 1986; 250: H151-8.
9. Nakatani T, Takano H, Taenaka Y, Umezu M, Tanaka T, Yutani C, Matsuda T, Iwata H, Noda H, Nakamura T, Takatani S, Seki J, Hayashi

K, Akutsu T, Manabe H. Therapeutic effect of left ventricular assist device on induced profound left ventricular failure. -Evaluation by left ventriculography- Trans Am Soc Artif Intern Organs 1984; 30: 533-9.

10. Kinoshita M, Takano H, Taenaka Y, Mori H, Takaichi S, Noda H, Tatsumi E, Yagura A, Sekii H, Akutsu T. Cardiac disuse atrophy during LVAD pumping. Trans Am Soc Artif Intern Organs 1988; 34: 208-12.

## CHAPTER VIII

### EFFECT OF LONG-TERM APPLICATION OF LEFT VENTRICULAR ASSIST DEVICE ON THE ISCHEMIC HEART

#### 8.1 INTRODUCTION

As was described in the previous chapters, acute experiments on the normal heart model indicated that LVAD pumping in the electrocardiogram (ECG) synchronous modes at the duty ratios of 1:1 and 2:1 are most effective to maintain the systemic circulation and to reduce the left ventricular mechanical work, respectively (1).

Based on these results, acute experiments on the ischemic heart model were carried out, and the results obtained showed that LVAD reduces the regional mechanical work done in the normal region, keeping the work done by the ischemic myocardium at near zero level, and decreases the bulk mechanical work of the left ventricle (2).

Subsequently to these acute experiments, a series of chronic experiments on goats with the normal hearts were performed to confirm the feasibility of long-term use of the sono-micrometers, and to study chronic effects of LVAD on the left ventricular mechanics (3). This study showed that LVAD exhibits a powerful unloading effect for a long period of time and that there might appear a subendocardial atrophy if applied under a continuously high unloading condition: these results imply that too much unloading may delay the recovery of damaged heart.

Even from these experiments, it is still unclear (i) whether the ischemic myocardium can be recovered by LVAD pumping, and (ii) how the

left ventricular function recovers. Although these subjects are very important, very few studies have been done.

The main purposes of the studies described in this chapter are to know chronic mechanical effects of LVAD on the ischemic heart and to analyze recovery process of the left ventricular function from myocardial damage.

## 8.2 METHOD

### 8.2.1 Experimental procedure

Eight goats of both sexes weighing between 25 and 35 kg (average 31.5 kg) were used for this study. Each animal was anesthetized with the mixture gas of fluothane and oxygen after administration of ketamine hydrochloride. While ventilation was maintained by a positive pressure respirator (Servo Ventilator 900C, Siemens-Elema, Sweden), left thoracotomy was performed at the 5th intercostal space, and the pericardium was widely opened.

The same LVAD system as that described in CHAPTER VII was implanted between the left atrium (LA) and the descending thoracic aorta as shown in Fig. 8.1.

Nine pairs of miniature ultrasonic sensors (around 2 mm in diameter) (4) were implanted in the left ventricle to measure left ventricular diameter, myocardial segment length, and wall thickness (Fig. 8.1).

Three pairs of these sensors were attached to the endocardial surface of the left ventricle to measure a long axis diameter (LD), and two short axis diameters parallel (SDp) and perpendicular (SDn) to the septum. The technique used for the implantation of these sensors was the same as that stated in the previous chapters (1-3).

A similar method to that described in CHAPTER VI was used to compare the behavior of normal myocardium with infarcted one. The central area of the left ventricular free wall was chosen as the 'normal' area and the distributing area of the left anterior descending coronary artery (LAD) as the 'ischemic' area, since the heart failure

was induced in the LAD distributing area as shown later.

Two pairs of sensors were embedded in the subendocardium to measure the segment length in the equatorial and meridian directions. The segment lengths in the equatorial and meridian directions are denoted by SSn and LSn, respectively, for the 'normal' area, and SSi and LSi, respectively, for the 'ischemic' area.

One pair of sensors were used for the measurement of left ventricular wall thickness (WTh and WTi for the 'normal' and 'ischemic' positions, respectively), which were embedded near the sensors for the measurement of segment length.

Left atrial pressure (LAP), aortic pressure (AoP), left ventricular pressure (LVP), pulmonary arterial flow (PAFd), and pump bypass flow (BFd) were measured in the same way as that described in CHAPTER VII. The extracorporeal pressure transducers used for the measurements of LAP and AoP were calibrated prior to each experiment and periodically during the experiments. The implantable pressure transducer for LVP was also calibrated prior to each experiment, and the long-term stability test showed that the drift of the output was low within 1.8 mmHg for 1 month, as was shown in CHAPTER VII (3). PAFd and BFd were normalized in the same way as that stated in CHAPTER VII.

After all the sensors and probes were implanted, the left anterior descending coronary artery (LAD) was ligated at the distal position to the first diagonal branch, and all small arteries in the LAD distributing area were ligated.

To maintain the systemic circulation under good condition, LVAD pump was driven in the asynchronous pumping mode (30 %-systole at 60 bpm pumping rate) during the implantation of the sensors and probes and the induction of left ventricular failure.

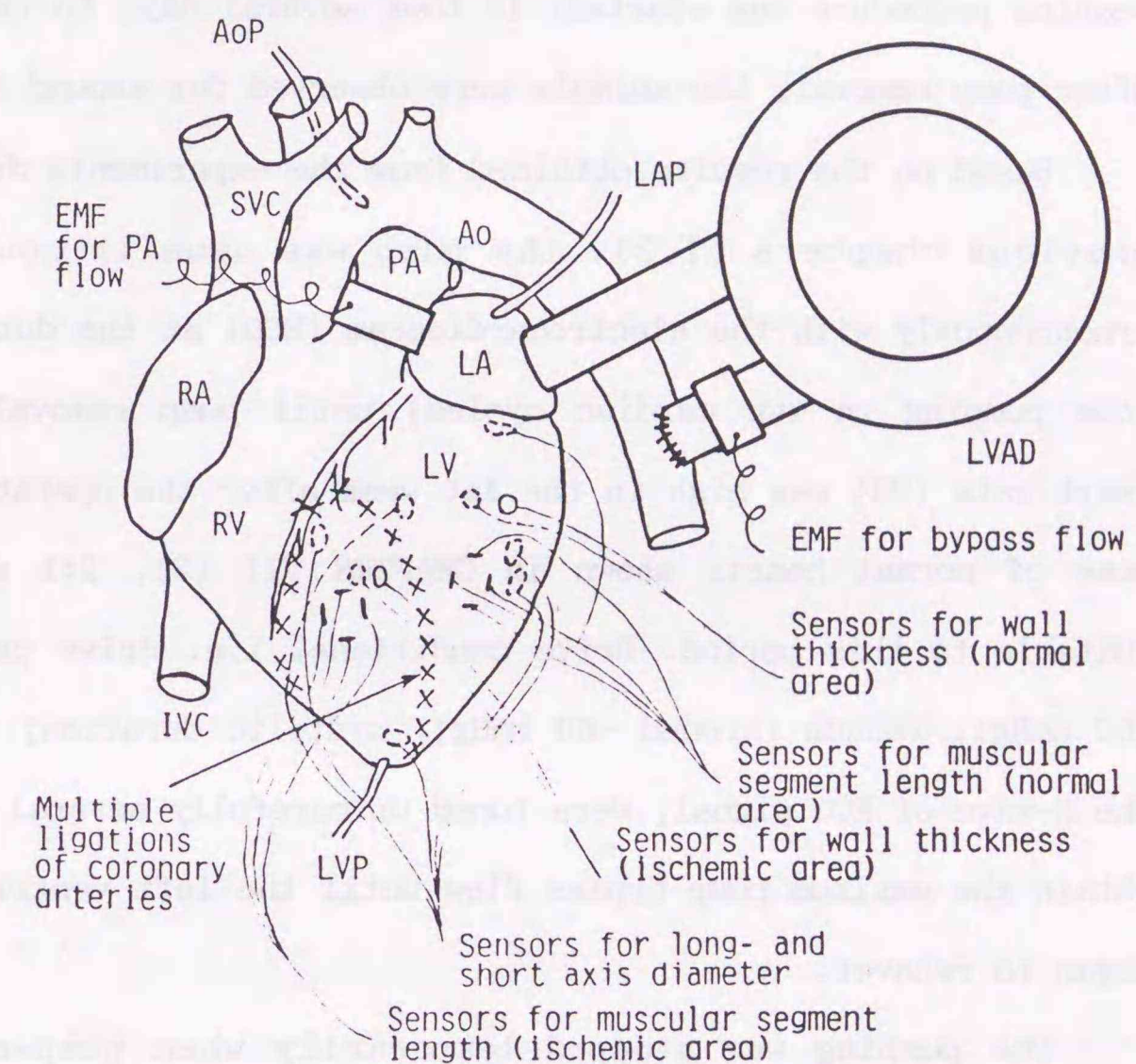


Fig. 8.1 Experimental arrangement. Ao, aorta; AoP, Ao pressure; EMF, electromagnetic flowmeter; IVC, inferior vena cava; LA, left atrium; LAP, LA pressure; LV, left ventricle; LVAD, LV assist device; LVP, LV pressure; PA, pulmonary artery; RA, right atrium; RAP, RA pressure; RV, right ventricle; SVC, superior vena cava.

### 8.2.2 Post-operative care

After the operation, the LVAD pumping was continued until pump removal. When the left ventricular function began to recover, the pump-weaning procedure was started. It took several days to remove the LVAD. After pump removal, the animals were observed for around 1 month.

Based on the results obtained from the experiments described in the previous chapters (1,2), the pump was usually counterpulsated synchronously with the electrocardiogram (ECG) at the duty ratio of 2:1 (one pumping in two cardiac cycles) until pump removal. Because the heart rate (HR) was high in the 1st week after the operation as was the case of normal hearts shown in CHAPTER VII (3), 2:1 drive mode was suitable to this period. Drive conditions, i.e. drive pressure (around 200 mmHg), vacuum (around -60 mmHg), systolic duration, and delay from the R-wave of ECG signal, were tuned up carefully several times a day to obtain the maximum pump bypass flow until the left ventricular function began to recover.

The pumping was stopped temporarily when pump-off data were acquired. During this procedure, the left ventricular function was evaluated by the left arterial pressure (LAP) level. If LAP did not exceed 20 mmHg when pumping was stopped, pump-weaning procedure was started: pump bypass flow was reduced slightly by reducing the drive pressure/vacuum and/or %-systole. This procedure was repeated once a day for several days until the bypass flow (BF) was reduced to 2 l/min which is the minimum flow for prevention of thrombus formation in the pump (5). If LAP became lower than 20 mmHg when pumping was stopped, the pump was removed under anesthetic condition, and the remained pump conduits were plugged by silicone stoppers in sterile environment. It took around

5 days to complete the pump-weaning and removal.

Each animal was kept for around 1 month thereafter to observe the recovery course and, then, sacrificed.

### 8.2.3 Post-operative data acquisition

Data were acquired once a day until sacrifice of animals, and recorded on magnetic tape for around 15 s each time by a data recorder (XR-510, Teac, Tokyo, Japan) and on the pen oscillographs (Polygraph 361 and Recti-Horiz 8K23, NEC San-ei, Tokyo, Japan).

Prior to the data acquisition, pumping condition was tuned to obtain the desired bypass flow. After all parameters became stable (usually within several minutes), hemodynamic and dimensional data were recorded during LVAD pumping in the 2:1 mode. Because the ultrasonic displacement meter has only 8 channels, the measurement was performed twice to obtain a series of data on 9 parameters. First, LD, SDp, SDn, SSn, LSn, SSi, and LSi were measured and, then, the channels for SSi and LSi were exchanged to measure WTh and WTi, respectively, and data were acquired again.

After that, pumping was temporarily stopped to obtain data under pump-off condition. If the left atrial pressure (LAP) elevated and reached 30 mmHg, the data acquisition was stopped and pumping was started again immediately. This procedure was repeated to obtain all data.

Usually, the pumping mode was then returned to 2:1 mode, and the drive condition was tuned up to obtain a desired bypass flow. Or in the case that LAP was less than 20 mmHg and BF was more than 2 l/min, bypass flow was reduced slightly after pumping was restarted. Or in the case that both LAP and BF were low enough, the pump was removed.

After pump removal, only pump-off data were acquired for around 1 month in the same method as mentioned above. At autopsy, the heart was resected carefully and it was checked whether the implanted sensors and

probes positioned properly. Body weight (BWA) and left ventricular weight (LVW) were measured. To calculate regional wall tension in the 'normal' and 'ischemic' myocardia, positions of the ultrasonic sensors for the segment length were measured on the equatorial plane, as explained in APPENDIX A.2 (2).

All data shown in this chapter are expressed as mean values  $\pm$  one standard error (SE) unless otherwise stated.

#### 8.2.4 Data analysis

Data analysis was carried out in the same fashion as that mentioned in CHAPTER VI (2). A mini-computer system (PDP-11/44, DEC, Maynard, Massachusetts, U.S.A.) was used to analyze the data recorded on magnetic tape.

Left ventricular volume, LVV, was calculated by eq. (3.1). Bulk external mechanical stroke work done by the left ventricle during a cardiac cycle was obtained from the method described in CHAPTER III. This stroke work was normalized by the left ventricular weight (LVW) measured during the autopsy, and multiplied by the heart rate (HR) to obtain the bulk mechanical work per second (BMW).

Left ventricular wall tension in the 'normal' and 'ischemic' regions,  $Tw_n$  and  $Tw_i$ , respectively, were obtained using eq. (6.1). Subendocardial rhombus area,  $Am_n$  and  $Am_i$ , surrounded by two pairs of sensors for the measurement of segment length in the 'normal' and 'ischemic' regions, respectively, were calculated by eq. (6.2). Regional myocardial external stroke work done by the local myocardium was obtained by the method stated in CHAPTER III. This work was normalized by the regional myocardial volume and multiplied by the heart rate to obtain the regional mechanical work per second (RMWn and RMWi for 'normal' and 'ischemic' area, respectively). Each myocardial volume was calculated by multiplying the averaged  $Am_k$  ( $k = n$  and  $i$ ) in a cardiac cycle by the averaged wall thickness.

#### 8.2.5 Histology

Myocyte diameter was used as a histological parameter as was in CHAPTER VII. Myocardial segments were cut out from the normal and infarcted areas, and histological specimens were made and stained with hematoxylin-eosin. Myocyte diameter of the normal myocardium was measured using the same method as that shown in CHAPTER VII. The diameters obtained from the subendocardial, middle, and subepicardial one-third layers were compared with the control data shown in CHAPTER VII.

### 8.3 RESULTS

Table VIII.I summarizes basic data of all experiments. Four goats out of 8 died under LVAD pumping: causes of death in these cases were ventricular fibrillation, poor lung function, septicemia, and low cardiac output, respectively. Three of the remaining 4 animals, P8627, P8703 and P8725, were recovered well by the LVAD pumping and the pumps were removed successfully on the 13th, 11th, and 15th post-operative day (POD), respectively.

The remaining animal, P8712, did not recover well in spite of 27 days' pumping together with long-term administration of digitalis. Until the 18th post-operative day, the left atrial pressure (LAP) or end-diastolic left ventricular pressure (LVEDP) of this particular animal exceeded 30 mmHg whenever the LVAD pumping was stopped temporarily. After 27 days' pumping, the pump was removed intensively. After pump removal, in spite of continuous administration of digitalis, general condition of this animal was getting worse but she survived for 1 month.

Body weight of each survived animal measured at autopsy (BWA) was less than the initial weight (BWO) by 2 or 4 kg. Ventricular fibrillation (Vf) occurred in 3 of 4 pump-removed animals on the operation day and, sometimes, on the first or second post-operative day (POD) again, although they were recovered by a conventional defibrillation procedure. The animals having experienced Vf(s) needed administration of epinephrine for first several days post-operatively. Digitalis was administered to the animals, P8725 and P8712, at 8 and 14 days prior to pump removal, and it was continued for 16 and 38 days thereafter, respectively. Anemia was observed in 2 pump-weaned animals possibly due to their poor appetite. The surface area of thin and

fibrous myocardium in the pump-removed animals macroscopically observed at the autopsy was 10 to 70 % of that of the left ventricular wall including the septum and free wall.

Figures 8.2, 8.3, and 8.4 shows the waveforms of hemodynamics, ventricular diameter and segment length, and wall thickness, respectively, obtained (a) during pumping on the 4th POD (7 days before pump removal), (b) during temporary pump-off on the same POD, (c) on the 15th POD (4 days after the pump removal), and (d) on the 36th POD (25 days after pump removal) in the successfully recovered P8627 animal. LAP measured under temporary pump-off condition before pump removal was slightly higher than that after pump removal. LD, SDn, SDp, and LSi became greater at the later stage of the experiment compared with those at the earlier stages (Fig. 8.3(d)). The waveforms of LSi and SSi were out of phase from those of the other segment length and ventricular diameter. The wall thickness, Wtn and WTi, decreased after pump removal (Fig. 8.4). WTi was out of phase from Wtn. The peak-to-peak amplitudes of left ventricular dimensions, especially SDn, SDp, SSn and Wtn, measured during LVAD pumping ((a) in Figs. 8.3 and 8.4) were smaller than those obtained under pump-off condition ((b) in Figs. 8.3 and 8.4). Their amplitudes observed after pump removal were larger than those obtained under temporary pump-off condition before pump removal. The changes in these amplitudes were mainly due to the changes of the dimensions in the end-diastolic phase.

Table VIII.I Summary of experiments.

Exp. no.	Sex	BWO (kg)	BWA (kg)	LVW (g)	VF (times)	VT (times)	EA (day)	DA (day)	PP (day)	CD	FA (%)	Remarks
P8624	F	28	--	109	6	--	4	--	4	Vf	--	--
P8627	M	28	26	93	--	--	--	--	13	TS	40	--
P8703	F	35	31	92	2	--	2	--	11	TS	10	Anemia
P8710	M	35	--	82	1	1	1	--	5	SP	--	Anemia
P8712	F	34	30	66	4	1	2	38	27	TS	70	--
P8718	M	33	--	--	2	--	--	--	2	PL	--	Anemia
P8720	M	25	--	--	1	2	2	--	2	LO	--	--
P8725	F	34	30	78	2	1	1	16	15	TS	50	Anemia

Key: BWO, body weight before operation; BWA, body weight at autopsy; LVW, left ventricular weight; VF, number of times of ventricular fibrillation; VT, number of times of ventricular tachycardia; EA, duration of post-operative administration of epinephrine; DA, duration of post-operative administration of digitalis; PP, pumping period; CD, cause of death; FA, percentage of thin and fibrous area; Vf, ventricular fibrillation; TS, scheduled termination; SP, septicemia; PL, poor lung function; LO, low cardiac output.

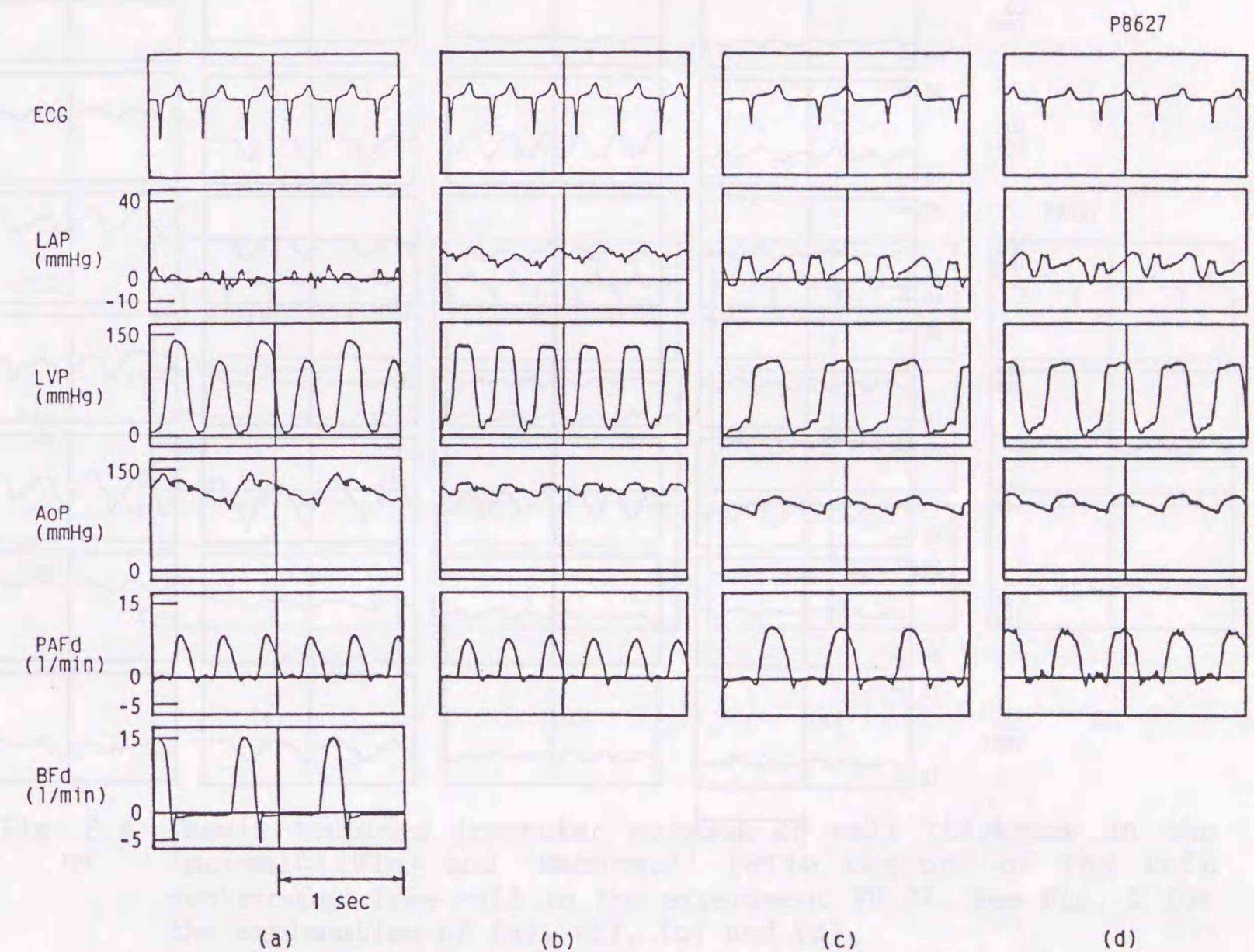


Fig. 8.2 Examples of phasic tracings (computer output) of electrocardiogram (ECG), left atrial pressure (LAP), left ventricular pressure (LVP), aortic pressure (AoP), pulmonary arterial flow (PAFd), pump bypass flow (BFd) in the P8627 experiment. Data were obtained (a) during pumping on the 4th post-operative day (POD) (7 days before pump removal), (b) under temporary pump-off condition on the same day, (c) on the 13th POD (4 days after pump removal), and (d) on the 36th POD (25 days after pump removal).

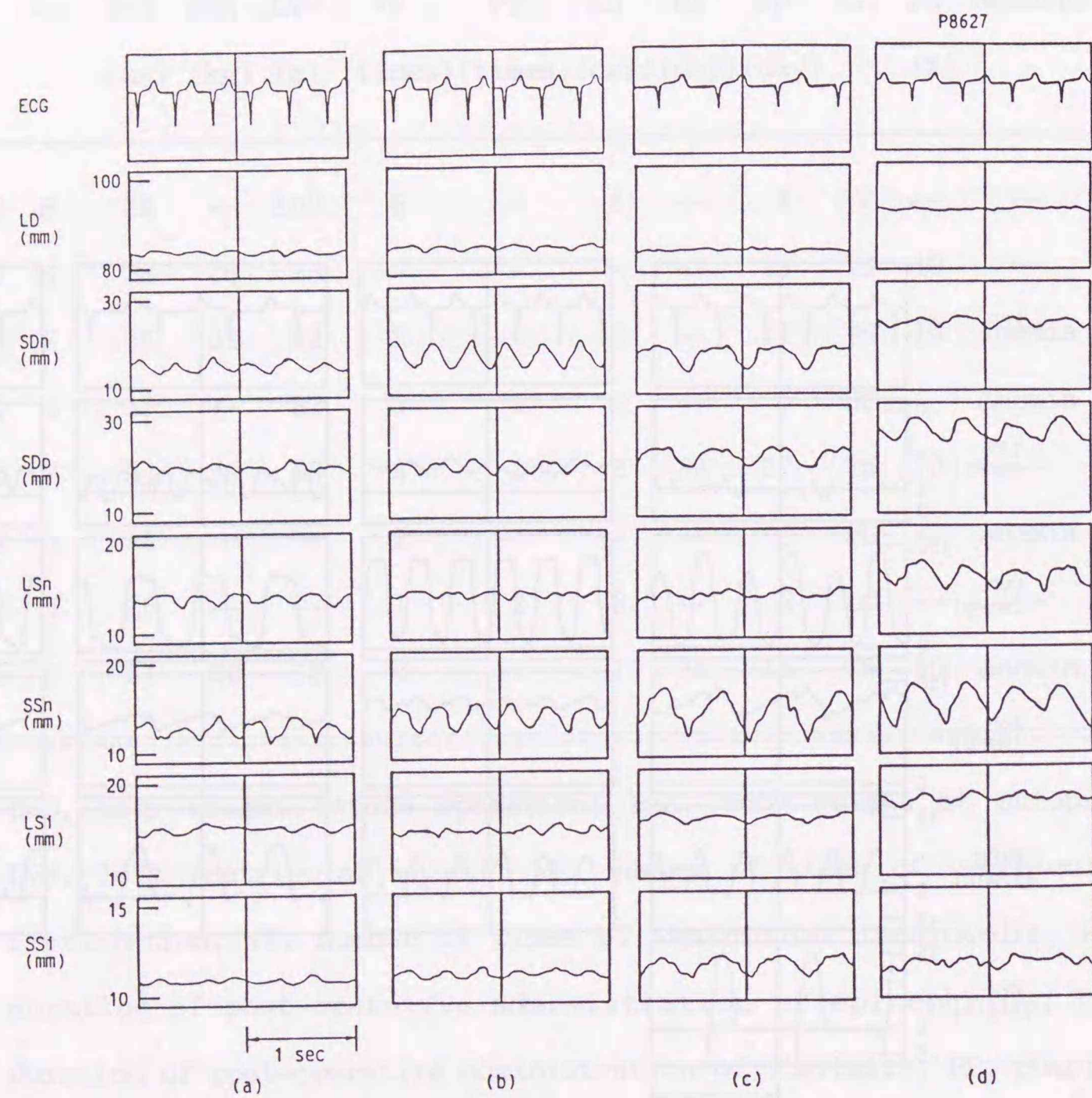


Fig. 8.3 Phasic tracings (computer output) of electrocardiogram (ECG), long axis diameter of the left ventricle (LD), short axis diameters perpendicular (SDn) and parallel (SDp) to the septum, meridian (LSn) and equatorial (SSn) segment length in the 'normal' region of the left ventricular free wall, and meridian (LSi) and equatorial (SSi) segment length in the 'ischemic' region in the experiment P8627. See Fig. 2 for the explanation of (a), (b), (c) and (d).

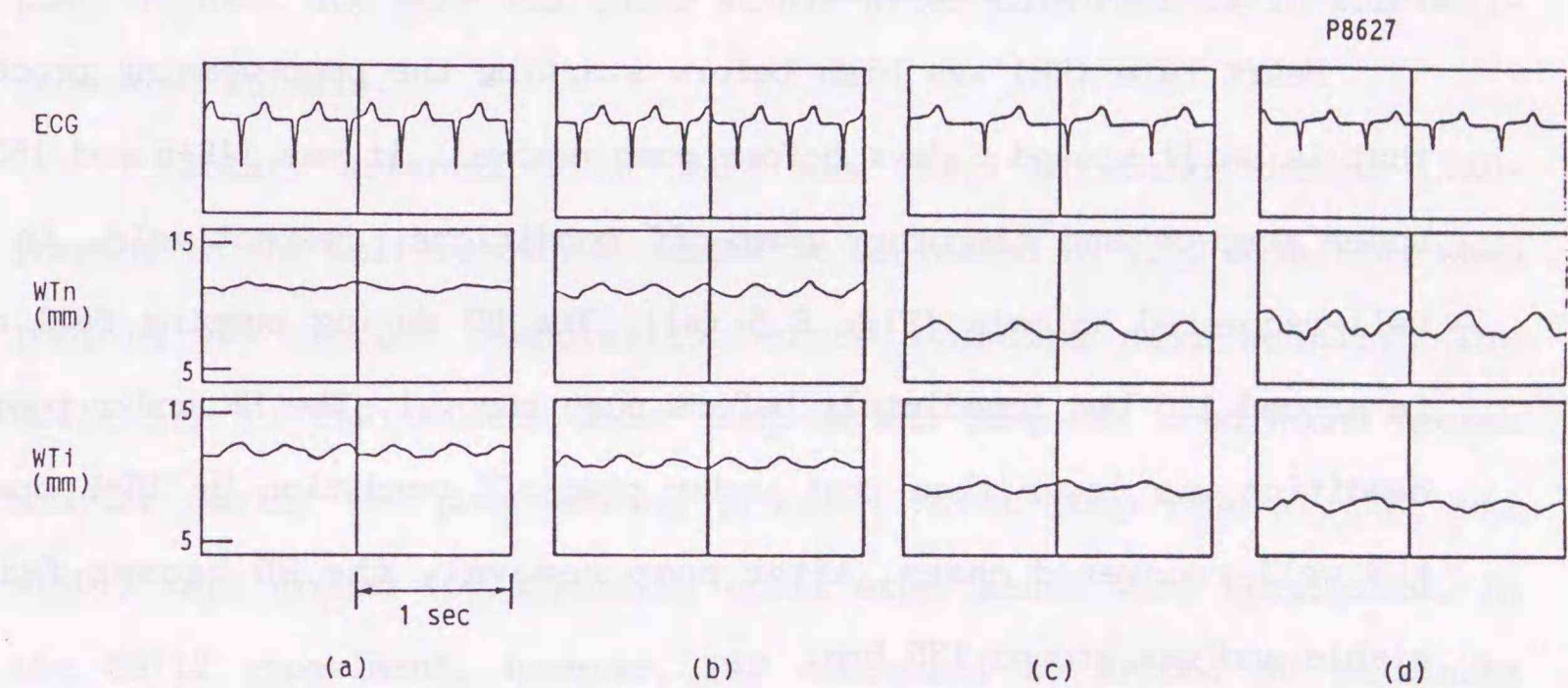


Fig. 8.4 Phasic tracings (computer output) of wall thickness in the 'normal' (Wtn) and 'ischemic' (WTi) regions of the left ventricular free wall in the experiment P8627. See Fig. 2 for the explanation of (a), (b), (c) and (d).

### 8.3.1 Hemodynamics

Figure 8.5 (a) and (b) shows the hemodynamic data obtained from well-recovered animals (P8627, P8703 and P8725) and a poorly recovered animal (P8712). The minus attached to the period (day) in the horizontal axis means the time before pump removal. Since in the P8712 experiment the catheter for the measurement of LAP was blocked on the 15th post-operative day, left ventricular end-diastolic pressure (LVEDP) was shown in the Fig. 8.5 (b) thereafter.

Heart rate (HR) was high before starting the pump-weaning process, that is until around 5 days before pump removal: it was  $148 \pm 5$  and  $163 \pm 6$ , under pump-on and temporary pump-off conditions, respectively, in the well-recovered animals (Fig. 8.5 (a)). The HR during pumping fell down to around 110 bpm immediately before pump removal. The HR under pump-on condition was lower than that under pump-off condition by  $18 \pm 2$  bpm in the well-recovered cases. After pump removal, the HR became fairly stable and was around 135 bpm.

The temporary stop of pumping reduced the mean aortic pressure (mAoP) by  $4 \pm 8$  mmHg in the well-recovered animals. The mAoP in P8712 was lower than that observed in the well-recovered cases by around 20 mmHg. After the mAoP decreased to  $87 \pm 2$  mmHg for 10 days after pump removal in the well-recovered animals, it increased to  $101 \pm 4$  mmHg at the last stage of experiments.

Peak left ventricular pressure (pLVP) in the poorly recovered animal was also lower than that observed in the well-recovered animals by around 20 mmHg. It was around 100 mmHg during pumping in the well-recovered cases. The pLVP was not changed much by the temporary stop of pumping. Again, the pLVP was low ( $95 \pm 3$  mmHg) for 10 days after pump

removal in the well-recovered cases and, then, increased to  $108 \pm 2$  mmHg at the last stage of experiments.

Mean left atrial pressure (mLAP) was higher under temporary pump-off condition by  $14 \pm 3$  mmHg than that during pumping in the well-recovered animals; the mLAP was kept low ( $4 \pm 1$  mmHg) during pumping. Although the mLAP during pump-off was as high as  $19 \pm 2$  mmHg immediately before pump removal in the well-recovered cases, it dropped to  $11 \pm 3$  mmHg only 1 day after. However, in the P8712, LVEDP remained high after the pump removal. The mLAP was quite stable after pump removal in the well-recovered animals.

Pulmonary arterial flow (PAF) was  $100 \pm 5$  ml/min/kg during LVAD-pumping in the well-recovered cases. It decreased by  $22 \pm 2$  ml/min/kg when pumping was stopped temporarily before starting pump-weaning. The difference of PAF between under pump-on and pump-off conditions became smaller during the pump-weaning process. After pump removal, PAF was stably kept around 100 ml/min/kg until experiments were terminated. In the P8712 experiment, however, PAF decreased to around 80 ml/min/kg after pump removal.

Pump bypass flow (BF) was  $97 \pm 12$  ml/min/kg before starting pump-weaning procedure in the well-recovered animals: bypass ratio (BF/PAF) was around 97 %. The BF was reduced gradually during the pump-weaning process. In the P8712 experiment, the BF was kept low for a fairly long period, that is for 18 days, and the mLAP increased much during this period.

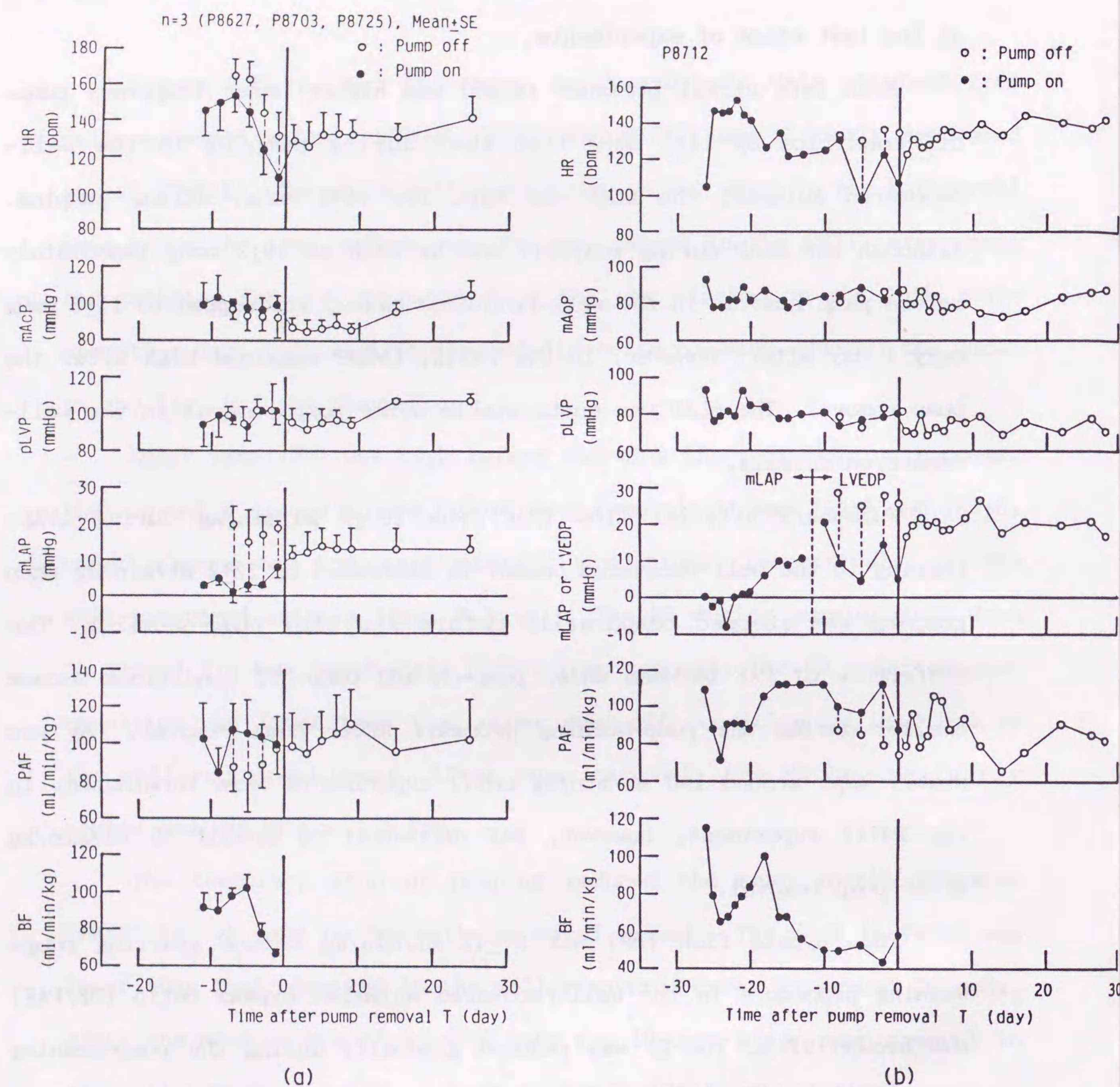


Fig. 8.5 Temporal change of hemodynamic parameters obtained of well-recovered three animals (P8627, P8703 and P8725) (a) and a poorly recovered animal (P8712) (b). HR, heart rate; mAoP, mean aortic pressure; pLVP, peak left ventricular pressure; mLAP, mean left atrial pressure; LVEDP, left ventricular end-diastolic pressure; PAF, pulmonary arterial flow; BF, pump bypass flow. Data in (a) are demonstrated by means  $\pm$  SEs.

### 8.3.2 Left ventricular dimension

Figure 8.6 shows changes in the left ventricular dimensions observed in the experiment P8627; they are averaged values in a cardiac cycle. Left ventricular diameters (LD, SDn and SDp) all increased with time, which implies that the left ventricular cavity enlarged to do necessary mechanical work, compensating for the debilitated heart. The LD and SDn increased much for 10 days after pump removal. The segment length in the 'normal' area (LSn and SSn) did not change much throughout the experiment, whereas those in the 'ischemic' area (LSi and SSi) increased slightly after pump removal. The wall thickness in the 'normal' area (WTn) decreased much when pump was removed; it was stable thereafter. The wall thickness in the 'ischemic' area (WTi) decreased gradually throughout the experiment.

Figure 8.7 shows the waveforms of the left ventricular volume (LVV) and the myocardial rhombus areas in the 'normal' and 'ischemic' regions ( $Am_n$  and  $Am_i$ , respectively) which were calculated from the data demonstrated in Fig. 8.3 using eqs. (3.1) and (6.2). When pumping was temporarily stopped, the diastolic LVV and  $Am_n$  increased, although the systolic LVV and  $Am_n$  did not change;  $Am_i$  did not change even in the diastolic phase. The averaged LVV, and peak-to-peak amplitude and average of  $Am_n$  increased when pump was removed, and they continued to increase thereafter. Before pump removal, the waveform of  $Am_i$  was out of phase from that of  $Am_n$ , although it became in phase after pump removal. The average of  $Am_i$  also increased when pump was removed, and it continued to increase thereafter.

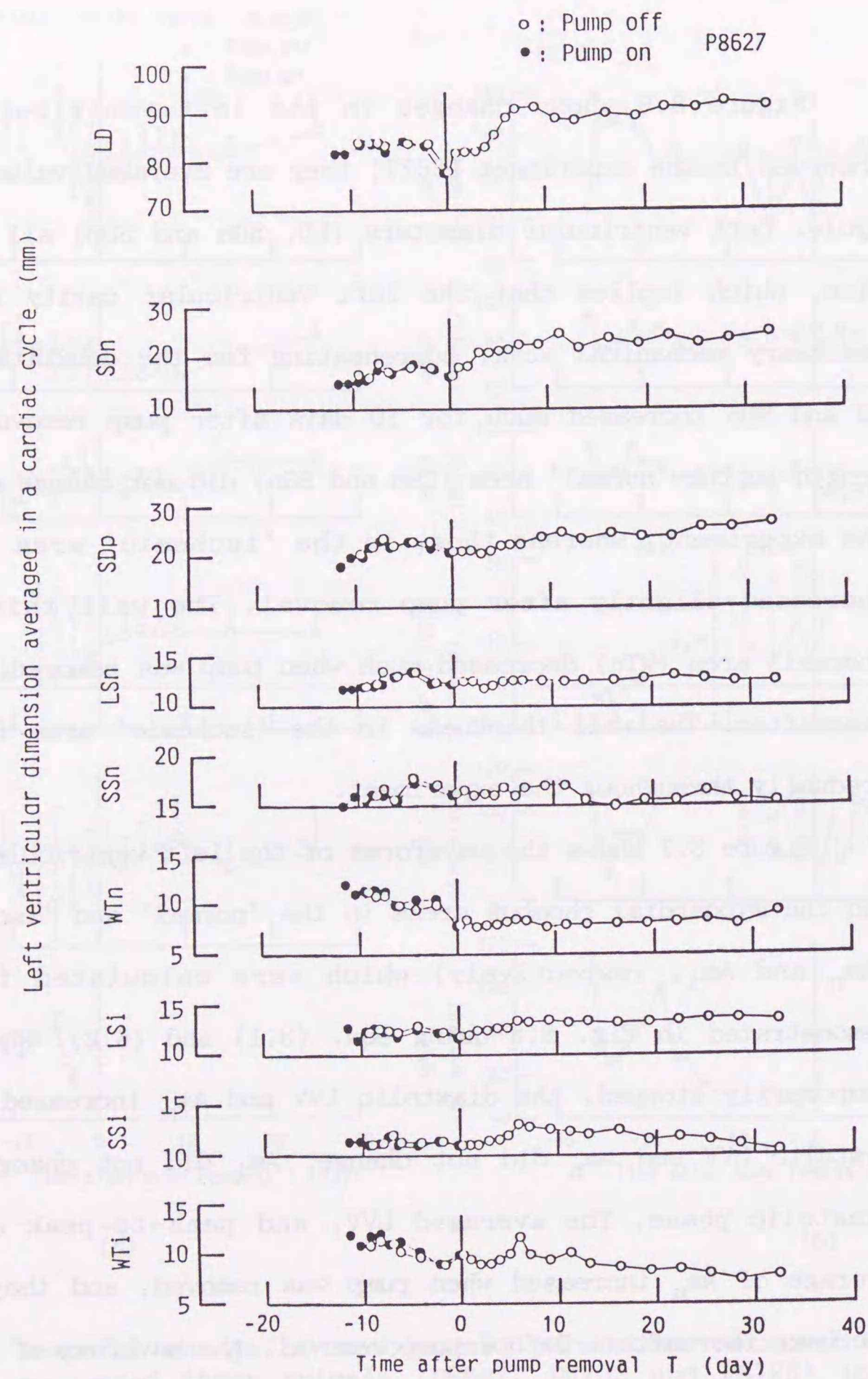


Fig. 8.6 Temporal change of cardiac dimensions averaged in a cardiac cycle (experiment P8627). The abbreviations are the same as those appeared in Figs. 8.3 and 8.4.

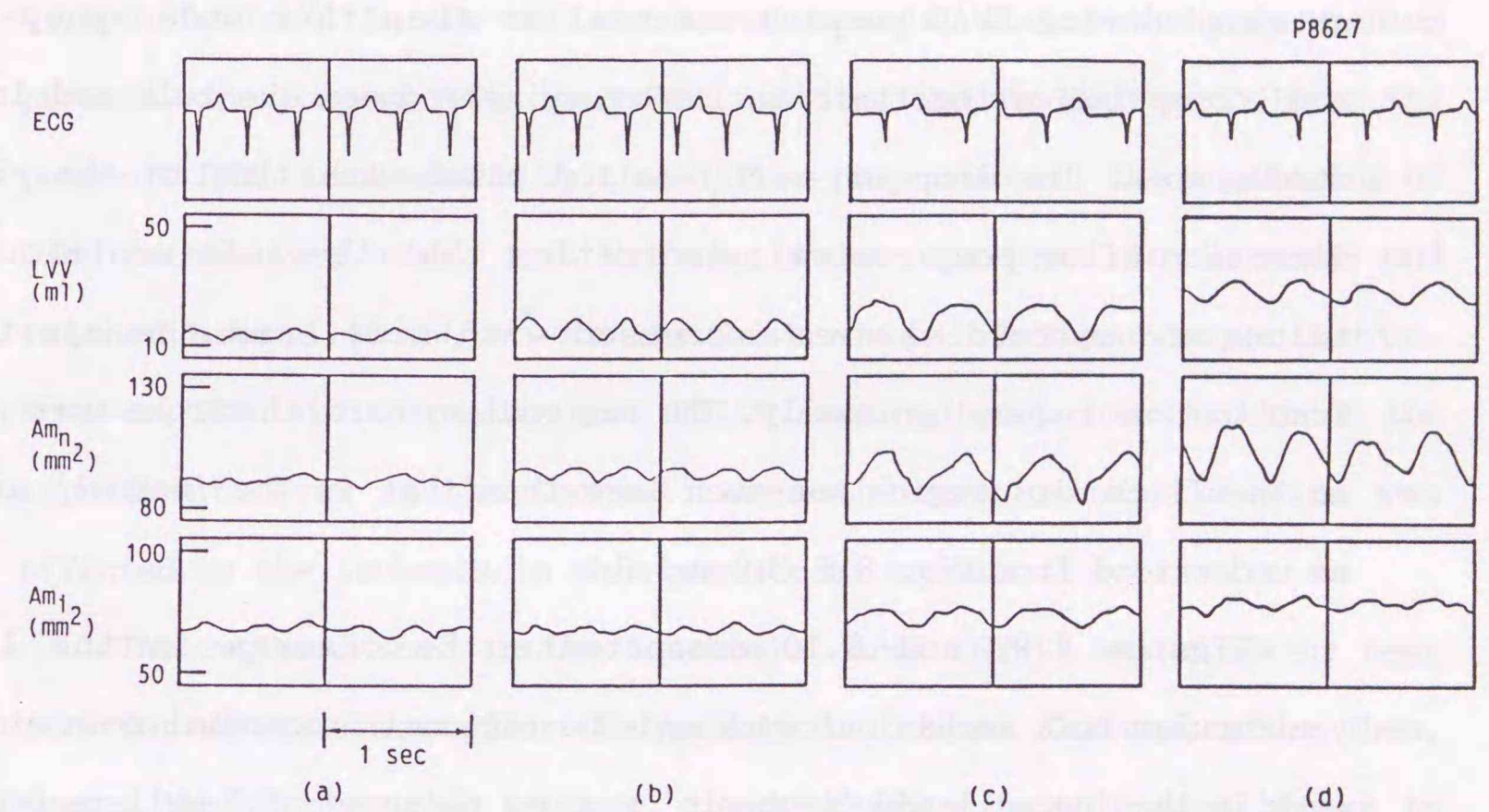


Fig. 8.7 Phasic tracings (computer output) of left ventricular volume (LVV) and regional subendocardial rhombus area in the 'normal' ( $A_{m_n}$ ) and 'ischemic' ( $A_{m_i}$ ) regions calculated from the data shown in Fig. 8.3 (P8627). See Fig. 8.2 for the explanation of (a), (b), (c) and (d).

### 8.3.3 Bulk and regional mechanical work

Figure 8.8 shows examples of left ventricular pressure-volume loops (a), and wall tension-area loops of the myocardia in the 'normal' region (b) and 'ischemic' region (c) which were drawn from the data demonstrated in Figs. 8.2 and 8.7. Successive 2 loops are depicted for the pump-on data. In Fig. 8.8 (a) and (b), the area inside the loop obtained during LVAD pumping was smaller than that under pump-off condition, indicating that the LVAD pumping reduced the bulk and local stroke work. The loop of each relation moved with time to the right direction after pump removal, indicating that the left ventricular volume and myocardial area increased with time, and the ejection fraction was reduced gradually. The regional myocardial stroke work done in the 'ischemic' region was much less than that in the 'normal' area, as understood from Fig. 8.8 (b) and (c).

Figures 8.9, and 8.10 demonstrate the changes in the left ventricular bulk mechanical work and the regional myocardial mechanical work in the 'normal' and 'ischemic' regions observed of 3 well-recovered animals (P8627, P8703 and P8725) (a) and a poorly recovered animal (P8712) (b).

The bulk mechanical work (BMW) obtained when the pumping was stopped temporarily was  $0.22 \pm 0.01$  W/(100 g LVW) in the well-recovered animals and was larger than that obtained during LVAD pumping. The BMW during pumping was  $0.08 \pm 0.01$  W/(100 g LVW) before starting pump-weaning procedure in these animals, and it increased during the weaning process. The difference between the BMW obtained under pump-on and -off conditions decreased with time in the well-recovered cases, whereas it did not in the experiment P8712. After pump removal, the BMW continued

to increase gradually for around 10 days in the well recovered cases; thereafter it became stable at a level of  $0.33 \pm 0.03$  W/(100 g LVW). In the experiment P8712, however, it decreased gradually after pump removal.

Before starting the pump-weaning procedure, the regional mechanical work obtained of the 'normal' area (RMWn) during pumping ( $1.5 \pm 0.4$  mW/cm<sup>3</sup>) was much smaller than that obtained under pump-off condition ( $4.3 \pm 0.9$  mW/cm<sup>3</sup>) in the well-recovered animals; during the pump-weaning process, the pump-on RMWn increased rapidly, and the difference from the pump-off RMWn decreased with time. After pump removal, the scattering of RMWn became very wide, and the mean value continued to increase and reached around 10 mW/cm<sup>3</sup> at the last stage of these experiments. However, RMWn in the experiment P8712 remained very low throughout the experiment: even in the 'normal' area the myocardial function was affected by the ischemia in this particular animal.

The regional work in the 'ischemic' area (RMWi) was minus or near zero for several days after the induction of heart failure; after then, during the pump-weaning process, the myocardium in this area became to do some external work under pump-off condition in the well-recovered cases although it was small ( $0.5 \pm 0.2$  mW/cm<sup>3</sup>). After pump removal, the RMWi was kept at a similar level to that observed under temporary pump-off condition immediately before pump removal in these animals. In the animal P8712, however, the RMWi remained at near zero level throughout the experiment.

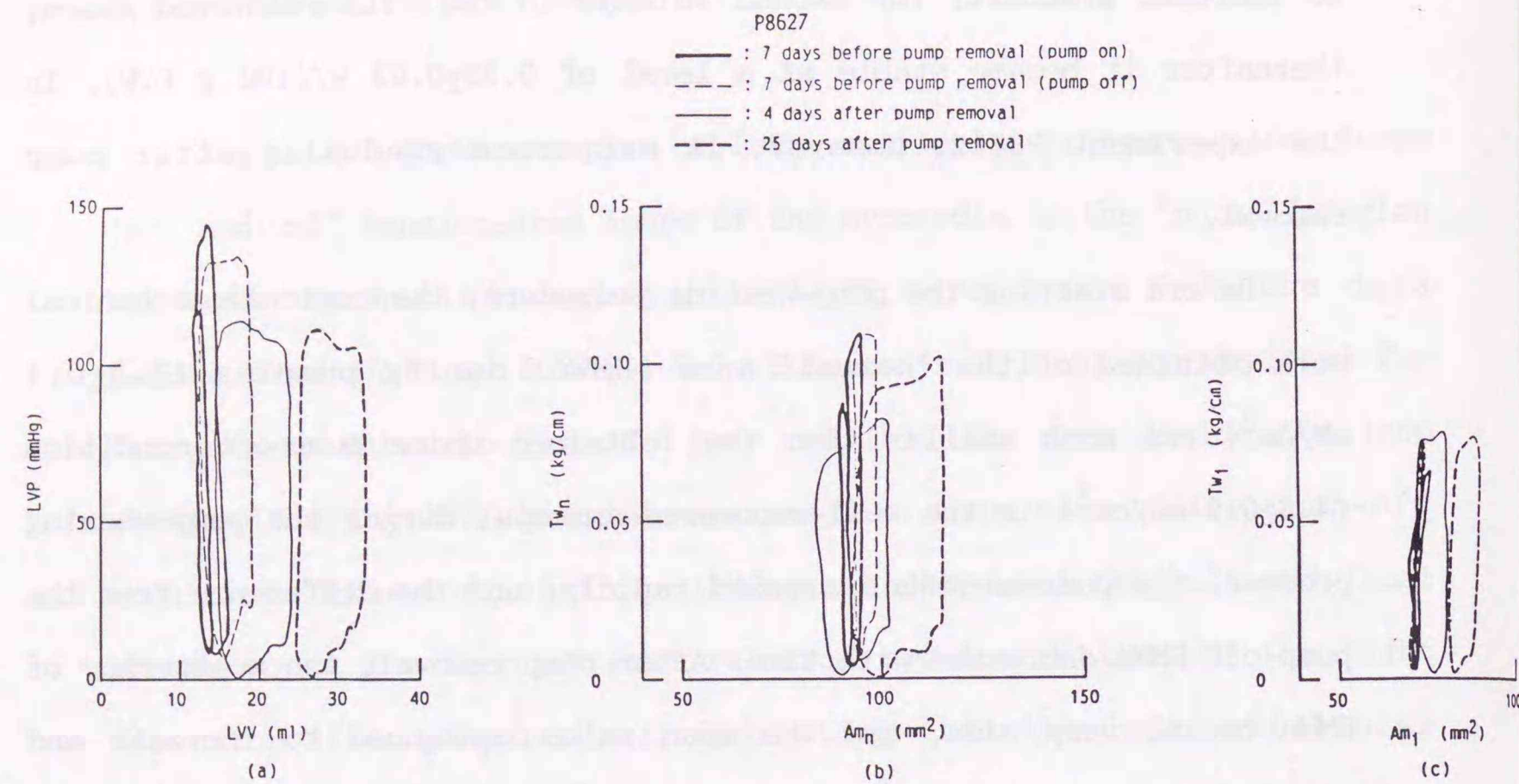


Fig. 8.8 Relationships between (a) left ventricular pressure (LVP) and volume (LVV), (b) regional wall tension ( $T_{w_n}$ ) and area ( $A_{m_n}$ ) in the 'normal' region, and (c) regional wall tension ( $T_{w_i}$ ) and area ( $A_{m_i}$ ) in the 'ischemic' region, all obtained from the data shown in Figs. 8.2 and 8.7 (P8627). Relations in the 2 successive cardiac cycles were shown for pump-on data.

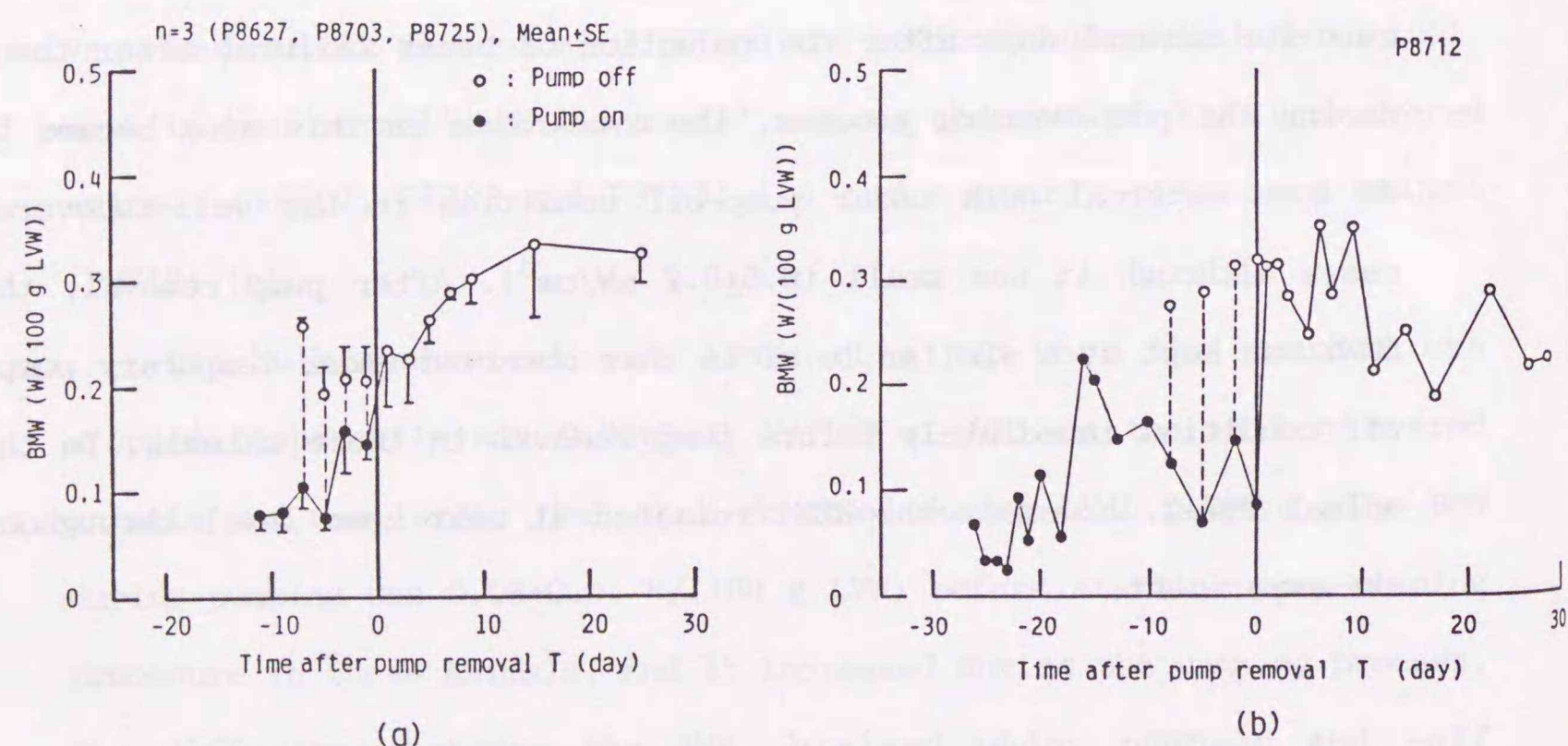


Fig. 8.9 Temporal change of bulk mechanical work of the left ventricle (BMW) obtained of well-recovered animals (P8627, P8703 and P8725) (a) and a poorly recovered animal (P8712) (b). Data in (a) are expressed as means  $\pm$  SEs.

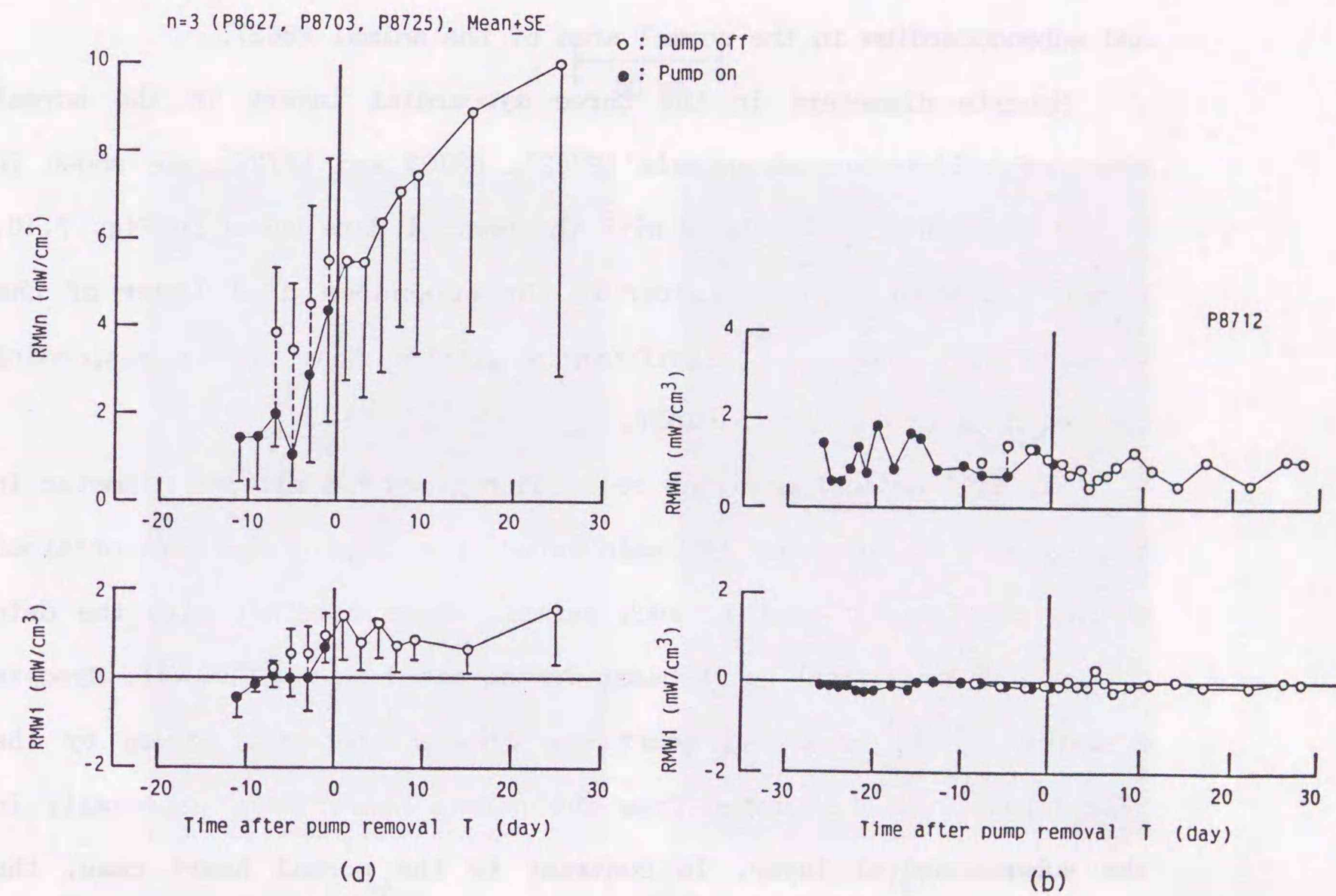


Fig. 8.10 Temporal change of regional mechanical work done by the 'normal' (RMWn) and 'ischemic' (RMWi) myocardia obtained of well-recovered animals (P8627, P8703 and P8725) (a) and a poorly recovered animal (P8712) (b). Data in (a) are expressed as means  $\pm$  SEs.

#### 8.3.4 Histological study

Figure 8.11 shows microstructure of the specimens obtained from the infarcted and normal regions. Clear differences are observed between them. Fig. 8.12 shows microstructure of subepicardium, middle myocardium and subendocardium in the normal area of the animal P8627.

Myocyte diameters in the three myocardial layers in the normal areas of well-recovered animals (P8627, P8703 and P8725) are shown in Fig. 8.13, which are compared with the control data shown in Fig. 7.10. Except for the myocyte diameter in the subendocardial layer of the animal P8627, they were significantly greater than the corresponding control data ( $p < 0.001$  to  $0.05$ ).

Fig.8.14 demonstrates the relation between the myocyte diameter in the normal myocardium and BMW calculated by averaging the data obtained during the last 10 days in each animal, shown together with the data obtained of the normal heart cases demonstrated in CHAPTER VII. Myocyte diameter in the infarcted heart was greater than that given by the regression lines calculated from the normal heart data, especially in the subendocardial layer. In contrast to the normal heart case, the myocyte diameter in the heart with smaller BMW was larger than that with greater BMW.

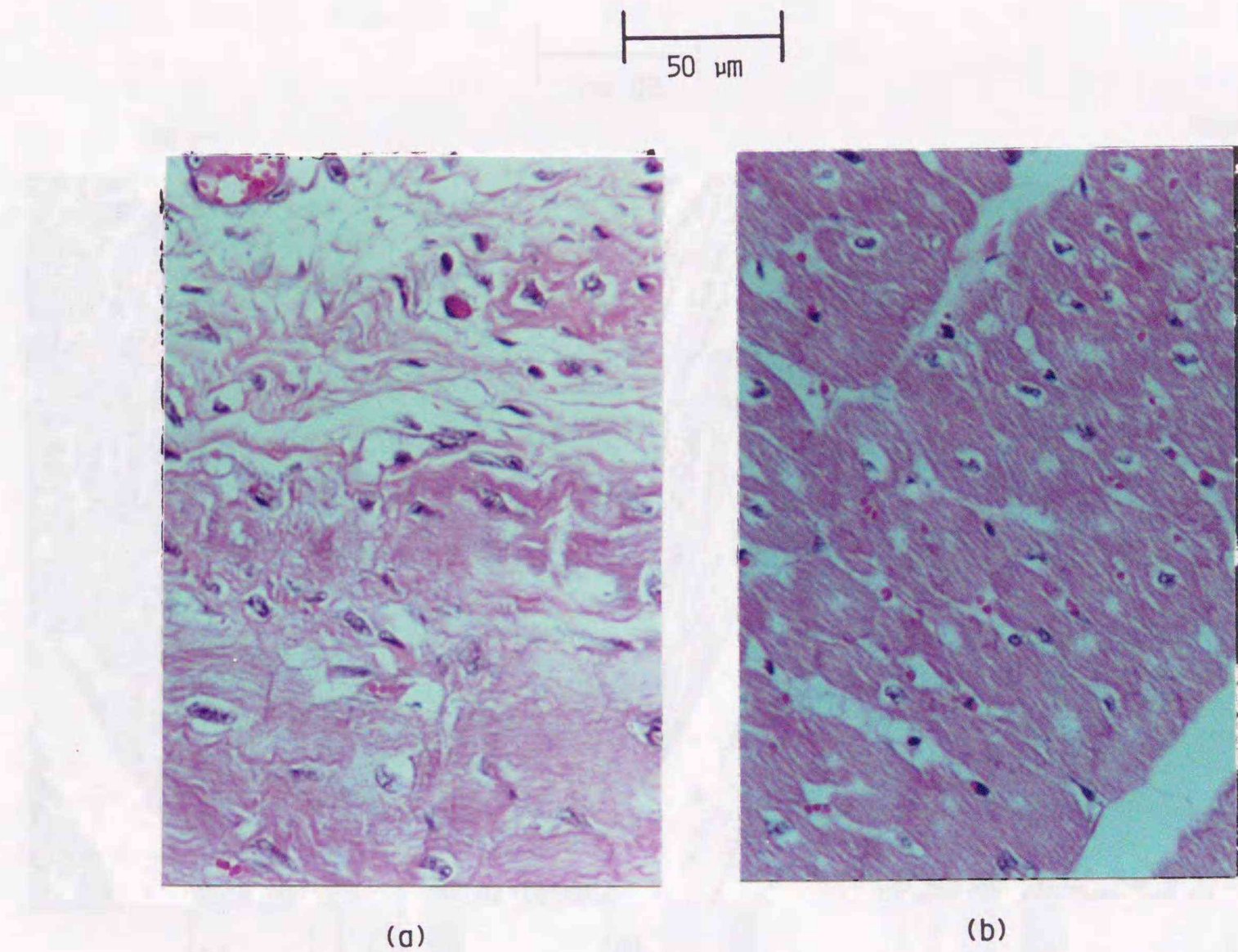


Fig. 8.11 Hematoxylin-eosin stained histological specimens obtained from the infarcted (a) and normal (b) areas (P8627).

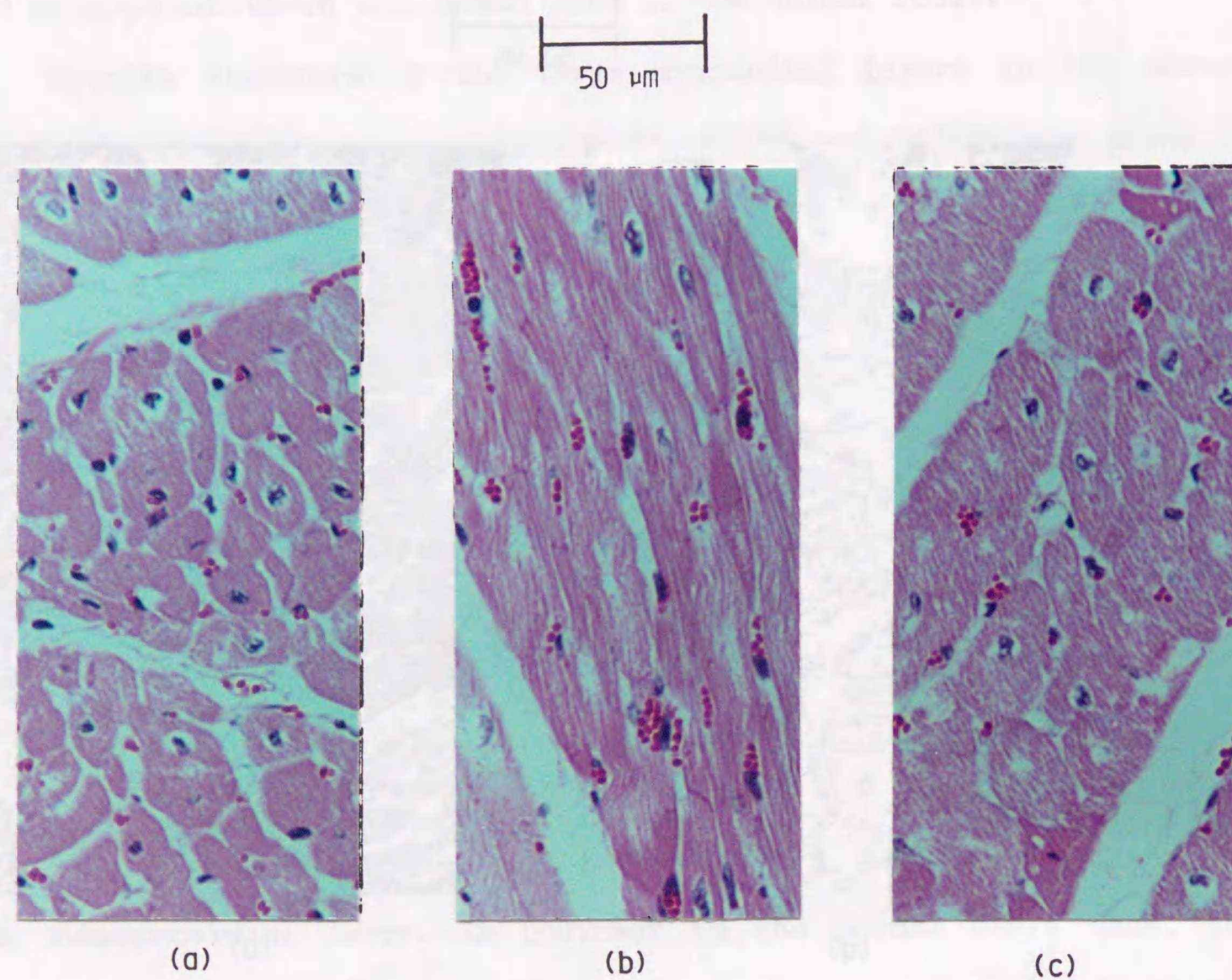


Fig. 8.12 Microstructure of subepicardial (a), middle (b) and subendocardial (c) layers of a myocardial specimen obtained from the normal region, stained with hematoxylin-eosin (P8627).

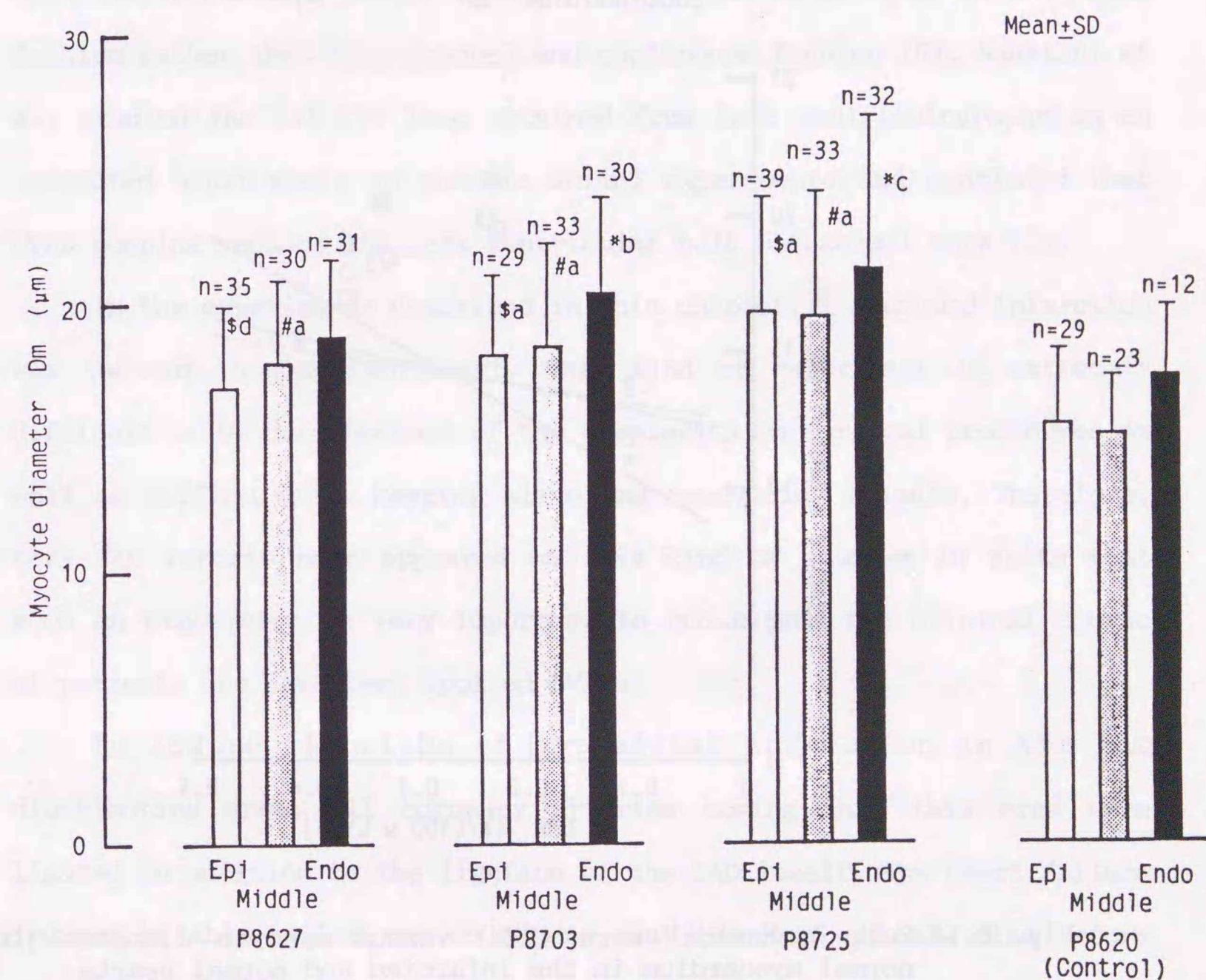


Fig. 8.13 Myocyte diameter (Dm) in the subepicardial, middle and subendocardial one-third layers (Epi, Middle and Endo, respectively) of the normal myocardium. Data are demonstrated by means±SDs. Key: a,  $p < 0.001$ ; b,  $p < 0.01$ ; c,  $p < 0.02$ ; d,  $p < 0.05$ ; \*, compared to the subendocardial data of the control animal; #, compared to the middle myocardial data of the control animal; \$, compared to the subepicardial data of the control animal.

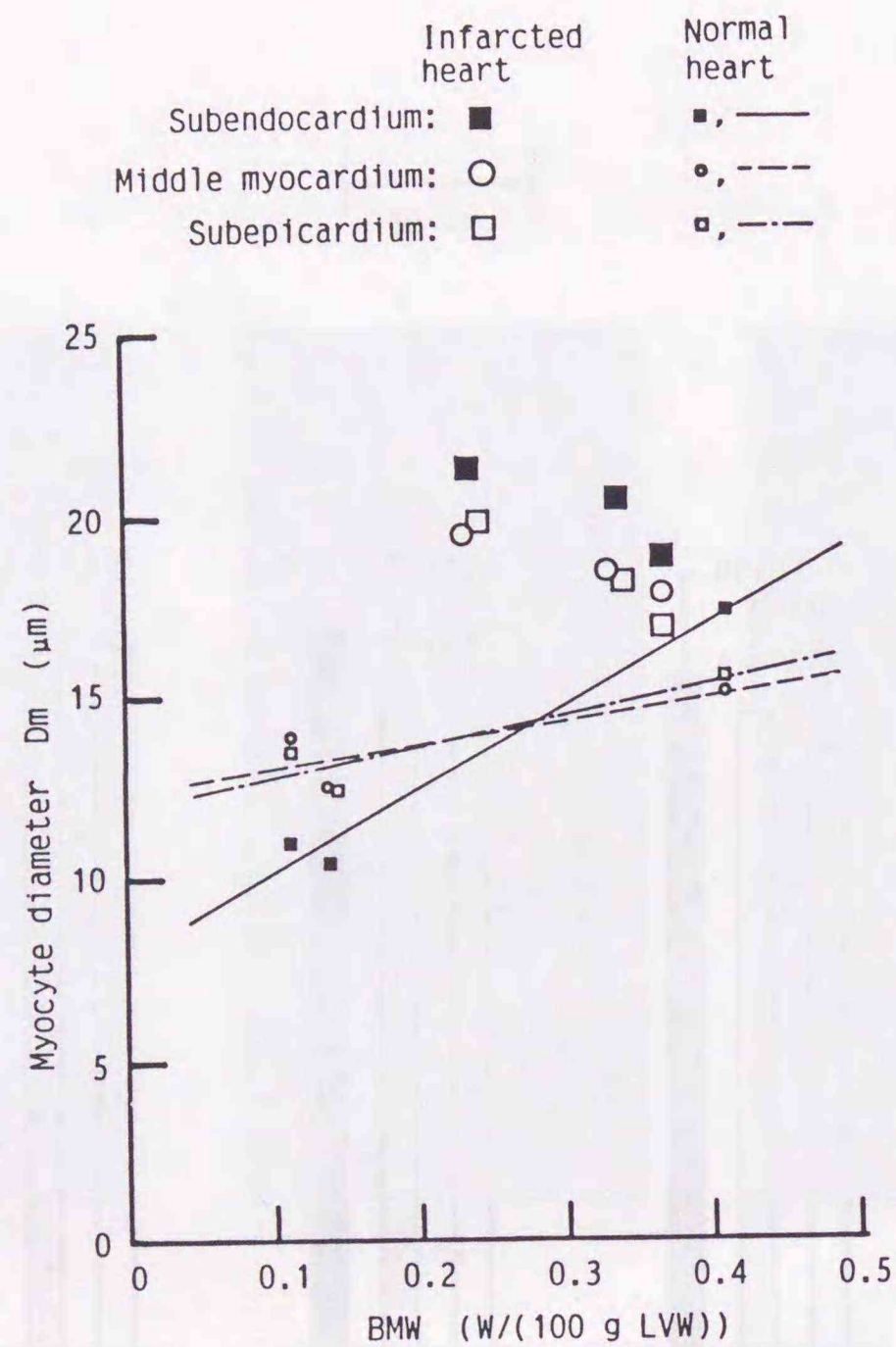


Fig. 8.14 Bulk mechanical work (BMW) versus myocyte diameter (Dm) of normal myocardium in the infarcted and normal hearts.

Until now very few studies have been conducted on the recovery process of the infarcted heart by LVAD pumping. Brugger et al. classified left ventricular activity into 5 stages in clinical cases, using aortic pressure of the patients supported by LVAD, and reported that the left ventricular function recovers with time in a cyclic fashion rather than in a gradual and continuous fashion (6). Nakatani et al. studied the LVP-LVW loop obtained from left ventriculography on an infarcted heart model in chronic animal experiments and concluded that LVAD pumping reduces the left ventricular bulk mechanical work (7).

In the experiments described in this chapter, a profound infarction was induced in the goat heart. This kind of experiment is extremely difficult to be done because of the complexity in surgical procedures as well as difficulty in keeping alive and recovering animals. Therefore, very few reports have appeared on this kind of studies in spite that such an experiment is very important to understand the clinical course of patients who have been applied LVADs.

To insure induction of myocardial infarction in the LAD distributing area, all coronary arteries coming into this area were ligated in addition to the ligation of the LAD itself. The heart failure induced by this method was so severe that the half animals died before weaning the LVADs. Although the infarction size could not be determined quantitatively during operation, the induced heart failure was profound enough to evaluate the effects of LVAD pumping. Because of too severe heart failure, the animal of P8712 was under a very poor condition and the condition got worse with time. Therefore, the data from this animal were not used for the study on the animals well-recovered by LVAD

pumping.

Based on the results obtained from the previous acute experiments (1,2), the ECG synchronous mode having the duty ratio of 2:1 was selected for the LVAD pumping. The drive pressure, vacuum, delay from the onset of cardiac cycle, and %-systole of pumping were adjusted manually several times a day to obtain the desired pump bypass flow.

In the successfully recovered cases, heart rate (HR) started decreasing at the same time when we recognized that the heart started recovering (Fig. 8.5 (a)). However, the decrease in HR may be attributable simply to the animals' recovery from surgical damage. It is impossible to determine the cause of decrease, because the pumping duration was rather short.

Before starting pump-weaning process, mean left atrial pressure (mLAP) increased much when the pumping was temporarily stopped (Figs. 8.2 and 8.5 (a)). The mLAP observed under the temporary pump-off condition was used to evaluate the heart recovery in this study: when it became lower than 20 mmHg, pump-weaning procedure was started. To simulate clinical cases, the pump-weaning was done by decreasing the bypass flow rate very gradually to 2 l/min for around 5 days.

After pump removal, mean aortic pressure (mAoP) and peak left ventricular pressure (pLVP) were slightly low for around 10 days (Fig. 8.5 (a)), while bulk mechanical work (BMW) and regional mechanical work in the 'normal' area (RMWn) increased much (Figs. 8.9 (a) and 8.10 (a)). These results imply that it needs around 10 days after pump removal for the left ventricle to stabilize the function.

Long axis diameter (LD), short axis diameter perpendicular to the septum (SDn) of the left ventricle, and meridian and equatorial myocardial segment lengths in the 'ischemic' area (LSi and SSi,

respectively) increased much for several days after pump removal (Fig. 8.6); BMW and RMWn increased much during this period, but regional mechanical work in the 'ischemic' area (RMWi) did not (Figs. 8.9 (a) and 8.10 (a)). Although meridian and equatorial segment lengths in the 'normal' area (LSn and SSn, respectively) did not increase in P8627 during this period (Fig. 8.6), it is presumed that the normal myocardium in the other areas was elongated and that the LVP-LVV and  $Tw_n-Am_n$  relations moved toward the right with time (Fig. 8.8). These results coincide with the data reported by Nakatani et al. (7). The elongation observed in the 'ischemic' area (LSi and SSi) must be a passive phenomenon caused by an active contraction of the normal myocardium. It is widely known that the longer the cardiac muscle is, the greater power it can produce under some limit. In the case of this study, since some part of myocardium could not function due to the heart failure, the remaining normal myocardium was elongated to generate the necessary power.

Wall thickness in the 'normal' area (WTn) decreased immediately after pump removal, whereas that in the 'ischemic' area (WTi) decreased gradually, rather independently of the event of pump removal. These results may support the above-mentioned phenomenon.

Bulk mechanical work (BMW) and regional mechanical work in the 'normal' area (RMWn) done during pumping was smaller than those done under temporary pump-off condition, respectively. These differences were mainly ascribed to the changes in the end-diastolic volume and area developed by the temporary stop of pumping, which coincides with the results observed in the normal heart (3). The BMW obtained under pump-on and temporary pump-off conditions ( $0.08 \pm 0.01$  and  $0.22 \pm 0.01$  W/(100 g LVW), respectively) were close to those obtained in the normal heart

experiments (around 0.12 and 0.21 W/(100 g LVW), respectively) and described in CHAPTER VII (3). The BMW in the stable state after pump removal ( $0.33 \pm 0.03$  W/(100 g LVW)) was slightly smaller than that obtained from the control animal ( $0.43 \pm 0.07$  (mean $\pm$ SD) W/(100 g LVW)) stated in CHAPTER VII (3), possibly due to the remained infarction.

Before pump removal, the RMWn showed a similar change with time to that of the BMW. The RMWn during pumping was quite low for a couple of days after the induction of heart failure and, then, increased gradually during pump-weaning process, which reduced the difference from that obtained under the temporary pump-off condition.

The RMWn at the last stage of experiments (around  $10 \text{ mW/cm}^3$ ) was much greater than the regional myocardial work in the normal heart (RMW, around  $4.3 \text{ mW/cm}^3$ ) which was shown in CHAPTER VII (3). Before pump removal, the RMWn ( $4.3 \pm 0.9 \text{ mW/cm}^3$ ) under pump-off condition was similar to that in the normal heart. After pump removal, however, it increased gradually and 2 weeks after, it reached as much as around twice of the RMW in the normal heart. This phenomenon indicates that the normal part of the myocardium works more to compensate for the disabled myocardium in the infarcted area. The wide scattering of the RMWn observed after pump removal might be due to the differences of the recovery level in the three animals.

LVAD pumping reduced the RMWn without inducing adverse effect on the 'ischemic' area for several days after surgical operation (Fig. 8.10 (a)), which was the same as that observed in the acute experiments (2). Although the myocardium in the 'ischemic' area could not work for the first several days after surgery, it became to do some but slight external work at several days before pump removal. It continued to do work after pump removal. The recovery of the damaged myocardium is

attributable not only to the load reduction by virtue of LVAD but also possibly to the growth of co-lateral arteries: they reduced the oxygen-demand/supply ratio in the damaged myocardium.

The results obtained from this study indicate that load reduction caused by LVAD pumping somewhat recovers the myocardium from damage if LVAD was applied before the damage became fatal (8,9). However, the functional recovery of the heart is mostly due to the compensatory increase of the work done by the remaining normal myocardium rather than that by the damaged but slightly recovered myocardium. These results coincide with the phenomena observed by other researchers in canine and human hearts implanted with no LVAD (10-12). The myocardium in the 'normal' area which is to be exposed to high stress condition after some myocardium has been infarcted becomes powerful during the pump-weaning process and after pump removal. It took around 10 days after pump removal until the left ventricular function became apparently normal and stable.

Histological data on the myocyte diameter plotted against BMW support the above-mentioned phenomenon. They showed that the myocyte diameter in the normal area of the infarcted heart was greater than that of the normal heart even in the case that BMW in the infarcted heart was less than that in the control heart (Fig. 8.14). The myocyte diameter was larger when BMW was smaller, which might mean that the normal portion of myocardium comes up in doing more BMW by thickening the muscle fibers. Such a compensatory behavior as observed in the normal myocardium might result from some adaptation of myocardium to mechanical environment.

The health condition of a poorly recovered animal P8712 was getting worse in spite of long-term administration of digitalis. This animal was

considered as a critical case between pump-dependent and recoverable. In such a case, heart transplantation, or replacement with a permanently implantable LVAD or an artificial heart should be applied.

In the well-recovered animals (P8627, P8703 and P8725), the surface area of thin, rigid and fibrous regions was below 50 % of the left ventricular myocardium including septal muscle; it was 70 % in the animal P8712. These results show that LVAD can rescue even the patients having such severe heart failure as the infarcted area of 50 % of the myocardium. However, if the remained normal myocardium is less than 30 %, it is difficult to recover even if supported by LVAD.

## 8.5 SUMMARY

Pneumatically driven, diaphragm type left ventricular assist devices (LVADs) were implanted into 8 goats who were induced profound infarction in the left ventricle by multiple ligations of the left anterior descending coronary artery (LAD) as well as small arteries in the LAD distributing area. Left ventricular diameters, regional myocardial segment lengths and wall thickness were measured by sonomicrometers.

After the left ventricular function seemed to be recovered, the LVADs were weaned off after decreasing the pump bypass flow gradually for several days. The hemodynamic and cardiac parameters were observed for around 1 month thereafter.

Three animals were recovered successfully by virtue of LVAD pumping. Before starting pump-weaning procedure, the bulk mechanical work (BMW) done by the left ventricle during LVAD pumping and under temporary pump-off condition were  $0.08 \pm 0.01$  (mean  $\pm$  SE) and  $0.22 \pm 0.01$  W/(100 g left ventricular weight (LVW)), respectively, while the regional mechanical work done by the normal myocardium (RMWn) were  $1.5 \pm 0.4$  and  $4.3 \pm 0.9$  mW/cm<sup>3</sup>, respectively. BMW and RMWn obtained under pump-on condition both increased gradually during the weaning process. Even after pump removal, they continued to increase and reached constant values of around 0.3 W/(100 g LVW) and 10 mW/cm<sup>3</sup>, respectively, around 10 days after pump removal. Although the myocardium in the infarcted area did no work for the first several days after surgical operation, it recovered to do some but slight external work by virtue of LVAD pumping. Myocyte diameter of remaining normal myocardium was larger than those of normal heart. Recovery of the left ventricular function owed much to the

compensatory increase of the ability of the remaining normal myocardium rather than to the recovery of the damaged myocardium. LVAD could salvage severely damaged hearts unless the infarcted area exceeds 50 % of the left ventricular wall including the septum and free wall.

#### REFERENCES

1. Nakamura T, Hayashi K, Seki J, Nakatani T, Noda H, Takano H, Akutsu T. Effect of drive mode of left ventricular assist device on the left ventricular mechanics. *Artif Organs* 1988; 12: 56-66.
2. Nakamura T, Hayashi K, Seki J, Nakatani T, Noda H, Fukuda S, Takano H, Akutsu T. Effects of cardiac assist on the bulk and regional mechanics of the ischemic left ventricle in dogs. *Artif Organs* 1990; 14: 57-68.
3. Nakamura T, Hayashi K, Seki J, Nakatani T, Noda H, Fukuda S, Takano H, Akutsu T. Sonomicrometric studies on the effects of long-term pumping of cardiac assist device on the bulk and regional mechanics of the normal left ventricle in goat. *Heart and Vessels* (submitted).
4. Nakamura T, Hayashi K, Seki J. Eight-channel ultrasonic displacement meter for implantable miniature sensors. *Med & Biol Eng & Comput* 1987; 25: 355-8.
5. Takano H, Taenaka Y, Nakatani T, Akutsu T, Fujita T, Manabe H. Circulation control of experimental and clinical profound left ventricular failure by automatic left ventricular assist system. *Jap Circ J* 1984; 48: 302-11.
6. Brugger JP, Odermatt R, Meli M, Hahn C. Periodic failure and recovery pattern during cardiac assistance procedures. *ASAIO J* 1985; 8: 182-5.
7. Nakatani T, Takano H, Taenaka Y, Umezumi M, Tanaka T, Yutani C, Matsuda T, Iwata H, Noda H, Nakamura T, Takatani S, Seki J, Hayashi K, Akutsu T, Manabe H. Therapeutic effect of left ventricular assist device on induced profound left ventricular failure. -Evaluation by left ventriculography- *Trans Am Soc Artif Intern Organs* 1984; 30:

533-9.

8. Lavalley M, Cox D, Patrick TA, Vatner SF. Salvage of myocardial function by coronary artery reperfusion 1, 2, and 3 hours after occlusion in conscious dogs. *Circ Res* 1983; 53: 235-47.
9. Bush LR, Buja LM, Samowitz W, Rude RE, Wathen M, Tilton GD, Willerson JT. Recovery of left ventricular segmental function after long-term reperfusion following temporary coronary occlusion in conscious dogs: comparison of 2- and 4-hour occlusions. *Circ Res* 1983; 53: 248-63.
10. Askenase AD, Naccarella FF, Weintraub WS, Klein LW, Agarwal JB, Helfant RH. Contractile function and reserve during acute ischaemia in the canine lateral border zone. *Cardiovasc Res* 1988; 22: 122-30.
11. Lew WYW, Chen Z, Guth B, Covell JW. Mechanisms of augmented segment shortening in nonischemic areas during acute ischemia of the canine left ventricle. *Circ Res* 1985; 56: 351-8.
12. Ginzton LE, Conant R, Rodrigues DM, Laks MM. Functional significance of hypertrophy of the noninfarcted myocardium after myocardial infarction in humans. *Circulation* 1989; 80: 816-22.
13. Schoen FJ, Palmer DC, Bernhard WF, Pennington DG, Haudenschild CC, Ratliff NB, Berger RL, Golding LR, Watson JT. Clinical temporary ventricular assist. *J Thoracic Cardiovasc Surg* 1986; 92: 1071-81.
14. Didisheim P, Olsen DB, Farrar DJ, Portner PM, Griffith BP, Pennington DG, Joist JH, Shoen FJ, Gristina AG, Anderson JM. Infections and thromboembolism with implantable cardiovascular devices. *Trans Am Soc Artif Intern Organs* 1989; 35: 54-70.
15. Icenogle TB, Smith RG, Cleavinger M, Vasu MA, Williams RJ, Sethi GK, Copeland JG. Thromboembolic complications of the Symbion AVAD system. *Artif Organs* 1989; 13: 532-8.

16. Termuhlen DF, Swartz MT, Pennington DG, McBride LR, Szukalski EA, JE Reedy, Ruzevich SA. Thromboembolic complications with the Pierce-Donachy ventricular assist device. *Trans Am Soc Artif Intern Organs* 1989; 35: 616-618.

## CHAPTER IX

### SUMMARY

LVAD is one of the most powerful and useful circulatory assist means to salvage patients having profound yet recoverable heart failures and to keep alive patients having unrecoverable heart diseases until cardiac transplantation is available. To apply the LVAD system more effectively, fundamental studies on the effect of LVAD pumping on the hemodynamics and the left ventricular mechanics are indispensable. However, very few studies have been carried out on the effects of LVAD on the ventricular and myocardial mechanics although hemodynamic studies have been done rather extensively. The main purpose of this study is to analyze bulk and regional left ventricular mechanics during LVAD pumping.

This study was conducted to know: (i) the most effective drive mode for LVAD, (ii) mechanical effects of LVAD on the normal and ischemic myocardium as well as on the whole left ventricle, (iii) long-term effects of LVAD, and (iv) recovery process of the failing heart supported by LVAD.

First of all, heart diseases and their treatment methods were surveyed in CHAPTER I. It was emphasized that very few studies have been conducted on the effects of LVAD pumping from the view point of cardiac mechanics. The purpose of this study was also stated in this chapter.

In CHAPTER II, general concept of LVAD system and importance of LVAD for the patients having severe heart diseases were stated. And then, it was described that a pneumatic driven, diaphragm-type LVAD was

used in this study and that it was inserted between the left atrium and the descending thoracic aorta to bypass the left ventricle.

It was pointed out in CHAPTER III that the bulk and regional mechanical work are useful and important parameters for the evaluation of the mechanical effects of LVAD on the left ventricular and myocardial function. As the preparation for obtaining these works, equations for the calculation of left ventricular volume, myocardial local wall tension, and local myocardial area were introduced.

In order to obtain these volume and area, an 8-channel ultrasonic displacement meter and implantable miniature sensors were developed for the measurements of ventricular diameter and myocardial segment length. The design specifications and performance of the system were described in CHAPTER IV. This ultrasonic system was used in a series of acute and chronic animal experiments.

First, effects of drive mode of LVAD on the hemodynamic and left ventricular functions were studied by acute animal experiments on dogs having normal hearts. Two fixed rate modes (pumping rates of 60 and 80 bpm) and three electrocardiogram-synchronous counterpulse modes at different duty ratios (1 pumping in 1, 2 and 4 cardiac cycles) were evaluated. It was shown in CHAPTER V that the synchronous mode at 2:1 duty ratio was most effective to rest the left ventricle and that the same mode at the ratio of 1:1 was best to maintain the systemic circulation.

Then, acute effects of LVAD pumping on the hemodynamic and cardiac functions was studied on dogs induced with ischemia in the heart by ligating the left anterior descending coronary artery (LAD). Based on the results described in CHAPTER V, the 2:1 and 1:1 synchronous modes were used to drive LVAD. The method for this experiment and the results

obtained were described in detail in CHAPTER VI. Briefly, there was little difference in the effects between two pumping modes in the case of ischemic heart. LVAD reduced myocardial work in the normal area, while exerting no load to the ischemic region and keeping the work in this region at near zero level.

After these acute experiments, chronic animal experiments were conducted to know the long-term effects of LVAD pumping as well as to study the recovery process from heart failure.

As the first series of chronic animal experiments, goats having the normal hearts were implanted with LVADs and were kept alive for 1 month as was described in CHAPTER VII. LVAD had a capability of decreasing the bulk left ventricular and local myocardial work for a long duration as observed in the acute experiments. Myocyte diameter in the subendocardial layer observed after 1 month LVAD pumping was thinner than that in the middle and subepicardial layers and that in the subendocardial myocardium of normal heart. It increased with the left ventricular mechanical work although those in the middle and subepicardial layers did not change. Long-term feasibility of the ultrasonic system was confirmed by the animal experiments.

Finally, recovery process of the natural heart induced with myocardial infarction and supported by LVAD was studied using the similar techniques to those explained in the previous chapters, and the results obtained were shown in CHAPTER VIII. When the left atrial pressure measured under temporary pump-off condition became lower than 20 mmHg, LVAD was weaned-off. Recovery process of the left ventricular function was observed for around 1 month after pump removal. Although the myocardium in the ischemic area recovered slightly to do some work, overall function of the left ventricle owed much to the compensatory

work done by the myocardium in the remaining normal area. Myocyte diameter in the normal area of this ischemic heart model was greater than that in the normal heart model described in CHAPTER VII. In the animals recovered successfully, percentage of the area occupied by normal myocardium was more than 50 % of the whole left ventricular free wall and septum.

In conclusion, it was demonstrated from the stand point of cardiac mechanics that LVAD is a very powerful and useful mean to salvage severely debilitated left ventricle. Bulk and regional mechanical work of the left ventricle measured in this study were very useful parameters to evaluate the left ventricular and myocardial function during LVAD pumping. The effects of LVAD on the infarcted left ventricle are summarized as follows: LVAD can maintain the systemic blood circulation under good condition until the remained normal myocardium becomes capable of producing necessary bulk left ventricular work without LVAD pumping, while salvaging a part of ischemic myocardium slightly. It is expected that the results obtained from this fundamental study contribute much to more effective use of LVAD in clinical cases as well as to better understanding of the left ventricular function in the field of cardiac mechanics.

ACKNOWLEDGMENT

This research work has been supported by many persons and has NEVER been completed without their enormous cooperation and encouragement. First of all, the author greatly appreciates Dr. Kozaburo HAYASHI, Professor, Department of Biomedical Control, Research Institute of Applied Electricity, Hokkaido University, for affording an opportunity of conducting this work, supervising, and encouraging to fulfill this work.

Most of the animal experiments were carried out at National Cardiovascular Center Research Institute, Osaka. The author appreciates Drs. Hisateru TAKANO, Yoshiyuki TAENAKA, Takeshi NAKATANI, Masayuki KINOSHITA, Hiroyuki NODA, Sachito FUKUDA, Takehisa MATSUDA, and Mitsuo UMEZU of the Department of Artificial Organs, and Junji SEKI, Tadashi KATO and Keiichi TAKAMIZAWA of the Department of Biomedical Engineering for their cooperation in the experiments, invaluable comments, suggestions and discussions. The author also expresses his sincere thanks to the other members of the Department of Artificial Organs for their intensive assistance in the animal experiments.

Finally, the author would like to express his special appreciation to Drs. Tetsuzo AKUTSU, Vice-Director, and Hiroyuki SUGA, Head of the Department of Cardiovascular Dynamics, National Cardiovascular Center Research Institute, for their invaluable discussions, continuous support and encouragement.

This work was supported financially in part by the Grant-in-Aid for

the Encouragement of Young Scientists (T. Nakamura, nos. 58770914, 59770983 and 60771079) and the Grant-in-Aid for the Scientific Research (K. Hayashi et al., no. 63480316) from the Ministry of Education, Science and Culture in Japan.

APPENDIX

A.1 Algorithm for calculation of loop area

The areas inside the LVP-LVV and Tw-Am loops in a cardiac cycle were calculated by the following algorithm (Fig. A.1) using a mini-computer system:

1. The maximum and minimum values of LVP or Tw in a cardiac cycle were searched.
2. The LVP or Tw in the cardiac cycle was equally divided into 100 levels between the maximum and minimum values. The height of each leveled band area,  $h$ , is expressed as:

$$h = \frac{\text{max. (LVP or Tw)} - \text{min. (LVP or Tw)}}{100} \quad (\text{A.1})$$

3. The maximum value of LVV or Am ( $\text{LVV}_x$  or  $\text{Am}_x$ ) and the minimum value of LVV or Am ( $\text{LVV}_n$  or  $\text{Am}_n$ ) were searched in each band.
4. The area of the  $i$ -th band,  $A_i$  ( $i = 0, 1, \dots, 99$ ), is calculated by:

$$A_i = h \frac{\sum_{j=i}^{i+1} ((\text{LVV}_x \text{ or } \text{Am}_x)_j - (\text{LVV}_n \text{ or } \text{Am}_n)_j)}{2}, \quad (\text{A.2})$$

assuming that the shape of the band is a trapezoid.

5. The area inside the loop,  $A$ , is calculated by:

$$A = \sum_{i=0}^{99} A_i. \quad (\text{A.3})$$

$$h = \frac{\text{max. (LVP or Tw)} - \text{min. (LVP or Tw)}}{100}$$

$$A_i = h \cdot \frac{\sum_{j=i}^{i+1} ((\text{LVV}_x \text{ or } \text{Am}_x)_j - (\text{LVV}_n \text{ or } \text{Am}_n)_j)}{2},$$

$$(i = 0, 1, \dots, 99)$$

$$A = \sum_{i=0}^{99} A_i$$

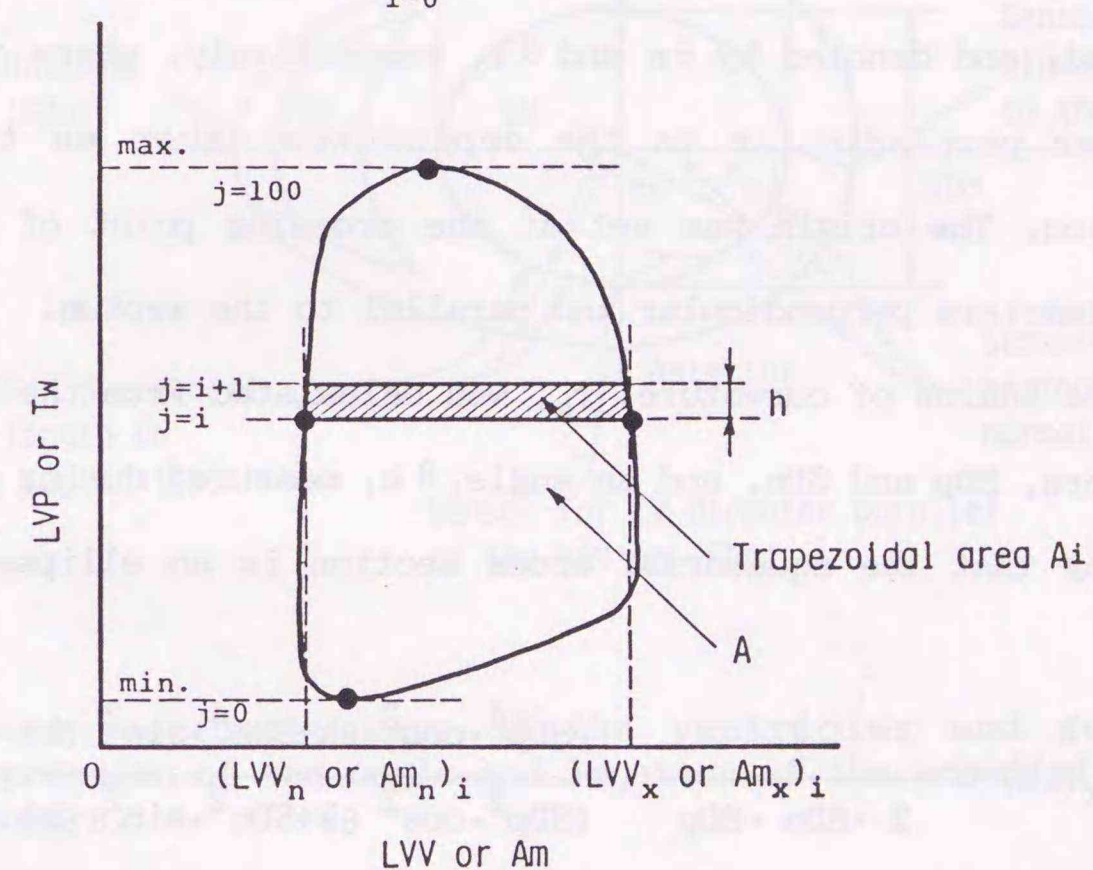


Fig. A.1 Calculation algorithm of the area inside the loop obtained from the relationship between the left ventricular pressure (LVP) and volume (LVV) or between the subendocardial wall tension (Tw) and regional rhombus area (Am) in a cardiac cycle.

## A.2 Calculation of local myocardial wall tension

The wall tension in the normal and ischemic regions of the left ventricle were calculated as follows.

After the experiments, the hearts were resected and cut equatorially at the level of the ultrasonic sensors for the measurement of the short axis diameter of the left ventricle (See Fig. A.2). The equatorial angles between the reference direction and the normal and ischemic regions where the ultrasonic sensors were embedded were measured, and denoted by  $\theta_n$  and  $\theta_i$ , respectively, where the short axis diameter perpendicular to the septum was taken as the reference direction. The origin was set at the crossing point of the two short axis diameters perpendicular and parallel to the septum.

The radius of curvature,  $r_k$ , was calculated from the two short axis diameters,  $SD_p$  and  $SD_n$ , and an angle,  $\theta_k$ , measured during the autopsies, assuming that the equatorial cross section is an ellipse. It is given by:

$$r_k(\theta_k) = \frac{1}{2 \cdot SD_n \cdot SD_p} \left[ \frac{(SD_p^4 \cdot \cos^2 \theta_k + SD_n^4 \cdot \sin^2 \theta_k)}{(SD_p^2 \cdot \cos^2 \theta_k + SD_n^2 \cdot \sin^2 \theta_k)} \right]^{3/2}, \quad (A.4)$$

where  $k = n$  and  $i$ .

The radii for the normal ( $r_n$ ) and ischemic ( $r_i$ ) regions were calculated from the above equation, and used to obtain the wall tension,  $Tw_k$ , by eq. (3.2). The wall tension is given by:

$$Tw_k = \frac{r_k}{2} \text{ LVP}, \quad (k = n, i) \quad (A.5)$$

where LVP is the left ventricular pressure.

$$r(\theta) = \frac{1}{2 \cdot SD_n \cdot SD_p} \cdot ((SD_p^4 \cdot \cos^2 \theta + SD_n^4 \cdot \sin^2 \theta) / (SD_p^2 \cdot \cos^2 \theta + SD_n^2 \cdot \sin^2 \theta))^{3/2}$$

$$r_i \equiv r(\theta_i)$$

$$r_n \equiv r(\theta_n)$$

$$Tw_n = \frac{r_n}{2} \cdot \text{LVP}$$

$$Tw_i = \frac{r_i}{2} \cdot \text{LVP}$$

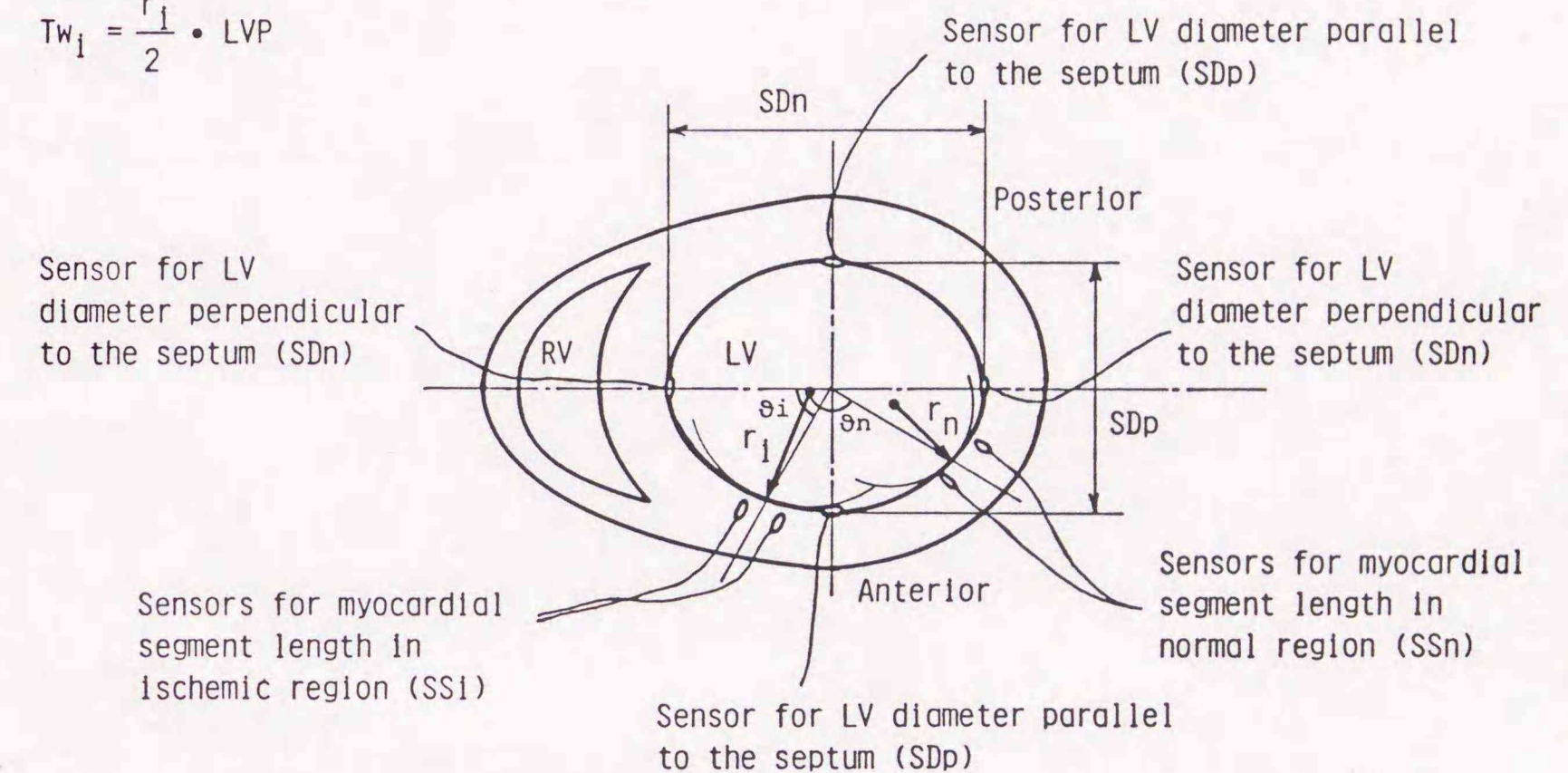


Fig. A.2 Cross-sectional shape of the ventricles and geometrical expression of the angle and location of the embedded ultrasonic sensors.

